Finanziato dall'Unione europea NextGenerationEU
Ministero dell'Università e della Ricerca
Italiadomani PIANO NAZIONALE DI RIPRESA E RESILIENZA
1506 UNIVERSITÀ DEGLI STUDI DI URBINO CARLO BO

UNIVERSITÀ DEGLI STUDI DI URBINO CARLO BO

Department of Pure and Applied Sciences

Ph.D. PROGRAMME IN:

Research Methods in Sciences and Technology (REMEST)

CYCLE XXXVIII

ANALYSIS OF SOLID TRANSPORT IN TORRENTIAL WATERCOURSES FOR HYDRAULIC AND HYDROGEOLOGICAL RISK MANAGEMENT

ACADEMIC DISCIPLINE:

GEOS-03/A

Thesis written with the financial support of a scholarship financed by Ministerial Decree no. 351 of 9 April 2022, under the PNRR - financed by the European Union - NextGenerationEU - Mission 4 ‘Education and Research’, Component 1 ‘Strengthening the supply of education services: from kindergartens to universities’ - Investment 4.1 ‘Extending the number of PhDs and innovative PhDs for public administration and cultural heritage - Domain: Generic

Coordinator: Prof. Luca Lanci

Supervisor: Prof. Stefano Morelli

Co-Supervisor: Prof. Alberto Renzulli

Ph.D. student: Erica Guidi

ACADEMIC YEAR
2024/2025

Happiness lies in small actions

ABSTRACT

Climate change is intensifying the frequency and magnitude of extreme weather events across Mediterranean regions, increasing the exposure of mountainous catchments to flash floods and related geomorphic hazards. To predict their morphological response and mitigate future impacts, it is essential to understand how sediment is supplied, transferred, and redistributed within these systems. This research integrates two complementary approaches to analyse sediment dynamics in the Burano River basin (Central Apennines, Italy), severely affected by the 15–16 September 2022 extreme flood. It is becoming more widely acknowledged that promoting the sustainable use of natural resources and reducing environmental consequences depend on effective sediment control and management. This thesis aims to investigate the intricate interactions between hydrodynamic forces, sediment delivery, and sediment availability, which are critical in determining how rivers react to extreme occurrences. In the first phase, a GIS-based framework was developed to identify and prioritise sediment supply areas and evaluate their structural connectivity using morphometric indices such as the Stream Power Index (SPI), Connectivity Index (IC), and Stream Length-Gradient Index (SL). The method has proven effective in identifying the spatial distribution of sediment source and connecting transport channels by considering the coupling processes between slopes and river channels. This approach is both time and cost-efficient and provides reliable information on sediment transfer with minimal input data requirements. In the second phase, a two-dimensional morphodynamic model (Iber) was applied to a critical Burano sub-basin (Tenetra stream) to simulate bed-load and riverbed evolution under the 2022 flood event conditions. Different scenarios of coarse sediment grain-size distribution (D_{50}) and abrupt sediment inputs were tested to assess how variability in sediment characteristics influences bed-load transport, channel morphology, and the efficiency of existing hydraulic works. The results of these applied techniques should offer important new information about the function of sediment availability, sediment supply understanding the river response to a grain-size variation in terms of morphological changes during flood events, both in the river under study and in similar fluvial systems. The integrated approach highlights how sediment availability and connectivity strongly control geomorphic adjustments during floods. Results demonstrate that neglecting bed-load transport can lead to underestimation of flood hazards, as morphological changes modify channel geometry, roughness, and flow conveyance capacity. The methodology offers a reproducible, time-efficient tool to support emergency planning and sediment management, providing valuable insights for predicting river responses to future extreme events and designing adaptive flood mitigation strategies in similar mountainous contexts.

Tables of contents

CHAPTER I
Background

According to the Intergovernmental Panel on Climate Change (IPCC - 2021), it is now well established that human-induced forcings have led to an increase in the frequency and/or intensity of certain extreme weather and climate events. An event is generally considered 'extreme' when the value of a variable exceeds or falls below a defined threshold, or when a pattern of severe weather conditions persists for a given period (Seneviratne et al., 2021). Analysis of variations in extremes have shown strong sensitivity to global warming. In the case of temperatures extremes, variations in magnitude often depend linearly on global surface temperature (Seneviratne et al., 2016; Wartenburger et al., 2017), whereas variations in frequency tend to be non-linear and can be exponential for higher levels of warming (Kharin et al., 2018). Similarly, precipitation extremes display clear intensification trends. Papalexiou & Montanari (2019) analysed globally the high-quality daily precipitation data from 1964 to 2013 and detected significant increases in both the frequency and, to a lesser extent, the intensity of extreme daily rainfall events. Kharin et al, (2018) further demonstrated that global warming of 2°C would produce substantially larger changes in the probability of extreme events than a 1.5°C increase. The relative increases (%) in extreme precipitation intensity exceed those of average annual precipitation by about 2-3 times (Kharin et al., 2013). According to the Clausius-Clapeyron relationship, the maximum annual amount of precipitation in a single day has increased by 7% for every 1°C of global average temperature (Westra et al. 2013). Consequently, both the rarity of the severe events and the magnitude of future warming play crucial roles in shaping the changing risk ratios of extremes (Kharin et al., 2018). These findings highlight how climate change has already altered the frequency and magnitude of extreme rainfall, creating new challenges for understanding the hydrological and geomorphological responses of catchments, especially in mountainous regions.

River systems that originate in mountainous regions are particularly sensitive to variations in climate regimes, especially changes in precipitation patterns, under a warming climate (Beniston, 1997). Climatic conditions, including long-term climate change, influence slope stability at multiple spatial and temporal scales (Seneviratne et al., 2012). The intensification of rainfall events (IPCC - 2014), combined with the complex geotechnical conditions of mountain slopes, is expected to increase frequency of shallow landslides and reduce the occurrence of deeper mass movements (Gariano & Guzzetti, 2016). When specific intrinsic or extrinsic thresholds are surpassed, rapid and significant changes in slope stability occur (Dijkstra & Dixon, 2010). Thus, slope stability can be interpreted through the concepts of system sensitivity and resilience at given time. Haque et al. (2019) documented a significant increase in fatal rainfall-induced over the past two decades in 128 countries, with a linkage to extreme rainfall events, particularly in densely populated areas. Although the proportion of landslides attributed to extreme rainfall remained stable, their absolute number rose in parallel with growing frequency and intensity of heavy precipitation (Haque et al., 2019). Understanding how climatic variables and their variability effects influence geo-hydrogeological risks, sedimentation and erosion processes

is now a fundamental issue for future forecasting and anticipate management (Walling, 2008; Coe and Godt, 2012; Dijkstra and Dixon, 2010; Gariano and Guzzetti, 2016; Semnani et al., 2025; Gariano & Rianna 2025).

Among the hydrogeological risks, floods represent one of the most severe and costly natural hazard globally (Nones & Guo, 2023). In response, the European Commission introduced Directive 2007/60/EC to address flooding in Europe, aiming to prioritize flood-risk management strategies. Flood events may be triggered by several mechanisms—including heavy or prolonged rainfall, snowmelt, the catastrophic release of glacial lakes, or the abrupt failure of water-control infrastructure (Vázquez-Tarrío et al., 2024). However recent studies emphasize that many extreme floods arise from multiple interacting drivers, such as soil moisture, precipitation, snow depth, and temperature, rather than a single overwhelming cause (Jiang et al., 2024). According to global hydrological models, river flooding is expected to increase in the near future, affecting broad areas. This increase may be exacerbated by people being more exposed to flood threats (Alfieri et al., 2017). Jiang et al. (2024) demonstrated that compound interactions among multiple flood drivers can amplify flood magnitudes, particularly for extreme events. Furthermore, inaccurate representation of sediment transport and morphological evolution in rivers may contribute to underestimating flood impacts, especially in active mountain watercourses subject to frequent geomorphic change (Nones & Guo, 2023). Understanding flood triggers in combination with sediment dynamics is therefore critical for improving predictive models and enhancing hydraulic and hydrogeological risk management.

While human-induced climate change is a dominant factor driving current environmental modifications (IPCC, 2021), other anthropogenic pressures, such as urbanization, deforestation and land-use changes, also play a crucial role in shaping Earth's surface processes and accelerating geomorphic responses (Remondo et al., 2024). Erosion and sediment transport processes, intrinsically linked with land cover and hydrology, are highly sensitive to both climatic and anthropogenic changes that affect sediment detachment, mobilisation, and transport (Walling, 2008). It has been proven that human activity has an impact on natural erosion processes and has caused a noticeable and significant rise in soil erosion rates throughout landscapes (Poesen, 2018). Climatic projections further suggest an intensification of the hydrological cycle that could promote a global increase in water erosion processes of approximately 30 to 66 % by 2070 (Borrelli et al., 2020; JRC, 2020). Such transformations are expected to alter sediment availability and transfer, reinforcing the need to integrate human drivers into hydro-geomorphological risk analyses. In this context, human-induced changes not only accelerate erosion and sediment delivery but also modify the natural connectivity between hillslopes and channels, thus reshaping sediment cascades and the functioning of entire catchment systems.

Understanding sediment production and its transfer through catchment networks has become increasingly essential for interpreting landscape evolution and managing hydrogeological risks. Based on connection-disconnection hypotheses between slopes and the channel network, the evaluation (relationship between hillside slope and sediment transport; Bracken et al., 2015) offers a thorough and novel method of system analysis. Recent years have seen a significant increase in the study of sediment production and river connection in geomorphology, particularly in the most thorough assessment of hillslope-channel coupling (Parsons et al.,

2015; Wohl, 2017). According to the theory of material transfer, connectivity is thought to be the most plausible relationship that water and sediments have. In a river basin, it may be described primarily by i) longitudinal connectivity, or coupling within the channel network, and ii) lateral connectivity, or hillslope–channel coupling, as well as the storage direction. Evaluating these forms of connectivity helps to identify the most effective sediment pathways and to detect critical zones where erosion, storage, and transfer interact. Such understanding is vital for anticipating the geomorphic and hydrological consequences of extreme events in mountainous catchments.

Sediment connectivity is determined by the structural characteristics of the catchment area, defined by its morphological and functional characteristics (Bracken et al., 2015; Najafi et al., 2021; Wainwright et al., 2011). The latter are defined as the interaction of structural connectivity characteristics through runoff processes, including the process of sediment transfer within the watershed (Commendador, 2021). Structural connectivity can be assessed by applying morphometric indices, such as the connectivity index (Borselli et al., 2008; Cavalli et al., 2013; Heckmann et al., 2018), which describe how efficiently sediment can be transferred between different compartments of the landscape. While structural connectivity captures the static framework of potential linkages, functional connectivity accounts for dynamic interactions controlled by hydrological processes, sediment availability, and triggering events (Turnbull et al., 2018; Wainwright et al., 2011). These components are deeply influenced by catchment morphology and external forcings (e.g., precipitation intensity or land cover) but also feedback into the system by modifying its geometry, altering channels, slopes, and depositional zones (Wohl et al., 2019; Zanandrea et al., 2021). Consequently, the study of sediment connectivity provides a key to understanding the complex feedbacks that regulate sediment cascades. It also represents a valuable tool for improving hazard prediction, especially in contexts where extreme rainfall events can abruptly reactivate or reorganize sediment pathways.

Effective hillslope-to-channel connectivity introduces sediment into the river system, influenced by size, mass, and shape. Coarse particles are transported mainly by rolling or saltation mechanisms in the lower water column, while finer fractions and dissolved sediment are carried in suspension within turbulent flow (Hjulström, 1935). It is estimated that around 95% of the sediment reaching oceans is transported by rivers (Commendador, 2021). The erosion rate and sediment load are two closely related factors, as the export of sediments from the catchment area provides a measure of the intensity of erosion in the upstream basin (Walling, 2008). The study of erosion rates and the related sediment loads transported by the world's rivers is therefore fundamental, as it represent a sensitive and significant indicator of environmental change and land denudation. The amount and composition sediment load recorded in the upstream river sections reflects the balance between erosion, storage and transfer processes occurring throughout the catchment. Sediment loads also pose significant challenges to water resource management, contributing to reservoir sedimentation, siltation, and higher water treatment costs, while altering nutrient and carbon cycles in lakes and coastal seas (Walling, 2008). Sediment load in rivers significantly influences morphodynamics, drainage basin hydrology, and erosion processes. The magnitude of these loads impacts the system's functioning. It impacts material fluxes, geochemical cycling, water quality, channel

morphology, delta development, and aquatic ecosystems and habitats (Walling, 2008). For these reasons, it is essential to approach sediment transport from a basin-wide perspective, integrating both upstream sediment sources and downstream morphological responses to understand how changes in sediment load can reshape the system's behaviour.

Recent studies show that increasing rainfall intensity leads to more frequent and extreme discharge events, which significantly enhance sediment production (Stryker et al., 2018). Higher precipitation rates increase the surface runoff, and consequently, sediment yields and transport (Wu et al., 2025). During extreme event, these processes intensify, resulting in complex hydraulic conditions that accelerate sediment movement and deposition dynamics. Model simulations have demonstrated that local increase in extreme precipitation can substantially amplify suspended sediment yields (Stryker et al., 2018). Moreover, human activities such as deforestation or urbanisation tend to increase hydrological-sedimentary connectivity, causing an increase in runoff and, consequently, erosion. Soil cover and surface roughness are important characteristics that can represent positive or negative feedback on surface runoff (Nordio et al., 2024). Extreme rainfall also affects flood peak magnitudes and timing, significantly influencing flood hydrographs (Tunas et al., 2021). Sediments and their characteristics play an important role in defining river flood hazard mapping. The short response time between intense precipitation and sediment-laden floods, especially in steep basins, highlights the high-risk potential of flash floods and debris flows (Borga et al.,2014). Hence, understanding how rainfall extremes control sediment mobilisation is key to improving predictive models of flood hazard and designing effective mitigation strategies in sediment-rich mountain catchments.

Sediment transport and river morphology are dynamically interlinked through feedback processes that influence each other over multiple spatial and temporal scales. The morphology of the riverbed depends on a number of factors, including the characteristics of the sediments transported upstream, the local geology, the local flow field and the flow rate (Hamidifar et al., 2020). Changes in sediment transport can alter channel morphology by modifying channel bed elevation, width, and sinuosity (Hamidifar et al., 2024), while variation in channel morphology, can affect sediment transport patterns by influencing flow velocities, shear stress distribution, and sediment deposition zones (Hamidifar et al., 2024). Bedload transport, particularly of coarser sediments, is one of the main drivers for the morphological change of gravel-bed rivers (Khosravi et al., 2020). The prediction of sediment transport in gravel-bed rivers is essential to the management of land, water, and ecological resources in mountain regions (Wilcock, 1998). Sensitivity analyses show that flow velocity, shear stress, flow discharge, bed shear velocity, bed slope, flow depth, median sediment diameter, and relative roughness are the main factors controlling sediment mobility (Khosravi et al., 2020). A riverbed's grain size mix is determined by how quickly various grain sizes are transported to the river and how fast the flow moves them. If the amount of water and sediment supply is altered, the river channel will start to modify its geometry and bed composition in order to adjust the new load (Wilcock, 1998). High-flow events can also mobilize large wood and coarse sediment determining the so-called disturbance regime that influences long-term channel evolution (Ruiz-Villanueva & Consoli, 2025). Intense sediment discharges contribute to an increase in the density of water-sediment mixtures

affecting flow velocity, stage-discharge relationships and flood thresholds (Vázquez-Tarrío et al., 2024). Consequently, sediment-laden floods may reshape channel geometry, influencing future flood behaviour by changing conveyance capacity and flow routing (Ruiz-Villanueva et al., 2023). Variations in sediment input can trigger downstream geomorphic adjustments, as confirmed by several studies (Tal and Paola, 2007; Dingle et al., 2019; Vázquez-Tarrío et al., 2024). Vazquez-Tarrío et al. 2024 showed that the most studies on the influence of sediment transport on flood risk have focused on mountain streams, as they are highly sensitive systems to changes in sediment supply. Furthermore, there are now opportunities to explicitly include sediment transport in flood hazard calculations thanks to recent advancements in hydrodynamic and morphodynamic numerical models. Magnitude and intensity of the hydro-geomorphic response may affect hazard and risk in the downstream channel system and the associated fans and floodplains (Borga et al., 2014). Grain size affects downstream transport distances for particles coarser than the riverbed's median grain size, while clast size has less of an impact on travel distances for particles finer than the bed sediment's median size (Church & Hassan, 1992). As we have seen, sediment balance and sediment flows can be disrupted by various factors, such as gravel extraction or hydraulic works, which sometimes occur simultaneously, creating overlaps and leading to changes in morphology and habitats. These changes lead to responses that propagate downstream, triggering a cascade of far-reaching geomorphological and ecological adjustments that persist long after the initial impact (Vazquez-Tarrío et al., 2023). Dams totally prevent the movement of coarse sediment, which causes channel deterioration. This usually leads to incision, bed coarsening, refilling (the buildup of fine material), and the separation of rivers from their floodplains (Ruiz-Villanueva & Consoli, 2025). Altogether, these processes illustrate that sediment transport is not only a geomorphic driver but also a central factor in hydraulic and hydrogeological risk. Understanding its dynamics from source to sink, and under changing climatic and anthropogenic conditions, is therefore fundamental to anticipate morphological evolution and to support sustainable management of torrential river systems.

1.1 Thesis objectives

The main objectives of this PhD project concern the promotion of greater awareness of the role of sediment transport within river systems, both along the channel and throughout the entire catchment. Understanding these processes is an important step towards predicting and preventing high-risk events, enabling the development of innovative methods applicable to different contexts. The research question, which is answered in this thesis, is how do rivers (and slopes) react to extreme events, especially in light of current changes in precipitation patterns (in terms of both frequency and intensity), given that mountain basins are particularly sensitive to these changes, being exposed to landslides, floods and strong sedimentary dynamics? A holistic approach that links hillslope processes with fluvial dynamics is essential to fully capture sediment connectivity and transfer mechanisms. Sediment mobilised from upland slopes represents the initial driver of downstream morphological adjustments, emphasising the need to analyse the entire catchment system rather than isolated channel reaches. The proposed framework integrates the identification of sediment source areas at the basin scale with a detailed investigation of riverbed dynamics during extreme rainfall events, offering a comprehensive understanding of how rapid

morphological adaptations develop under high-risk conditions. The selected study area is the Burano River sub-basin (Metauro River basin, central Italy), which was severely affected by the extreme flood event of September 2022. This system, not previously investigated from a geomorphological and morphodynamic perspective, proved to be an ideal case study for the analysis of torrential watercourses. Its morphological characteristics and the occurrence of a contemporary event of intense precipitation that triggered mass movements on the slopes and imbalances in solid transport in the riverbed make it an interesting case to be studied in depth using the identified methodology. The Burano River and its tributaries represent one of the areas that suffered the most severe consequences during the flood. In particular, the town of Cantiano experienced widespread damage; therefore, the study focused on tracking the movement and transfer of solid material in its upstream sector. The event caused numerous landslides, extensive hillslope erosion, and catastrophic flooding of the valley floor. Owing to the hilly morphology and the complex geological setting, the area exhibited an intricate pattern of material transfer between slopes and the channel network. This research aim to highlight a replicable case study that can serve as a reference for similar contexts, offering practical, rapid, and cost-effective tools for managing extreme rainfall and flood events. This dual approach is innovative, and provides constructive insights into sediment supply, connectivity, and riverbed evolution under extreme hydrological conditions. The method employs two distinct approaches that are used in sequence to identify the source areas of material and manage sediment in the riverbed through modelling that defines the morphological impacts. The procedure aims to expand knowledge about the solid river transport that is mobilised and transported during extreme conditions. It also has the purpose to provide effective tools to offers practical implications for hazard assessment and flood mitigation strategies. The structure of the thesis has been organised as a monograph containing two main articles that represent the core of this research. Each article has been introduced and discussed individually and represents *CHAPTER II* and *CHAPTER III* respectively. A general introduction forms the opening section of the thesis (*CHAPTER I*), and a final section conclusion forms the closing section, which acts as a binding element. Brief outlines of the objectives and methodology for each article are provided below.

CHAPTER II: "Optimising the identification of river sediment supply areas and their connectivity in the mountainous river basins of central Italy"

GIS-based approach, to quickly obtain the sediment availability and supply evaluating coupling with the drainage network. The transfer materials over slopes and major riverbeds could be defined by combining a geomorphological characterisation with three geomorphometric indices: the Stream Power Index (SPI), Connectivity Index (IC), and Stream Length-Gradient Index (SL). With just a digital terrain model, basic geological data, pre- and post-event evidence, and landslide inventories, the framework is intended to be transferable and operationally straightforward. This methodology is quick but effective and provides concrete assistance in identifying areas of instability that could be triggered by meteorological events.

CHAPTER III: "Modelling River geomorphic responses to abrupt sediment inputs and grain size variability during floods: insights from Burano River (Italy)"

A two-dimensional numerical model was employed to simulate river morphodynamics and to assess the effects of abrupt sediment supply, evaluate the efficiency of existing retention structures, and test different grain-size scenarios (D50 values ranging from 0.01 m to 1 m) to analyse their impact on sediment mobility and riverbed morphology. The study was applied to the Tenetra stream, a steep torrential watercourse free from anthropogenic influence, which was severely affected by the 2022 flood in the Marche region and experienced substantial morphological changes. Requiring only a limited amount of input data, this approach proves to be both practical and cost-effective, suitable for emergency response as well as for the design phase of protective works.

CHAPTER II

Optimising the identification of river sediment supply areas and their connectivity in the mountainous river basins of central Italy

Under review – Journal of Mountain Science

*Guidi E. [a, *], Pappafico G.F. [a], Confuorto P. [b], Morelli S. [a]*

a Department of Pure and Applied Sciences, University of Urbino Carlo Bo, Urbino 61029, Italy

b Department of Earth Sciences, University of Florence 50134, Italy

A B S T R A C T

Climate change is forcing Mediterranean countries to face more extreme weather events with increasingly destructive land effects, such as flash floods, debris floods, and rapid landslides. Understanding the processes supplying material into catchment areas is crucial due to the strong connectivity between upstream and downstream in mountainous regions. This can exacerbate vulnerabilities, cause localized flooding, and pose significant hazards. This study presents a semi-quantitative GIS-based procedure for optimising the identification of sediment supply areas and their structural connectivity in mountainous catchments of central Italy. The method combines three morphometric indices, the Stream Power Index (SPI), Index of Connectivity (IC), and Stream Length-Gradient (SL), starting from the geomorphological characterisation of the study area. The methodology is designed to delineate sediment-source areas and assess their degree of connectivity with the drainage network. It incorporates a linear morpho-hydraulic component, based on SL index and longitudinal profile analyses, which supports the interpretation of channel energy conditions and sediment transfer dynamics. Finally, a synoptic raster map is generated that visually highlights the most critical values of the three calculated indices. The approach was tested in the mountain portion of the Burano River basin (Central Apennines), severely affected by the 15 September 2022 flood. The analysis revealed strong correspondence between high-connectivity areas and zones of post-event instability, indicating effective identification of both sediment sources and preferential transport corridors. Validation was performed through multi-source comparison, integrating post-event NDVI difference analysis, UAV photogrammetry, and detailed traditional field surveys, thereby confirming the robustness of the results. This approach is both time- and cost-efficient, offering reliable insights into sediment transfer along slopes and river channels, coupling them into a unique final product, while maintaining a simplified operational structure.

Keywords: GIS analysis, Sediment supply assessment, Catchment-scale sediment connectivity, Quick analysis procedure.

2.1 Introduction

Sediment transfer in mountainous basins plays a fundamental role in landscape evolution, water quality, and natural hazard dynamics, influencing the frequency and magnitude of floods, debris flows, and other slope instabilities (Harvey, 2001; Fryirs, 2013; Bracken et al., 2015), as well as the sediment balance within the river networks (Liu et al., 2018; Sadeghi et. al., 2017). These fundamentally natural processes have been significantly altered by human activities, leading to issues such as accelerated erosion due to changing land use (e.g., urbanisation, rural abandonment, unsustainable agriculture) and the disruption of land–sea sediment transfer by trapping behind dams and infrastructure (Kemp et al., 2020; Syvitski et al., 2005). Understanding how sediments are mobilised and transferred through a catchment is essential to support risk mitigation and watershed management strategies (Fryirs, 2017; Wohl et al., 2019). In this framework, the concept of sediment connectivity has emerged as a key tool to describe the degree to which a system facilitates or impedes sediment transfer between sources, pathways, and sinks (Brierley et al., 2006; Cavalli et al., 2013; Heckmann et al., 2018, Najafi et al. 2021a).

International Sediment Initiative (ISI) was launched in 2002 by UNESCO's International Hydrological Programme (IHP) to promote sustainable sediment management globally (Liu et al., 2018). It aims to understand erosion and sediment transport by rivers to marine, lake or reservoir environments, aid in creating a decision-making framework for sediment management, and link science with policy and management needs. This framework offers guidance on legislative and institutional solutions applicable across diverse socio-economic and physiographic contexts in global change. In 2021, the Strategic Plan for the ninth phase of the IHP, titled "Science for a Water Secure World in a Changing Environment", was adopted by UNESCO in relation to the 2022 - 2029 period (Raphael et al., 2023). This phase identifies priority areas in support of Member States to achieve the Sustainable Development Goals (SDGs), focusing on the United Nations 2030 Sustainable Development Agenda and other water-related global agendas, such as the “Paris Agreement on climate change”, the increase “Sendai Framework on Disaster Risk Reduction” and the “New Urban Agenda” (UNESCO, 2022). The importance of understanding these phenomena is becoming increasingly evident, such as the concept of sediment production and its subsequent transfer to all potential minor collection basins. Considering the current increase in the intensity of rainfall events (Senatore et al. 2025), it is necessary to have rapid and practical responses, aligning with the objectives of global shared agendas. The assessment based on connection-disconnection hypotheses between slopes and the canal network (relationship between hillside slope and sediment transport; Bracken et al., 2015) is a comprehensive and innovative tool for analysing the system.

Research on sediment production and river connectivity have experienced considerable growth in the last years (Parsons et al., 2015; Wohl, 2017; La Licata et al. 2025), especially in the most comprehensive evaluation of hillslope-channel coupling. From this perspective, connectivity can be characterised in a river basin according to the storage direction and mainly by i) longitudinal connectivity, i.e. coupling within the channel network, and ii) lateral connectivity, i.e., hillslope–channel coupling. Moreover, connectivity can be conceptualised into two fundamental components: structural and functional connectivity (Wainwright et al., 2011; Shi et al., 2025). Structural connectivity refers to the arrangement and spatial layout of the system's compartments (Turnbull et

al., 2018). In contrast, functional connectivity pertains to the interactions facilitated by sediment transport processes, emphasising the actual occurrence and temporal fluctuations of sediment movement. Consequently, it depends not only on the inherent structural characteristics of the system but also on the influence of dynamic external factors, such as the characteristics of precipitation and antecedent terrain conditions (e.g., the soil moisture), which are essential for effectively transferring sediment between different landscape compartments (Zanandrea et al., 2021). However, structural and functional connectivity are closely linked (Wohl et al., 2019), as sediment transport often alters the system's morphology, which in turn influences the pathways of sediment movement. Given its static nature, structural sediment connectivity was the first to be quantitatively analysed using numerical and GIS-based models (Cavalli et al., 2013; Messenzehl et al., 2014; Cossart and Fressard, 2017, Martini et al., 2022).

In particular, the river sediment connectivity were explored through: i) assessment of the status of river sections, distinguishing between unconnected, partially connected, potentially connected, and disconnected areas (Hooke, 2003); ii) analysis of the complex mechanisms involved in small- and large-scale sediment transport (Bracken J. L., 2015); iii) development of approaches for morphological analysis using quantitative methods (Najafi et al. 2021a; Koreňová et al. 2024; La Licata et al. 2025); iv) development of morphometric indices (Mishra et al. 2019); v) introducing of new concepts such as (dis)connectivity in geomorphology associated with river and watershed management aspects (Poeppl et al. 2023).

According to Najafi et al. (2021b), that has analysed 117 papers about the sediment connectivity, the problem is usually addressed from five points of view that are based on: i) developing conceptual frameworks; ii) depicting spatial and temporal distribution of sediment source and sink areas (morphological approach); iii) developing sediment connectivity indices (geomorphometric modelling); iv) using and developing models (based on existing or new software); v) investigating sediment delivery likelihood through a network analysis approach. Over 50% of the reviewed literature in Najafi et al. (2021b) calculates connectivity indices, with the Index of connectivity proposed by Borselli et al. (2008) and its subsequent modifications being the most widely adopted, as reported by Shi et al. (2025). Approximately one-fifth of the studies employ morphological approaches, while alternative methods are less commonly applied. Similar studies have begun to address the explicit link between erosion and sediment connectivity and to understand how geomorphological processes are fundamental to accurately estimating the sediment yield of a river basin. More recently, La Licata et al. (2025) introduced a model (named HOSTED) that clearly and explicitly integrates all the above-mentioned components, delivering as output a single and comprehensive raster map. This GIS-based model was designed for assessing potential hotspots of sediment dynamics at watershed scale, integrating geomorphic spatial information with both structural and functional properties of connectivity.

In the present work, a semi-quantitative GIS-based procedure is proposed that assesses the sediment availability within a hydrographic basin combining three morphometric indices - the Stream Power Index (SPI, Abu El-Magd et al., 2021; Chowdhury, 2023), the Index of connectivity (IC, Borselli et al., 2008), and the Stream Length-Gradient Index (SL, Troiani et al., 2014) - starting from the geomorphological characterisation of the study area. The method has been developed to identify sediment supply areas and evaluate their coupling with

the drainage network. It explicitly includes a linear morpho-hydraulic component (SL and longitudinal profile analysis), which contributes to the interpretation of in-channel energy and sediment transfer processes. The method was tested to study on a central Apennines basin (Italy), which was severely affected by the 15 September 2022 flood, taking advantage by comparing pre- and post-event data. The combination of morphometric and topographic indices allowed the recognition of sediment source zones, transport corridors, and depositional areas.

A rainfall event occurred in September 2022 with intense and sudden magnitude, it struck violently mainly two river basins: the Burano basin, where the highest rainfall intensity was recorded in Cantiano, and the Misa basin. Misa basin is mostly characterized by the less permeable arenaceous and clayey rocks of the Argille Azzurre formation (Corti, M., et al., 2024) and even though it recorded a lower accumulated amount, it showed damage distributed along its path to the sea. The Misa river basin has been the subject of study by various institutions and Universities (Corti, M., et al., 2024, Confuorto, P., et al., 2025, Brenna, A., et al., 2025). Due to its small size and limited anthropogenic influence, the Burano basin has not been studied previously, which is why it was chosen as the study basin. The most significant damage occurred in the small town of Cantiano, which is why the study focused on observing the processes of movement and transfer of solid material in the upstream part of the town. This event triggered numerous landslides, widespread hillslope erosion, and severe flooding in the valley floors. The transfer of material between the slopes and the river network was intense and complex due to the mountainous conformation of the area and the varied geological composition. This approach was developed and tested a 92 km² fluvial basin. Although it has a very similar approach to that used by Licata et al. 2025, it differs from the above-mentioned work in terms of i) simplicity of the procedure; ii) fewer factors involved and greater fluidity; iii) difference in the erosion model; iv) a linear analysis performed on the grid is added to the method; v) the final maps are not combined together, introducing errors, but simply interpreted by a scientific heuristic method; and vi) multiscale approach, from the concept of the hydrographic basin and evaluation of the slopes, we move on to the hydrological system, narrowing the field. Using a pre-event digital terrain model, the marks left on the ground by this event were used to test the validity of the method. Owing to the availability of high-resolution post-event data, the validation process was conducted with a high degree of precision.

2.2 Study area

Geographical and climatic characteristics

The study area is located in the Northern Umbria-Marche Apennines (Central Italy), close to the boundary between the Umbria and Marche regions at about 50 km from the Adriatic coast (Fig. 1). This is a predominantly mountainous sector of the Marche Apennines, whose slopes decrease in the east direction towards the Adriatic coastline to turn into hills that gently decrease towards the littoral zone. The most imposing relief is the Catria mount (1701 m a.s.l.; Fig. 2), part of a complex structure of almost parallel orographic lineaments in the N/NW-S/SE direction. The climatic characteristics of the territory are influenced to the east by exposure to the Adriatic Sea and to the west by the presence of the Apennines, which obstruct the course of the western atmospheric currents, predominant in the local latitudes (Amici and Spina, 2002). Distance from the sea, altitude,

morphology, and exposure of the valley slopes are the most important geographical factors that define the climatic conditions. However, there may be variations in trends due to local influences. The climate of the study area can be classified as Mediterranean along the coastal zones, characterised by mild winters and hot summers. As elevation increases toward the Apennines, the climate transitions progressively toward continental conditions—with greater temperature swings and increased cold during winter months (Soldini and Darvini, 2025). In the low hills and intermediate terrain between the coast and the mountains, the climate exhibits traits of sub-Mediterranean transitional zones, reflecting gradual changes in temperature, precipitation, and daily range across the east-west gradient (Soldini and Darvini, 2025). According to the Köppen's classification system (Köppen, 1936), the territory is classified as having a moderate climate (class C). In particular, the climate can be identified with the sub-category Cfb (Latini, 2018), which is characterised by average annual temperatures varying between 13° and 10°, a temperature range that reaches 14°-15°, and annual rainfall that oscillates between 1000 and 1500 mm. From the rain gauge close to the Catria mount, an average annual rainfall of 1,291 mm has been estimated from the available data from 1951 to 2024 (Marche Region, 2022).

From a hydrographic point of view, the rivers flow from west to east, with the Metauro being the longest river (121 km) (Gentilucci et al., 2020). The study area chosen for this research includes the upstream part of the Burano basin, whose closing section is located downstream of the built-up area of Cantiano. Before the end of the study area, there are two points where the main tributaries of the Burano converge, the Bevano and Tenetra streams, which cross the underground of the historic centre. Since these three sub-basins have different hydrological responses and different effects on the territory, their main characteristics are sometimes considered separately and compared throughout this paper (Fig. 1).

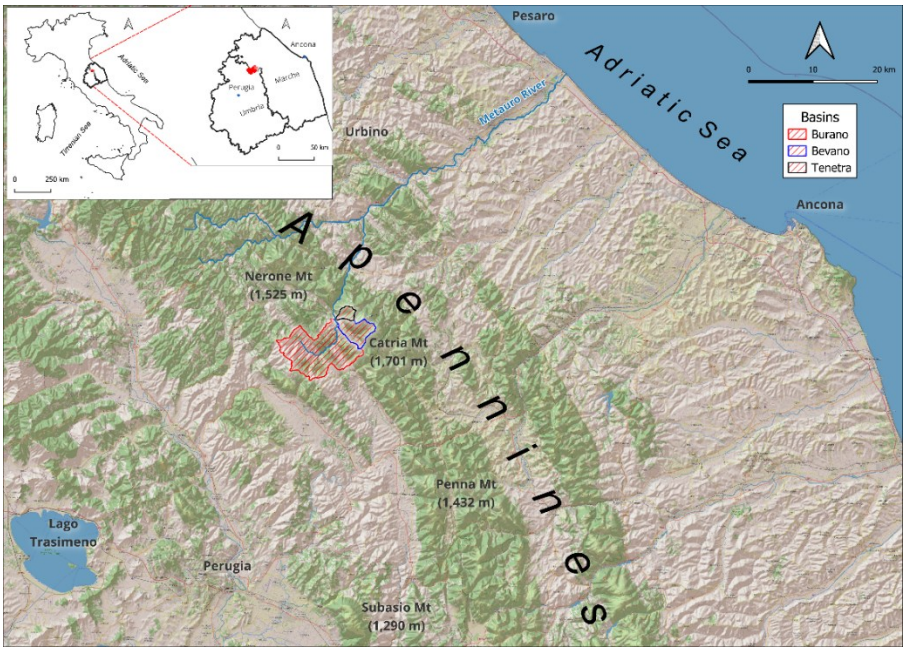

Fig. 1. Geographical location of the study area in the inner sector of the Northern Apennine Range. The three sub-basins are marked with differently coloured boundaries.

2.3 Geological setting

The study area is part of the Northern Apennines, a northeast-verging fold-and-thrust belt (Scisciani, 2009; Barchi et al., 2012). The outcropping lithological units in the investigated area belong to the Umbria-Marche succession and span a time interval from the Jurassic to the middle-upper part of the Neogene (Fig. 2). The westernmost Burano basin differs from the Bevano and Tenetra basins in terms of the type and age of the outcropping lithostratigraphic units.

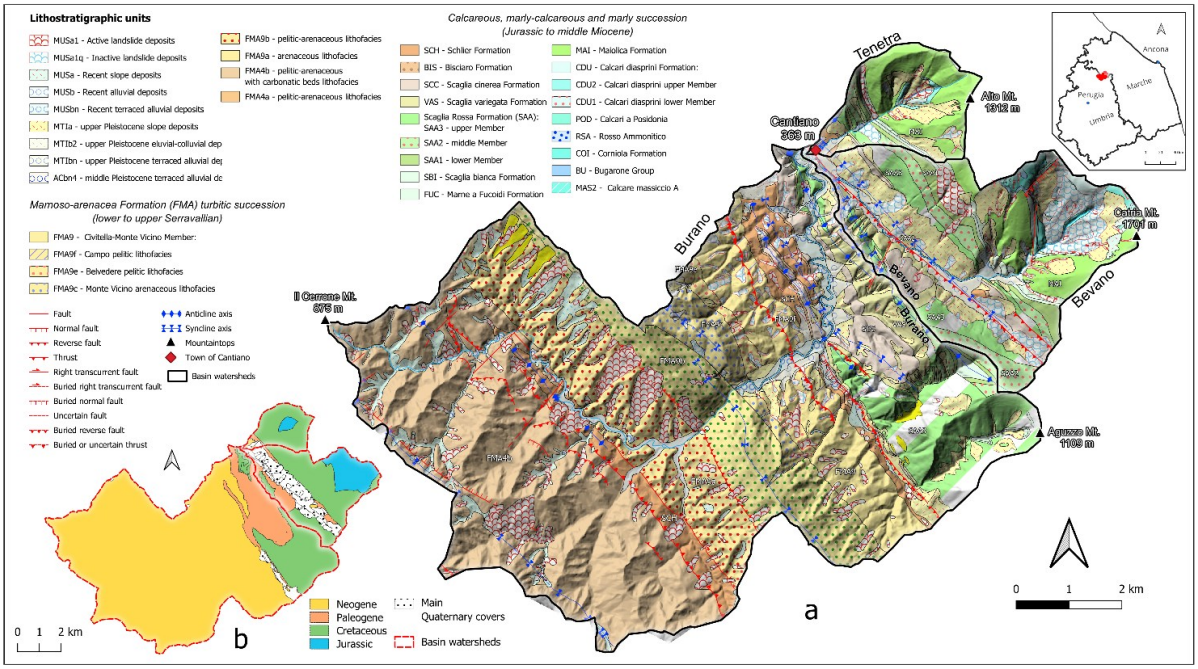

Fig. 2. a) Geological map with the lithostratigraphic units derived from the official Regional Geological Cartography of Marche and Umbria regions (CARG project 1996-2003); b) Synthetic geological scheme highlighting the differences in type and age of the lithologies between the two north-eastern basins of Bevano and Tenetra, containing Jurassic-to-Paleogene carbonate-marl units, and the more extended Burano basin containing predominantly Neogene siliciclastic-terrigenous units.

They also have different areal extents, the largest of which (Burano) includes predominantly Neogene siliciclastic-terrigenous units and a less extensive eastern portion adjacent to the other two basins, characterised by Cretaceous-to-Paleogene carbonate-marl units. The other two, less extensive river basins include Jurassic-to-Paleogene exclusively carbonate-marl lithostratigraphic units (Fig. 2b).

The different lithological characteristics of the upper Burano basin and its two tributaries make some of them more prone to producing material. In particular, the upper part of the Burano, upstream of Cantiano town, and the transition zones between one basin and another present materials with a higher degree of erosion, which tend to disintegrate into very fine grains similar to sand and/or silt. In this area, landslides have often been attributed to the debris flow landslide type. On the contrary, the two secondary basins, located at the foot of the main anticline, are much more consistent, with low degrees of erosion and the characteristic of producing material mainly by falling or due to the erosion of a large amount of water flow. Within the Tenetra basin, there is a layer called “fucoid marl,” which is more erodible and produces sediments comparable to flattened pebbles. A large landslide with a significant accumulation at the base has formed on this channel, which was already

present before the event. This paragraph does not take into account the deposits present before the event, but only the type of lithological composition.

This is reflected in the geomorphology of the territory, characterised by generally steeper slopes and more significant height differences in the two smaller basins compared to those of the larger basin (for more details, see section 4.1). Further, the distribution and areal proportion of the landslide types surveyed after the 15 September 2022 extreme event (Santangelo et al., 2023) seem to depend on the lithotypes occurring in the three basins and the type of slope detritus, which is abundant where predominantly carbonate terms crop out.

The lithological units are intensely fractured and contribute to the development, within the hydrographic basin system, of a dual-circuit groundwater network, which sustains baseflow even during dry periods. Structural lineaments trending NW–SE and SW–NE exert a strong control on both surface and subsurface hydrological dynamics, influencing the distribution of the springs and the orientation of the drainage network (Nanni and Vivalda, 2009; ISPRA-CARG, 2009). The combination of steep slopes, lithological variability, and tectonic complexity results in a highly sensitive landscape to geomorphological processes such as erosion, shallow landslides, and fluvial adjustments.

2.4 The 15-16 September 2022 pluviometric event

On the evening of 15 September, a V-shaped, stationary and self-regenerating thunderstorm was formed in the Apennine chain of central Italy from storm cells originating on the Tyrrhenian side of the peninsula after becoming loaded with moisture during their path. Such a physical condition originated from a warm and humid mass of air moving from North Africa, and simultaneously by the development of some air convective systems favoured by the presence of humidity coming from the Tyrrhenian Sea and by the orography of the peninsula and its largest islands (Morelli et al., 2023). The event led to high precipitation amounts in a very short time (Table 1). It resulted in widespread criticality in the mountain areas of the basins on the eastern slopes of the Apennine chain and along some main courses up to their mouth (Fig. 3). The highest cumulated rainfall value was recorded at the rain gauge of Cantiano, with 419 mm in 12 hours (Table 1; Donnini et al., 2023), resulting in one of the most conspicuous events in the recording history of this area. Then, in the subsequent transit towards the coastal areas of the Adriatic Sea, the storm system gradually weakened, losing intensity and progressively depleting. The pluviometric event covered a total area of 5,000 km^2 (Santangelo et al., 2023).

Table 1

Cumulative precipitation in mm of the 15th-16th Sep 2022 event, measured by rain gauges of 9 stations located in the basins affected by the rainfall event: maximum measurements at 1, 3, 6, 12 and 24 hours (Marche Region, 2022). Averages of annual extremes at the rain gauge in Cantiano (PU), which has a historical series of 71 years of records.

RAIN GAUGE		BASIN	*1 HOUR*	*3 HOURS*	*6 HOURS*	*12 HOURS*	*24 HOURS*
	Cantiano	*Burano*	101.4	256.6	384	419	419
Cantiano	*Average Intensity in the Hour Interval (mm/H)*		101.4	85.5	64	34.9	17.5
	Long-Term Average		26.5	37.7	8.8	66.6	88.7

ano						
Monte Acuto	*Cesano*	107.2	248.4	343.0	384.2	384.4
Arcevia	*Misa*	47.0	94.8	117.8	128.8	129.2
Barbara	*Misa*	50.8	111.4	121.2	127.0	127.2
Colle	*Misa*	77.4	162.4	186.4	204.0	204.0
Sassoferrato	*Sentino*	-	62.8	99.8	99.8	100.4
Colleponi	*Sentino*	42.4	68.0	122.0	122.2	122.6
Monte San Vicino	*Musone-Esino*	65.8	108.2	120.0	192.8	193.6
Cingoli	*Musone*	93.6	160.4	184.6	247.2	247.6

Table 1 shows the data recorded by rain gauges distributed throughout the Marche region. The first three rows are associated with the Cantiano sensor and therefore refer to the Burano Basin, the river under consideration. The first row shows the millimetres of water measured, the second the intensity in mm/h and the last one the long-term average trend defined by the historical series of this station. There are no other sensors, and these data are considered valid for the Burano basin upstream of Cantiano and for its two minor tributaries that flow into it laterally. Below the rows defining the values for Cantiano, we find a comparison with other rain gauges that recorded the same event in different river basins. The Misa and Cesano rivers suffered extensive damage as a result of the same extreme event.

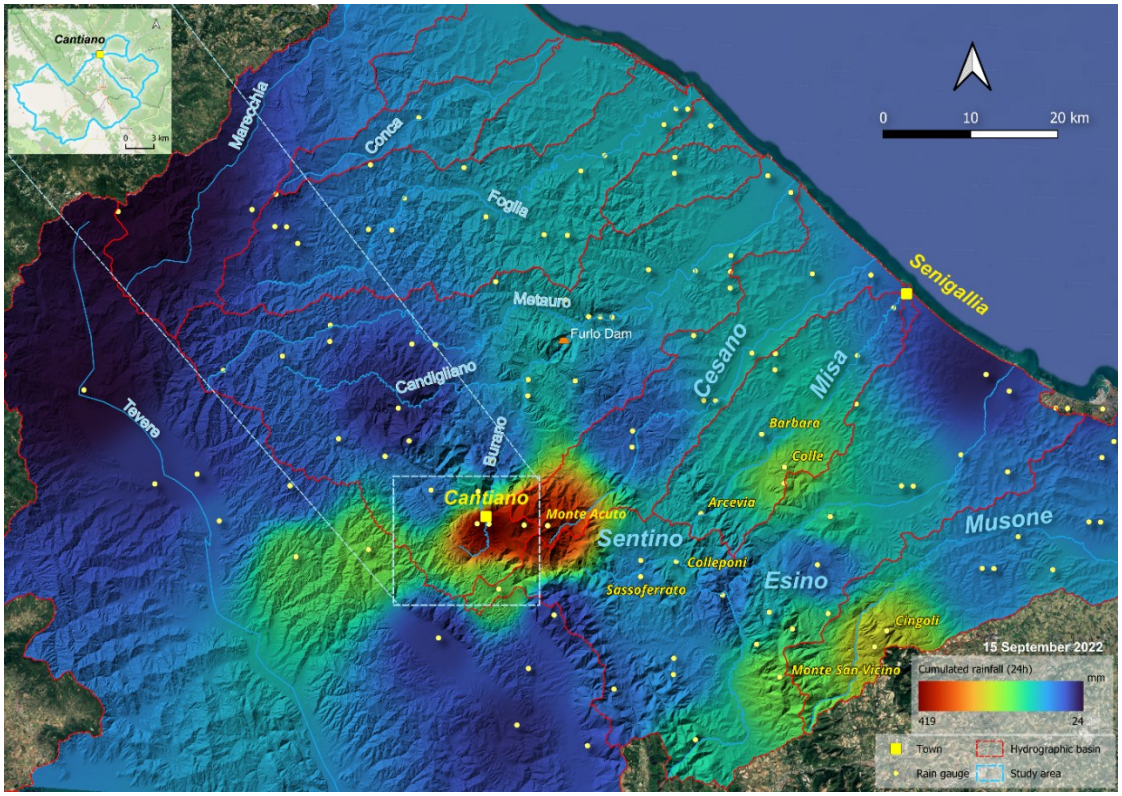

Fig. 3. September 2022 rainfall distribution concerning the main watercourses and related hydrographic basins. The position of the two most affected urban areas is highlighted (Senigallia is the most affected city in the plain area by the flood wave coming from upstream).

Before the thunderstorm, the soil was substantially dry after a long summer drought. Rainfall network data show no significant precipitation within the 30 days before the event. Only about 61.4 mm cumulative between August 15 and September 1 and just a few mm in the first 15 days of September were recorded from the pluviometer of Cantiano (RT-2972) of the Civil Protection Marche.

The combination of this aspect with the amount of rainfall led to the rapid rise in the hydrometric levels of the Burano river course and its tributaries. Sudden and destructive floods were triggered, leading to numerous landslides phenomena that contributed significantly to the downstream solid transport, although widespread residual risk conditions persisted along the slopes (Donnini et al., 2023).

The town of Cantiano was one of the areas affected the most by floods. In a very short time, the local riverbeds were crossed by large, turbulent flows and filled up by transported solid load, quickly exceeding the containment limit and overflowing uncontrollably. Many buildings in the historic centre were flooded by water, mud and debris and the urban paths of the watercourses were severely damaged, sometimes in association with connected sewers (Fig. 4). At the same time, the city became isolated due to landslides along the external main communication routes and bridge damage due to flooding activity and mass movements, even in combined action.

Fig. 4. Location of the effects of the high flow rates in the artificial stretch of riverbeds and sewer system within the built-up area of Cantiano. (a) pavement and road torn off by the overflowing water of the Bevano creek; (b) outlet of the underground river bed of the Tenetra stream and related material transported; (c) break in the sewerage network in front of the Municipality; (d) natural protections set up during the emergency; (e) breaking point of the culvert caused by the high hydraulic pressure created.

Several circumstances were primarily decisive in generating the critical issues of this site: i) the stationing of exceptional precipitation in the surrounding mountains over an arid terrain, ii) the local geology in its capacity to create debris, iii) the proximity, with its historic centre, to the confluence of two creeks (Bevano and Tenetra) with the main river (Burano) (Fig. 4), iv) the geomorphologic conformation of the reference water catchment areas and their natural hydraulic network (deeply discussed in section 4.1), and v) the response of hydraulic layout of urbanised stretches where the three watercourses converge (Fig. 4). The latter is a consequence of a historic anthropic activity intervening heavily on the original fluvial path and geometry that almost definitively cancelled out any character of naturalness and functional specificity over time (Morelli et al., 2023).

The Burano River was diverted in the upstream stretch of the town in the late 1920s through an 80 m tunnel (8 m wide and 9 m high) (Morelli et al., 2023) at a high angle to the original path (Fig. 5). The original course, consisting of a meander that ran alongside the town's ancient buildings on one side and the rocky slopes of a mountain relief on the other, was permanently blocked by a high wall and filled with material behind it. The upstream portion preceding the underground diversion work is confined between artificial masonry banks. The Bevano Creek, which originally passed through the middle of the current Luceoli Square in the city's centre, was diverted in the late 1700s about 50 m North into a confined (Morelli et al., 2023), narrow, recessed curving

path. The shape has remained unchanged until today. At the end of the 1950s, it was covered with concrete slabs for a length of 200 m, as the concept of hygienic safety was increasingly pressing. At that time, there was no complete sewerage network or purification system. Subsequently, some houses were also built on some parts of the covered areas. In the mid-1700s, the Palazzo del Conte was built above the Tenetra Creek, creating the first underground riverbed in this area. This closure, built in masonry with an arched vault, was then modified over time until its current size (which was about 57 m in length) and the urban downstream section was channelised up to the confluence with the Tenetra Creek, beyond which it was confined until reaching the Burano River in more recent times.

Fig. 5. (a) River stretch before the detour, flood damage can be seen; below is a destroyed bridge; (b) Burano detour tunnel as seen from the road; (c) hydrometric level reached homes near the detour area.

2.5 Methodology

A comprehensive methodology combining various types of spatial analyses is proposed to investigate the interplay between slope dynamics and the river network at the watershed scale, as well as the overall movement capacity of the removable terrain within this context. The procedure involves two main stages: the first is the detailed geomorphological characterisation of the area, including previous and post-event instability, and the second is a GIS-based spatial analysis to understand how instability processes are distributed and what rules they follow in relation to the main water course during extreme events. Fig. 6 shows the flow chart relating to the structured work model.

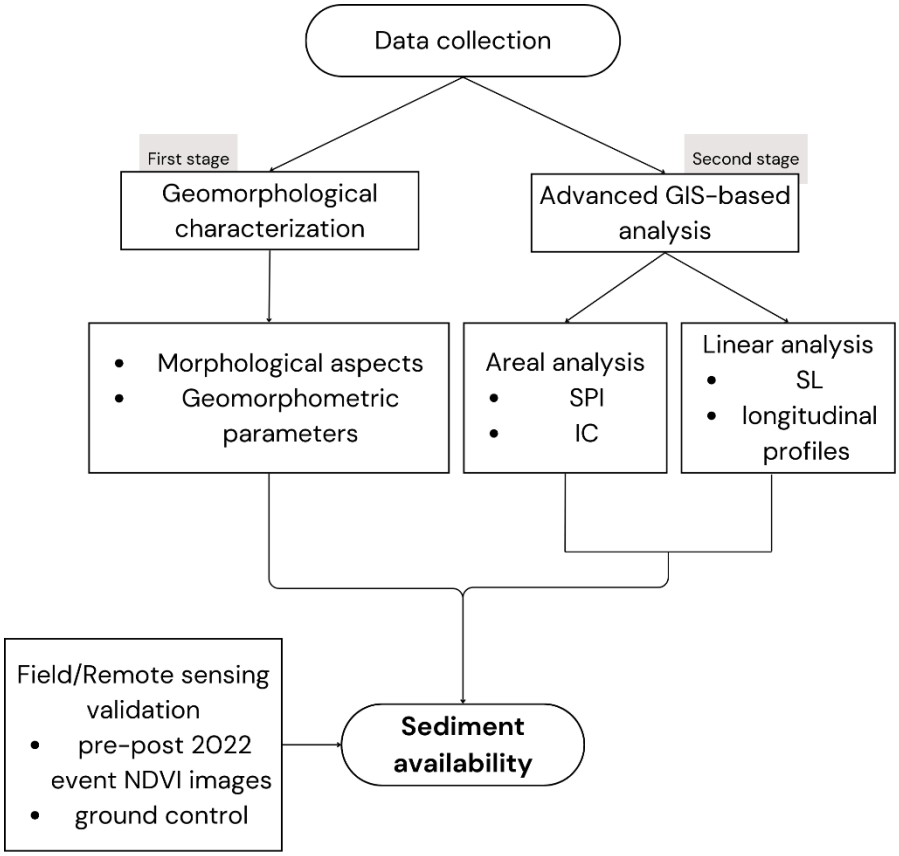

Fig. 6. Methodological flowchart highlighting all the steps of the applied procedure that lead to the sediment availability assessment validated by fields checks and remote sensing analysis

2.5.1 Geomorphological characterisation – morphological aspects

A detailed geomorphological map was arranged, basically including i) geomorphological complexes, corresponding to geological formations from the official Regional Geological Cartography (scale 1:10,000), grouped according to their degree of erodibility based on regionally different state of weathering, and adjusted based on observed hillslope conditions following the method of Moosdorf et al., (2018). In this approach, erodibility values are calibrated using real slope data for each lithology class to better represent the sediment production potential at the landscape scale. ii) Quaternary deposits extracted from the same source, and iii) existing and updated landslide distribution. The datasets corresponding to points i) and ii) represent a reasoned reprocessing of pre-existing information, whereas the dataset in point iii) is based on published inventories and has been verified through field inspections conducted as part of this study. A quantitative descriptive statistical analysis of the landslide inventory triggered by the 2022 extreme rainfall event (E-LIM database) was carried out to identify well-constrained sediment-mobilization areas, focusing specifically on the fraction of material with the highest mobility and runout capacity. Morphological features at all spatial scales were represented on the map as polygons when larger than 225 m2, and as points when smaller.

QGIS software (version 3.34.6) was used for this product following the guidelines indicated by the Italian Institute for Environmental Protection and Research of the Ministry of the Environment (Campobasso et al., 2021). A 10 m-resolution digital terrain model, called TINITALY DEM and released for free in the updated

version in 2023 by the National Institute of Geophysics and Volcanology, was used as a basic spatial datum (Tarquini et al. 2007; 2023; Tarquini and Nannipieri, 2017). Much data was inserted for landslides, available by catalogues with different information: the Italian Landslide Inventory with the characterisation type and other descriptive aspects (The IFFI Project, scale 1:25,000; Trigila et al., 2007; 2010; Trigila and Iadanza, 2008) and the 2022 post-event inventory (E-LIM Inventory, scale 1:15,000; Santangelo et al., 2023).

2.5.2 Geomorphological characterisation – geomorphometric parameters

From the river network and catchment layers, the main geomorphometric parameters (Table 2) were calculated in a GIS environment. Relief ratio (Rh), bifurcation ratio (RB), stream frequency (Fs) and drainage density (Dd) were used to parameterise the dimensional, morphological and topological properties of the drainage network and catchment areas. Rh expresses the overall relief energy of the basin and provides an indication of the potential for sediment mobilisation along slopes. RB describes the degree of branching of the drainage network, reflecting the efficiency with which runoff and sediment are channelled downslope. Fs represents the density of channels per unit area and therefore indicates the degree of hillslope dissection and the proximity of sediment sources to the fluvial network. Finally, Dd quantifies the total channel length per unit area and serves as a proxy for the capacity of the drainage system to intercept and convey sediments. Taken together, these morphometric indices provide quantitative measures of basin physiography and offer insight into the structural components that control sediment connectivity, thereby characterising the predisposition of the catchments to transfer sediments from hillslopes to the main channel.

Table 2
Methods and equations for the calculation of geomorphometric parameters (Shekar and Mathew, 2024).

Basin's morphometric parameters	**formula / description**
H *(m.a.m.s.l.)*	*Basin maximum elevation*
h *(m.a.m.s.l.)*	*Basin minimum elevation*
Lb *(m)*	*Basin length*
A *(km^2)*	*Basin Area*
P *(km)*	*Basin Perimeter*
Relief ***Bh***	*Bh = (H – h)*
Relief ratio ***Rh*** (Schumm, 1956)	*Rh = (Bh / Lb)*
Circularity ratio ***Rc*** (Miller, 1953)	*$Rc = (4\pi A / P^2)$*
Elongation ratio ***Re*** (Schumm, 1956)	*$Re = (2 [A / \pi]^{0.5}) / (Lb)$*
Gradient ratio ***Gr*** (Sreedevi et al., 2005)	*Gr = (a-b) / Ls*
Basin major stream's morphometric parameters	**formula / description**
a *(m.a.m.s.l.)*	*Major stream's source elevation*
b *(m.a.m.s.l.)*	*Major stream's mouth elevation*
Ls *(m)*	*Major stream's length*
Total Stream number ***Nu*** (Horton, 1945)	*$\sum Nu_n$ (Nu_n stream number of the $_n$ order)*
Total Stream length ***Lu*** *(km)*	*$\sum Lu_n$ (Lu_n stream length of the $_n$ order)*
Bifurcation ratio ***Rb*** (Horton, 1945; Strahler, 1964)	*Rb = (Nu / Nu + 1)*
Stream frequency ***Fs*** (Horton, 1945)	*Fs = (∑ Nu) / A (A area of the basin)*
Drainage density ***Dd*** (Horton, 1932)	*Dd = (Lu) / A*

This analysis was used to preliminary define the spatial and typological availability of sediments. By overlaying these layers within a GIS environment, the intersection of the different parameters highlights locations where predisposing factors co-occur, delineating hotspots that are most prone to sediment availability and potential mobilisation. These critical areas are typically associated with zones of flow acceleration, hydraulic jumps, and topographic convergence, where water and sediment are preferentially concentrated. The areal GIS analysis made use of these information as a basis for controlling the results.

2.5.3 Advanced GIS-based analysis – areal assessment

This first stage of analysis characterised the entire catchment area, understanding the physical connections of removable sediment material inside it to the primary channel network and the link between the power of flowing water and the soil erodibility. The second one focused on the examination of the main river paths, with outputs referring only to the river line. For the spatial analyses, a 10 m-resolution digital terrain model, called TINITALY DEM and released for free in the updated version in 2023 by the National Institute of Geophysics and Volcanology, was used as a basic spatial datum (Tarquini et al. 2007; 2023; Tarquini and Nannipieri, 2017).
In particular, the basin analysis envisaged the assessment of two morphometric indices:

- Stream Power Index (SPI), based on modified Abu El-Magd's equation (Abu El-Magd et. al., 2021), using ArcGis Pro version 3.3 to compute it.
- Index of Connectivity (IC), based on Borselli's original equation (Borselli et al., 2008), using a modified equation from (Cavalli et al., 2013) in the SedInConnect software (free, open-source and GIS-independent stand-alone tool (Crema and Cavalli, 2018).

Moreover, a linear analysis along rivers was performed the Stream Length Gradient Index (SL) of Piacentini et al. (2020) was selected as the morphometric index, and it was determined by using the equation provided by Hack (1973). Subsequently, this was compared with the geometric information derived by the river-long profile observation in the digital model using a QGIS plugin to generate topographic profiles (qProf). While the first analyses the average course of small sections chosen a priori in length, the second highlights the minor imperfections of the profile, such as sudden hydraulic jumps.

Stream Power Index (SPI)

SPI is one of the most popular attributes that can be calculated with single- and multiple-flow direction algorithms and it is based on the assumption that discharge is proportional to the specific catchment area (Wilson, 2012). SPI is conceptualised to visualise potential flow erosion and its relationship to landscape processes in the entire basin. The SPI regulates the potential erosive force of water flow and describes the potential for flow erosion at the specified surface point (Moore et al., 1991), to determine how regions with topographic potential for erosion and deposition are spatially distributed in a complex terrain.
The SPI concept (Moore et al., 1991) is expressed in the following formula:

$$SPI = SCA * \tan \beta \quad (1)$$

Where SCA is the specific catchment area, while β is the slope expressed in radians.

The SPI is obtainable from GIS using the tool "Raster calculator". The hydrological modelling tools integrated into ArcGIS Pro derive flow direction, flow accumulation, and slope functions from the DEM. Eq. (2) results from applying the variant (Abu El-Magd et al., 2021; Chowdhury, 2023). *0.001* is a constant introduced into the logarithmic function to reduce extreme values and handle values close to zero. In this case, the slope is in degrees, and division by 100 facilitates multiplication using the logarithm. The logarithmic function is applied to the first factor so that their distribution would more consistently reflect the trend; the slope contribution is kept in linear form (after a simple normalisation) to represent its impact in the SPI adequately.

$$SPI = Ln\ (As + 0.001) * (\beta/100 + 0.001) \quad (2)$$

Where *As* is the basin flow accumulation, β is the basin slope, and "*Ln*" is constant refers to the Napierian logarithm. The flow accumulation demonstrates regions that contribute to the overland flow (Abu El-Magd et al., 2021). This formula represents a valid empirical simplification that proves to be more compliant for workflows in a GIS environment.. The SPI determines the erosive power of the channel and expresses the topographic potential for deposition (for low or negative values) and erosive areas (positive values).

Index of Connectivity

The IC for sediment transport measures how easily sediment can be transported from one part of a landscape to another, often considering factors like slope, land cover, and drainage network. In particular, the IC index is used to calculate the structural morphometric connectivity of sediments. For each raster cell the degree of connection that controls sediment flows across the landscape is calculated by the SedInConnect software (Crema and Cavalli, 2018). The IC shows the potential connection between sediments eroded from hillsides in relation to a selected target feature, which is the main hydrographic network in this case study. Within the same watershed, each point (pixel of the basin) yields a probability value ranging from negative to positive infinity, while the target feature defined in the model determines the connectivity configuration (Cavalli et al., 2013). Providing a shapefile containing the sinks to be emphasised, the model ignores all the sub portions of the DTM which are not draining into this feature, excluding them from the computation (Crema and Cavalli, 2018). In this work the target was used in order to focus the analysis on the lateral slope to the main network, thus making it possible to distinguish smaller connective channels. This was represented by a linear shapefile with a buffer of 20 m on the main river, 10 m on its tributaries, and 5 m on less developed high-altitude watercourses. Therefore, maximum attention was given to the slopes by observing where high connectivity values were detected.. River flow and sediment may be connected as indicated by IC from Borselli et al. (2008) (Eq. 3). Specifically, it functions at the area level by comprehending the flow of material from the slope-based source areas to the main river course, which represents the zone of maximum depression in the topographic model. The following equation considers two primary factors: upslope and downslope (*Dup* and *Ddn*, respectively, in Eq. 3). The upslope factor is the potential for downward routing of the sediment-produced upslope. The downslope factor considers the distance a particle needs to travel to enter the drainage region. Since IC was defined in the

range of [−∞, +∞], the connectivity increases for larger IC values (Cavalli et al., 2013). The probability that the particle will end up in the main river course is more significant the shorter the distance to it.

$$IC = \left(\frac{Dup}{Ddn}\right) \quad (3)$$

SedInConnect (Crema and Cavalli, 2018) tool computes the IC index using the TAU DEM algorithm (Terrain Analysis using DEM). The software employs the Borselli equation, offering the flexibility to select some different input factors . In the modification made by Cavalli et al. (2013) a factor called W was added instead of the C factor based on soil classification, and it represents the flow impedance factor defined by the roughness of the surface. The choice to include the W factor is given by the morphological characteristics mentioned above and the minimal anthropogenic influence that makes land use non-descriptive and differentiated. Roughness is a factor that best describes areas with significant differences in slope over an area like the studied one, making it more suitable for the case. The W factor is extracted from the topographic model. The parameters required for processing were therefore the DTM, roughness and a selected target represented by the river segment of the entire drainage system derived from DTM hydrological extraction. On the other hand, vegetation (present here as "land use" data) is essentially homogeneous across the sectors of interest, with minimal differences for the study aims. Therefore, since it does not exhibit a distribution that could lead to different influences, it was excluded from the analytical considerations.

2.5.4 Advanced analysis GIS-based – linear assessment

Stream Length Gradient Index (SL)

The linear analysis was carried out by making longitudinal profiles and using them in SL (Troiani et al., 2014). The latter analyses the most significant topographic variations along the river path as the morphological footprint of surface and subsurface processes. This index strongly relates to the hydraulic gradient, often indicating a perturbation along the river course. SL is a proxy for stream power per unit length and is proportional to the total stream power available at a particular reach (Summerfield, 1991, Pérez-Peña et al., 2009). The index was developed in a GIS environment through an ArcGIS tool. DEM is the only input source of data, and the measurement unit of the output is the metre. In the practical procedure, points at known distances were inserted on the linear river element. The elevation value was interpolated on each of these points, and the equation described below was applied. From the literature (Troiani et al., 2014) for comparable sites with a small catchment area and a torrential character, typical of predominantly mountainous stretches like in the study area, the ΔL value in Eq. 3 that provided results with more accuracy is the distance of 50 m. This distance makes the tool efficient. This value is highly dependent on the size of the study area and, therefore, on the detail and precision of the pixels in the topographic model. With this analysis value, it was observed that fewer errors were introduced. Eq. 3 (Piacentini et al., 2020) was used to identify significant deviations from the concave-up shape of river longitudinal profiles of bedrock streams within mountainous catchments by highlighting the values of differential anomalies defined over the entire reticulum. *Knickzone* and *knickpoint* are the names given to these anomalies on the map. Usually, they can be attributed to a variety of features, the most significant ones being:

i) lithological differences in the substrate (geology), ii) the existence of a tectonic structure (tectonics), iii) the existence of a landslide in the riverbed (morphological evolution).

$$SL = \Delta H * L / \Delta L \quad (3)$$

where ΔH is the variation of elevation between two points of the stream channel, ΔL is the distance between the two points, and L is the total channel length from the channel initiation (Piacentini et al., 2020).

The first output of the SL model is represented by a set of point values. Therefore, following the suggested classification of Piacentini et al. (2020) it was considered the quartile distribution for the subdivisions in classes representative of the different possible erosional dynamic. Therefore, in this case a graded symbolism was set up to visualise five classes and distinguish the higher ones. This method divides the attributes into bins with the same number of features. The points with the highest values of steepness anomaly, here contained in last class (V class), are characterised by a light purple colour.

2.5.5 Validation method

The information acquired after the 2022 event made it possible to validate the model's results. The validation of the results obtained was carried out using two approaches. The first included a remote verification analysis using optical multispectral satellite images aimed at characterising the situation prior to the event. It was decided to use NDVI (Normalized Difference Vegetation Index) images downloaded from Planet (Planet Team, 2022), which represent a graphical indicator for the analysis of measurements obtained from satellite remote sensing. PlanetScope provides up to 3 m multispectral imaging with daily revisits and is made up of many CubeSat (Doves and Super Doves) flights in sun-synchronous orbit. The earlier-generation Dove satellites (Standard PlanetScope) gather multispectral imagery in four bands: blue, green, red, and near-infrared. Launched since 2020, SuperDoves (upgraded PlanetScope satellites) provide 8-band multispectral imaging with calibrated and smaller bands in the wavelength range of 430–860 nm. By carefully selecting two days, one before and one after the event, with 0 cloud cover, it was possible to assess the changes in terms of vegetation variations in just a few days. Planet images are supplied already orthorectified and radiometrically calibrated with corrected reflectance. The bands used were red and NIR (Confuorto et al., 2025). A formula that measures the difference between near-infrared (NIR) and red light reflectance is used to generate the Normalised Difference Vegetation Index (NDVI), which quantifies vegetation. NDVI is calculated as follows: (NIR - Red) / (NIR + Red). Similar to other satellite data, planet imagery can be used to compute NDVI, which offers information on the density and health of the vegetation. NDVI change detection was performed to localise landslides occurred, where the vegetation on the slope is removed or partially destroyed, leading to a decrease of NDVI value (Confuorto et al., 2025). The software chosen for use is ENVI (Environment for Visualising Images).

The second methodology adopted a conventional framework. Utilizing a heuristic approach, the most critical areas were identified through terrestrial and UAV photogrammetry. Subsequently, pre-defined control points, deduced from the final map, were compared against these findings for validation. A fundamental component of this study involved also benchmarking the predictive results against the spatial distribution of landslides triggered during the 2022 extreme weather event, as documented in the E-LIM Inventory.

2.6 Results

2.6.1 Geomorphological characterisation - morphological aspects

Based on the classification criteria defined by ISPRA (Campobasso et al., 2021), four lithological complexes were identified within the study area: pelitic-arenaceous, marly-mudstone, limestone-anhydrite, and arenaceous rocks. Each unit corresponds to a distinct geomorphological complex, represented by a specific background colour on the drawn geomorphological map (Fig. 7). This representation constitutes the basis on which the various specific thematic levels were subsequently superimposed. Regarding the post-event landslides, the E-LIM inventory provided the exact mapping of 351 landslides physically reachable during a field survey or visible from observation points on the ground.. Of the total number of landslides digitised after the event 156 polygons and 195 points are located, and 50 % of them are attributable to the earth slide type, 15% to the debris flow type, 10 % to the debris slide type, 11 % to the earth slide-flow type, 7 % to the debris slide-flow type, 6 % to earth flow type, and 1 % to the rockfall and rockslide types according to Hungr et al. (2014) classification. The events with the highest number of occurrences (earth flow/slide) are in the western part of the catchment area due to the local lithology. On the contrary, around Cantiano, debris flows, debris slides and rockfalls are more frequent due to the main limestone composition.

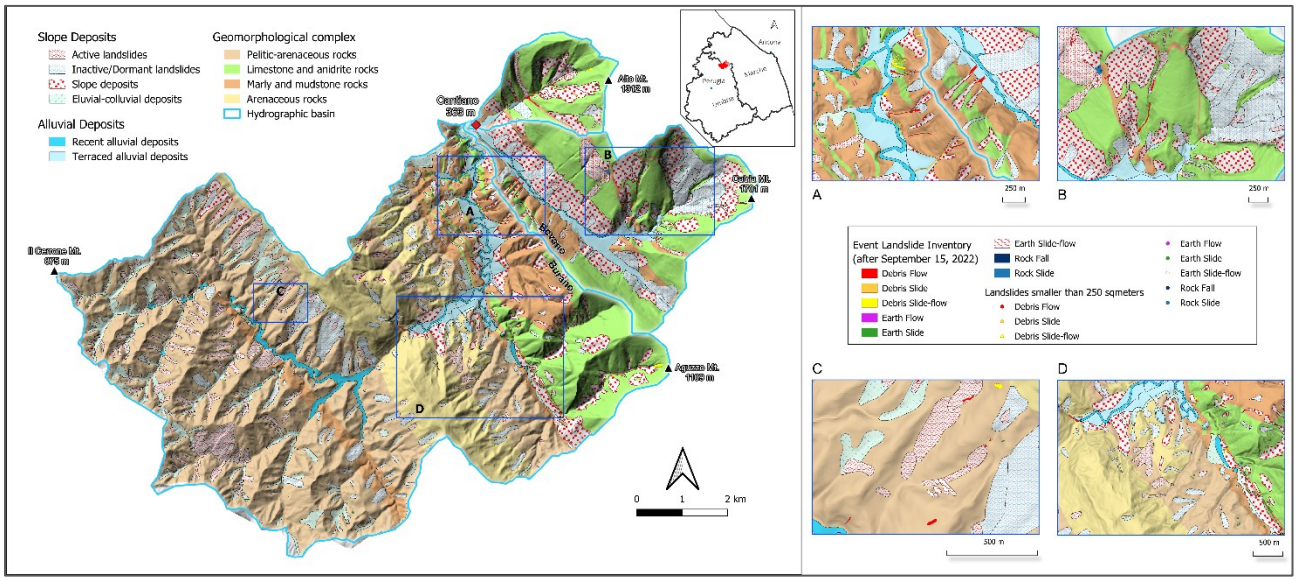

Fig. 7. Geomorphological map to understand sediment production (left), images from A to D (right), zoom on different sectors of the basin (see the left map for the position) where the small landslides inventoried by E-LIM are visible in detail.

2.6.2 Geomorphological characterisation - geomorphometric parameters

Geomorphometric parameters for characterising the basins' geomorphology and comparing the dynamic characteristics of their drainage patterns are listed in Tables 3 and 4 (Shekar and Mathew, 2022). The parameters defining the drainage texture (*Nu*, *Lu*, *Fs* parameters in Table 4) denote numerous shorter streams for the Burano basin compared with the stream patterns of the Bevano and Tenetra basins. This could be related to the less permeable bedrock of the basin, which is characterised by a significant surface runoff compared to the other basins. The drainage density (*Dd*) values of the Bevano and Tenetra basins (Table 4) can be mainly related to relief ratio (*Rh*) values higher than those of the Burano basin (Table 3). The latter parameter quantifies the

topographic evidence that the Bevano and Tenetra basins are shorter with higher gradients than the Burano basin. Lastly, the lower circularity (*Rc*) and elongation (*Re*) ratios' values of the Burano and Bevano basins (Table 3) indicate a lower propensity for runoff, erosion and sediment transport; on the contrary, the more 'oval-circular' shape of the Tenetra basin implies a greater concentration of flows and therefore a greater likelihood of runoff with energetic flows and thus may imply sediment transport. The much lower value of the slope ratio (*Gr*) of the Burano River confirms its lower sensitivity to runoff and a higher probability of flooding of flat areas due to a decrease in the system's energies, which in turn leads to a deposition of material.

Table 3
Basin's morphometric parameters calculated to characterise and compare the hydrological behaviour of the three basins. Abbreviations and definitions of the morphometric parameters are provided following Shekar and Mathew (2024).

Basin's morphometric parameters	**Burano**	**Bevano**	**Tenetra**
H *(m.a.m.s.l.)*	**1,101.36**	**1,701.53**	**1,319.90**
h *(m.a.m.s.l.)*	**360.15**	**360.16**	**360.37**
Lb *(m)*	**30,964.67**	**7,679.06**	**3,521.53**
A *(km^2)*	**102.93**	**20.69**	**6.25**
P *(km)*	**43.80**	**19.74**	**9.35**
Relief ***Bh***	**741.21**	**1,341.37**	**959.53**
Relief ratio ***Rh*** (Schumm, 1956)	**0.02**	**0.17**	**0.27**
Circularity ratio ***Rc*** (Miller, 1953)	**0.67**	**0.67**	**0.90**
Elongation ratio ***Re*** (Schumm, 1956)	**0.37**	**0.67**	**0.80**
Gradient ratio ***Gr*** (Sreedevi et al., 2005)	**0.03**	**0.11**	**0.25**

Table 4
Stream's morphometric parameters calculated to characterise and compare the drainage patterns of the three basins. Abbreviations and definitions of the morphometric parameters are provided following Shekar and Mathew (2024).

Basin major stream's morphometric parameters	**Burano R.**	**Bevano C.**	**Tenetra C.**
a *(m.a.m.s.l.)*	**874.00**	**1,225.00**	**1,225.00**
b *(m.a.m.s.l.)*	**350.00**	**360.00**	**350.00**
Ls *(m)*	**20,467.00**	**7,679.10**	**3,521.50**
Total Stream number ***Nu*** (Horton, 1945)	**5,153.00**	**876.00**	**220.00**
Total Stream length ***Lu*** *(km)*	**507.46**	**126.82**	**30.75**
Bifurcation ratio ***Rb*** (Horton, 1945; Strahler, 1964)	**1.95**	**1.89**	**1.67**
Stream frequency ***Fs*** (Horton, 1945)	**50.03**	**41.71**	**36.67**
Drainage density ***Dd*** (Horton, 1932)	**4.93**	**6.04**	**5.12**

2.6.3 Advanced GIS-based analysis – Stream Power Index Map

The graphic representation of SPI identified those areas where the erosive effects of surface runoff could be concentrated (Fig. 8). It describes the ability to load and transfer the sediment throughout the hydrological basin; in addition, the SPI was used to assess the flash flood risk in stream channels (Abu El-Magd et. al., 2021). Areas with high SPI values are those where the flow accelerates, increasing the potential for removal. These areas are mainly concentrated in the impluvia, where the slope and convergence increase. The SPI of the Burano basin ranges from −4,59448 to +4,99374. A pixel statistical analysis was used to establish a quantification of the spatial range. A calculation was conducted based on the three catchment basins, excluding values less than +1 from the raster to isolate the most vulnerable places.

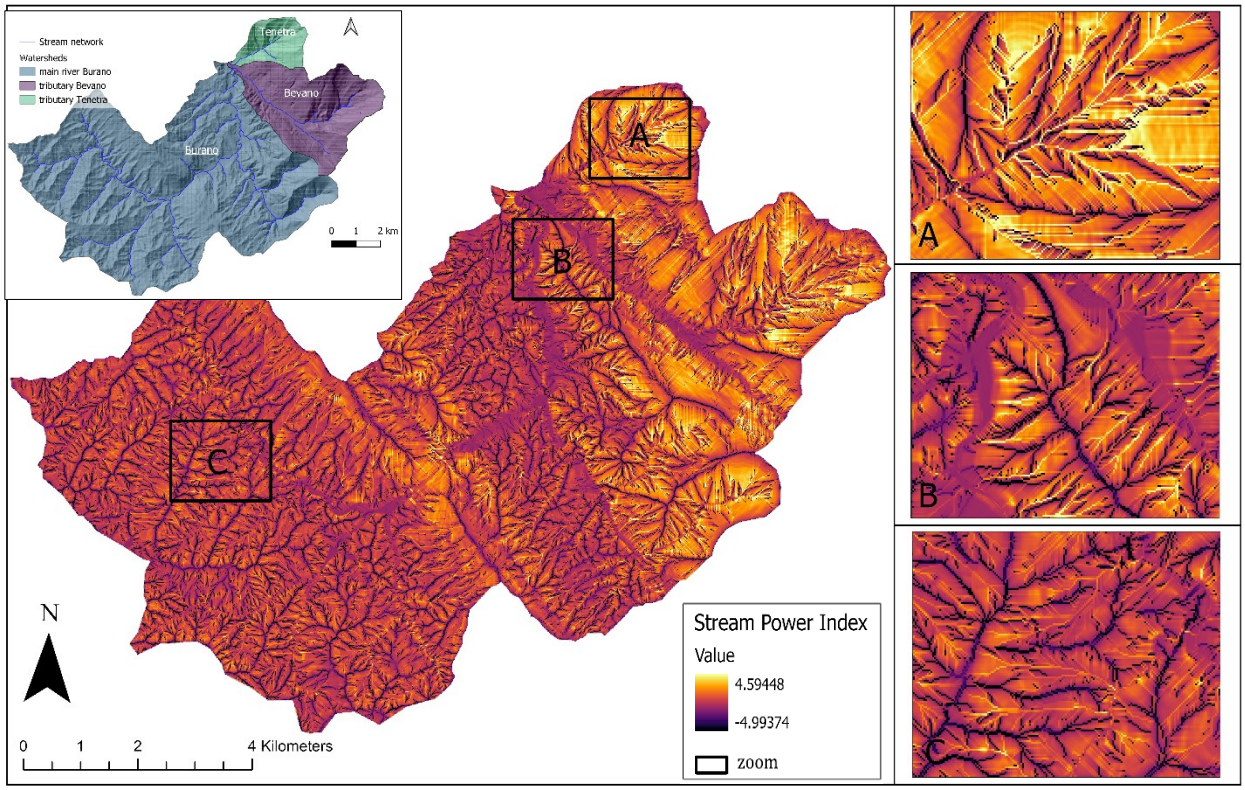

Fig. 8. Stream Power Index Map. Reflects the erosive power of streams defined for the upper Burano basin.

2.6.4 Advanced GIS-based analysis – Connectivity Index Map

The output map (Fig. 9) was categorised as a function of positive and negative values that range from 2.47555 (high) to -5.42555 (low) as logarithmic values. Positive values indicate a connectedness of the material, while negative values are a function of unconnected areas. Therefore, based on the distribution of output values, areas such as the Tenetra basin, the upper part of the Bevano, and the higher order impluvia in the main river course are categorised as having a high connectivity index indicating strong or effective connections between sediment sources and the transport pathways, facilitating sediment movement. Whereas sediment movement is hindered or obstructed in areas with a low connectivity index, which indicates weak connections. For areas exhibiting decoupling conditions, which means a negative value, it is possible to use terms like disconnected or unconnected, where disconnection implies the presence of an interruption; in contrast, non-connection represents the opposite extreme to the maximum connection.

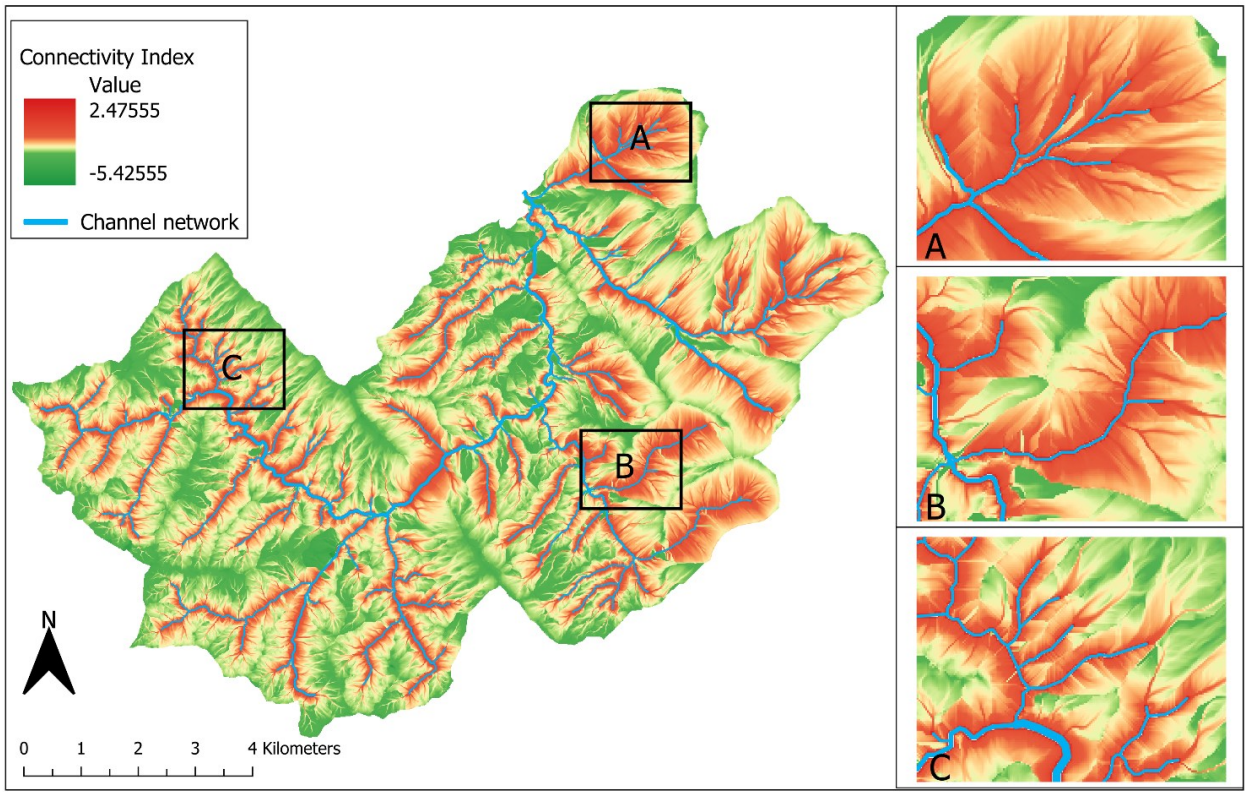

Fig. 9. Connectivity Index Map. Unconnected areas are highlighted in green, while connected areas are highlighted in red.

It must be considered that the connectivity index analysis is performed with the use of a target, in the present case, the extracted reticulum, which implies that a threshold value describing a level of detail has been defined and also allows the identification of areas of material accumulation on the slopes. Therefore, the positive pixels will be distributed around these river orders, not reaching the higher parts of the watershed. Different orders of connection and detail are identified in the figure by means of a graduated and stretched colour scale.

2.6.5 Advanced GIS-based analysis – Stream Length-Gradient (SL) Index Map

The output map (Fig. 10) was represented by points along the river path with values associated with different colours, thus immediately highlighting the areas where the main jumps are present . These do not include points that correspond to hydraulic works on the 1:10,000 scale topographic map, nor those considered invalid through a geomorphological interpretation (manual filtering). The obtained values were positive from a minimum of 0 (I class), areas where the gradient is shown to be low, to a maximum of 1,278 (V class). Most knickpoints with high values are found in the major river orders. The knickzones that acquire greater importance are where along-stream deviations are extensive from the typical concave-up shape in isolated river reaches (knickzones). In these cluster areas, an accumulation of material coming from secondary connection channels or lateral landslides could be considered responsible for the appearance of sudden high gradients. This difference in heights could indicate a (more or less recent) unconsolidated deposit which represents a potentially source area of material. River reaches with the fifth class are found in all the trunk streams of the three studied sub-basins, indicating that the potential for sediment entrainment is evenly distributed throughout the area (although in the

Burano it is more concentrated in the central section). However, these values have a different overall relevance when associated with the hillslope assessments.

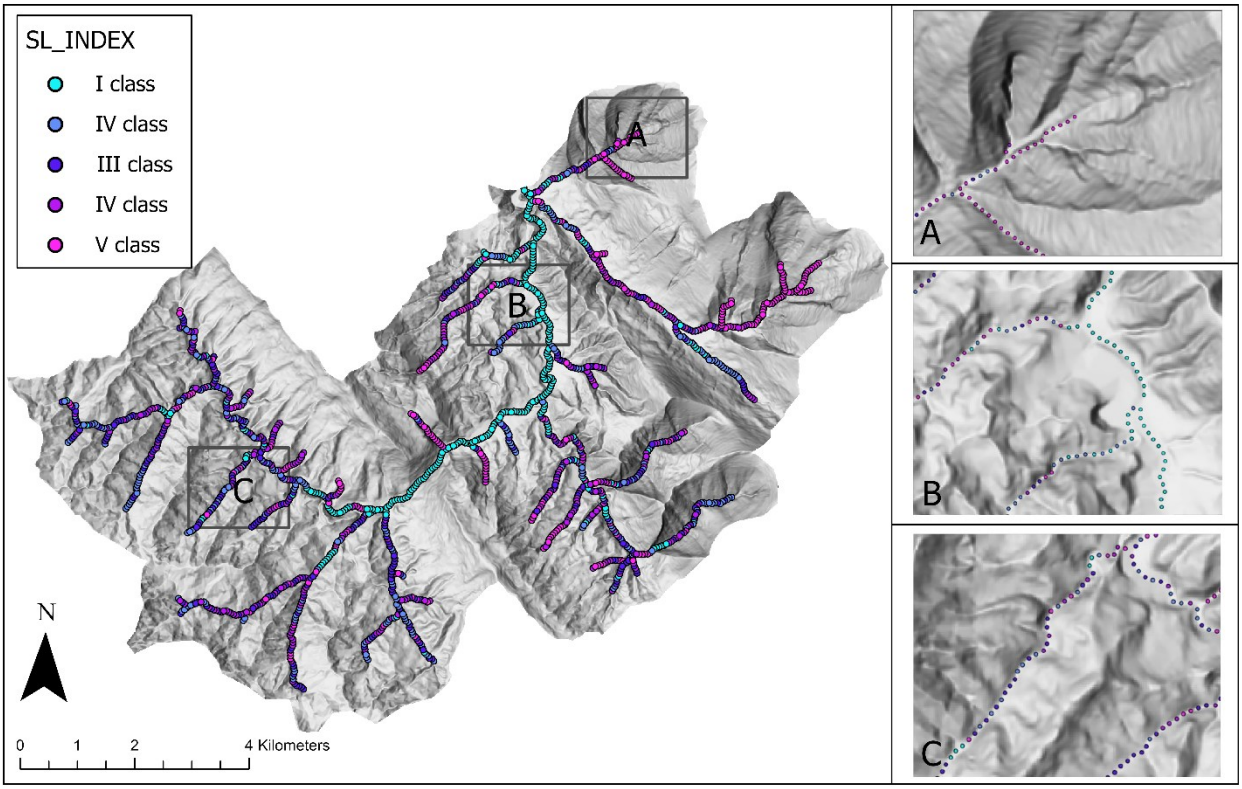

Fig. 10. Stream length Gradient Index processed using the SL tool and setting a V-class quartile classification. Larger values represent areas with the presence of knickpoints.

2.6.6 Advanced GIS-based analysis – River Long Profile

The longitudinal profile visualisation emphasised the spatial variation of morphology along the main river courses (Burano, Bevano, Tenetra), highlighting significant deviations in the topographic profile trend (Fig. 11). It is a way to visualise the abrupt slope transition of the riverbed, as local discontinuity in the general evolutionary context (therefore clearly detectable even for riverbed segments smaller than 50 m used for the SL index). Tenetra and Bevano have higher elevation springs and much shorter paths, making hydro-geomorphological processes more aggressive. In particular, the analysis of longitudinal profiles has proven helpful in identifying areas with localised hydraulic jumps, some of which are characterised by hydraulic structures while others are of natural origin without any anthropogenic influence on the site or nearby.

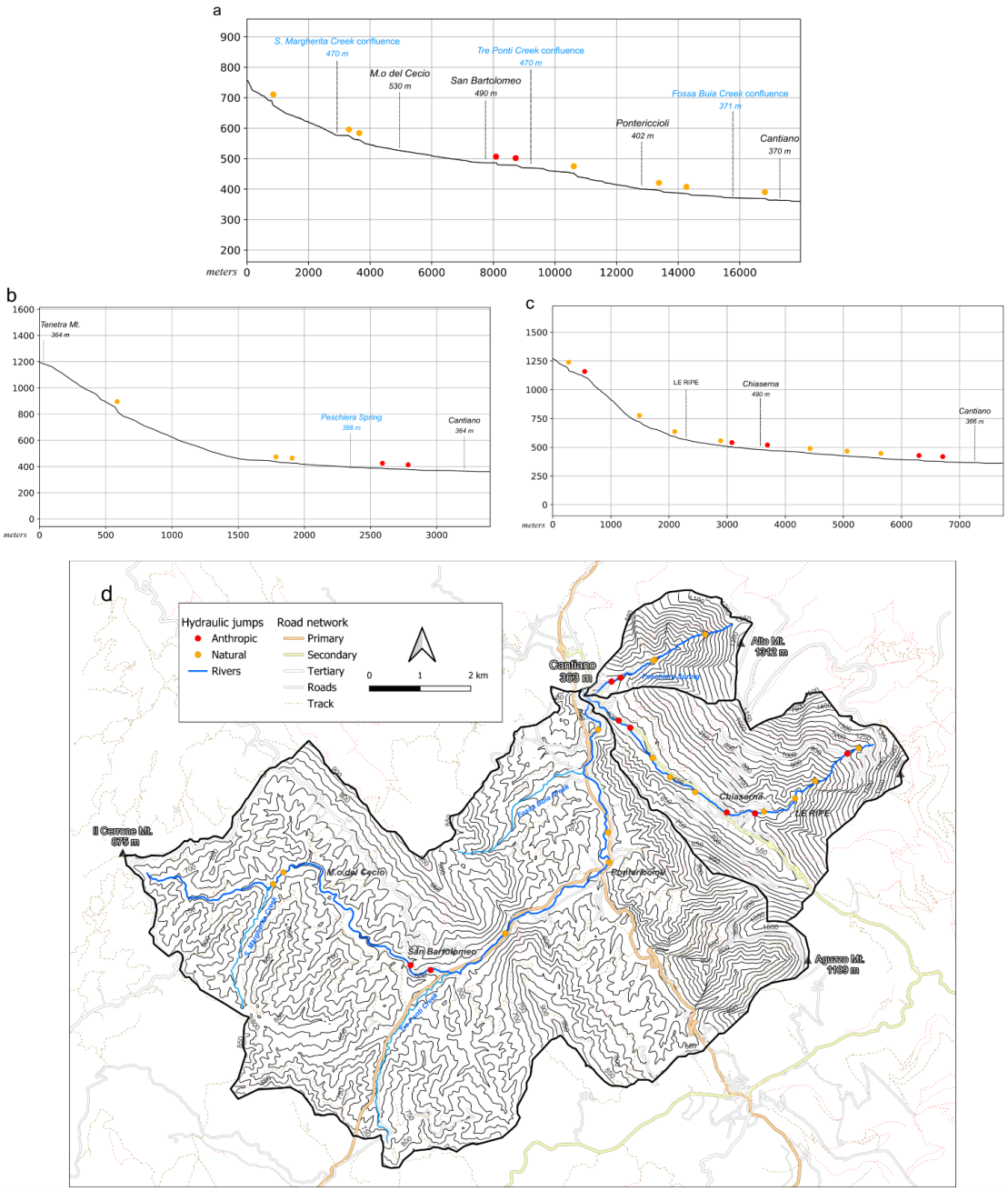

Fig. 11. River Long Profiles: a) Burano River; b) Tenetra Creek; c) Bevano Stream; d) Location map. Red and orange dots mark anthropic and natural hydraulic jumps, respectively. The toponymy derives from the official cartography of the Italian Military Geographic Institute (IGMI): in black, towns, built-up areas, and mountains; in blue, confluences with other water bodies.

2.6.7 Sediment Availability Map

A synoptic map that clearly integrates all the primary processed data was created to support a better interpretation of the zones that generate sediment and how these sediments can (or cannot) move. By creating a virtual raster with the resulting Connectivity Index and Stream Power Index maps and classifying them into 5 classes indicating the likelihood of transfer, a functional zoning of the river basin—comprising source, transfer, and storage areas—was derived. It has been provided an integrated representation of sediment dynamics and the morphodynamic energy of the flows involved on the slopes (Fig. 12). To define the sediment availability map, another important source of information is the mass movements extracted from the landslide inventories

(official Italian IFFI catalogue) of the area. Quiescent landslides and alluvial deposits were excluded from the analysis, taking into account only landslides with signs of evolution. The accumulations recorded in this area due to the topography are strongly related to the lithology of the area. The last defined index is the SL, which is an indicator of anomalous gradients in the networks of the channels analysed that can indicate a possible inflow/accumulation of material into the riverbeds. The use of the more classical longitudinal river profiles supported the interpretation of the detected morphological variation, identifying local and punctual morphological anomalies that can be associated to lithological jumps (especially those represented by rocks emerging from the riverbed) or anthropogenic works which on the contrary can indicate the presence of strong current, erosion and taking charge of the materials downstream of the jump. In this sense the integration of the two longitudinal analyses works very well in the interpretation of the variations. The raster representing the likelihood of material transfer has been categorised in 5 continuous classes, with red indicating high probability and green indicating low/zero probability. The stream length gradient index was classified using quantile counting, in blue are the most important knickpoints, which means also an increase of the steepness and energy consequently (Fig. 12).

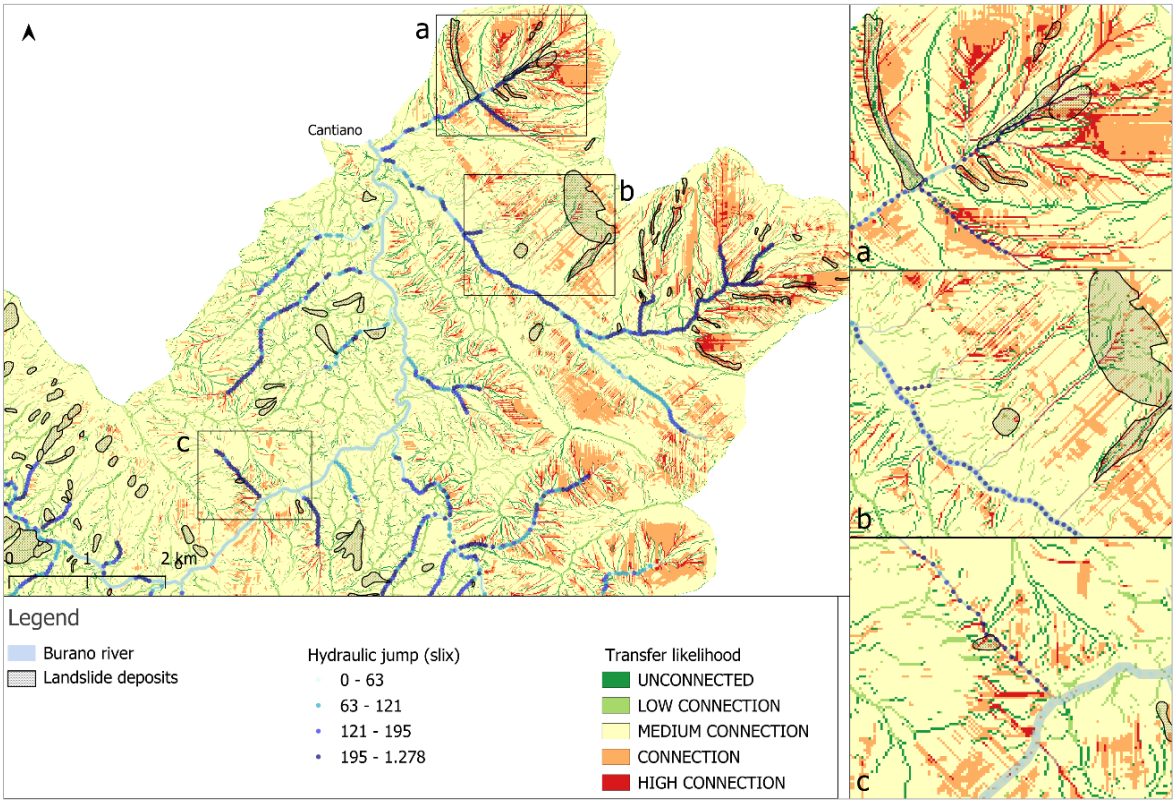

Fig. 12. Sediment availability map supported by fieldwork–sensitive values (IC and SPI), categorised in 5 classes indicating the high energy and connection (red colours) or the low energy and connection/unconnection (green colours); SLindex defined for the linear river element and classified in the quantile method in 4 classes. The black polygons define the evolutionary landslide with active indication.

Analysing the whole studied hydrographic system the Burano River flows through younger materials with marly arenaceous compositions, which allows it to more easily modify its course and riverbed promoting significant fluvial dynamics. In contrast, the lands crossed by Bevano and Tenetra watercourses mainly consist of limestone, which is reflected in the higher stream slope and elevation, and in a minor dynamism. For this reason, the

available sediment depends on the amount of unstable material that can be identified from the updated geomorphological map. The two basins most susceptible to sediment production can be described as follows: in the Bevano basin, Quaternary debris is identified by the presence of inactive or dormant landslides, whereas in the Tenetra basin a larger number of active landslides with clear signs of evolution are observed (most of them close to high values of IC).

2.6.8 Validation

The GIS analyses carried out in this work are based on a DEM created some years before the 2022 exceptional rainfall that profoundly affected the morphology of the territory with its consequences (landslides, linear and areal erosion along slopes, high solid transport in rivers, riverbank erosion). Therefore, the information deduced from the post-event observation and analysis was used to corroborate the spatial model's predictions and validate the methodology's reliability. Based on a comparison of pre- and post-rainfall events, it was possible to collect a valid archive with terrestrial and UAV photo documentation, satellite images elaborated like NDVI difference, and highlighted control points on the field (Fig. 13, Fig. 14).

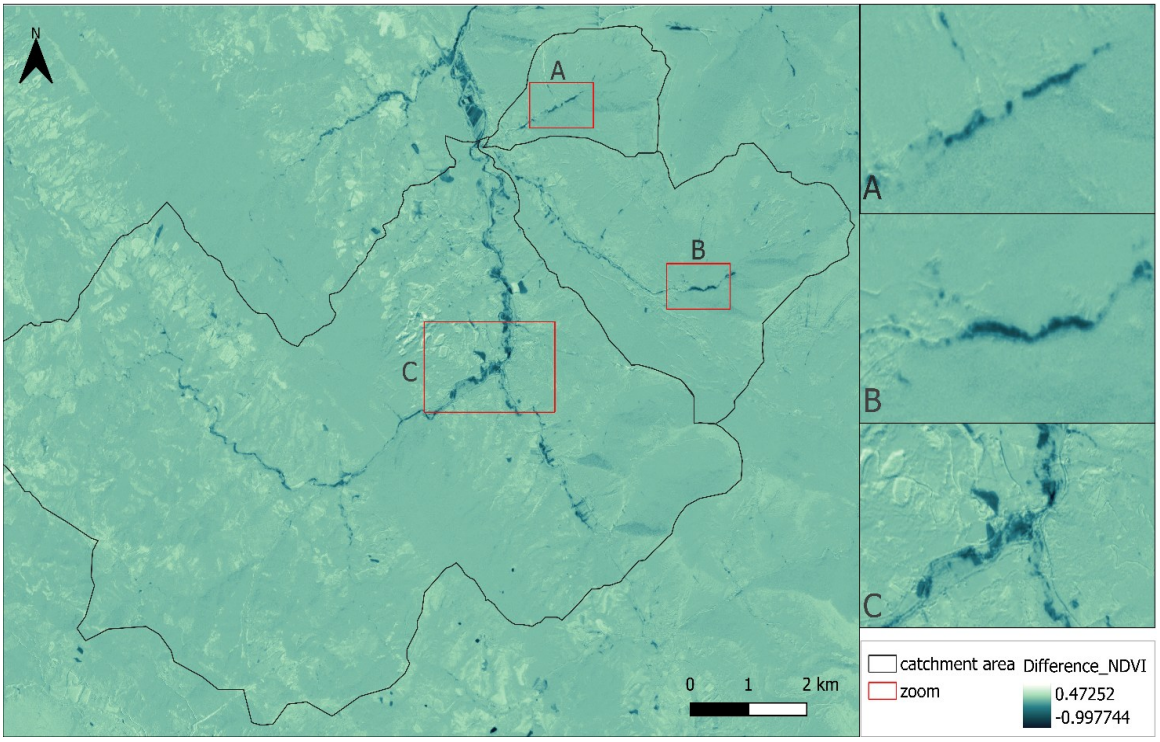

Fig. 13. NDVI – raster of difference of NDVI images – pre and post-flood event in Cantiano city – 12 September and 18 September. Image © 2022 Planet Labs PBC

A semi-quantitative remote analysis of the study area allowed to see morphological variation caused by the September 15 events and locate them in relation to study results. A difference analysis between two Normalised Difference Vegetation Index (NDVI) images (12 September and 18 September 2022; Fig. 13) highlighted a good correspondence between the results of the applied methodology and the actual case for the entire basin area in different geomorphologic contexts. DEM of Difference (DEM of Difference) analysis illustrates a noticeable reduction in vegetation. Given that the two images were acquired only a few days apart, the observed changes

can be reasonably attributed to the flood event that occurred in September 2022. The decrease in vegetation is shown as a negative value on the pixel. Evaluating the number of pixels with negative signs highlights that the area affected is 2.11 km^2 in the upper Burano River, 0.44 km^2 in the Bevano Creek and 0.13 km^2 in the Tenetra Creek.

The fieldwork included a series of general inspections carried out immediately after the event in September 2022 in collaboration with the Civil Protection Centre of the University of Florence and, subsequently, a lot of targeted examinations in the Bevano and Burano drainage areas in November 2023 and in the Tenetra basin in April 2024. The focus was on identifying the most sediment-producing areas, and in particular, the areas that may have caused damage to the basin and even to the city of Cantiano due to the merging of the three studied watercourses. UAV images were used to localise remotely the on-field control points. Based on a possible comparison of recently recorded information with the processing of older data, the fieldwork was carried out with extensive checking directly in the main areas identified as more mobilizable by the obtained maps (Fig. 14).

Fig. 14. Ground sites – Field validation. The map with the white icons highlights the points viewed, numbered according to the images taken in the field. Surveys were carried out in November 2023 and April 2024**.**

Due to the territorial and environmental conditions, the hydraulic network reached very high flow levels in a very short time with a large transport of solid material, composed of debris with an average size of a few decimetres and plant material mobilised by the riverbeds themselves and the surrounding high slopes. The highly concentrated fluid overflowed at several points of wall levees or riverbanks and caused anomalous and temporary transversal fluvial sections, sometimes collapsing banks or embankment walls. One of these levee overtopping places was located exactly at the Burano's diversion bend into the tunnel (after overflowing upstream as well), as the raging water flows reclaimed the original riverbed that flooded up to the town centre. Concurrently, in the urban section of Bevano, the abruptly channelling waters broke their cover along two stretches, causing their waters to spread through the downtown streets from multiple sources. Even the sediment-laden waters from the steep valley of Tenetra came with very high energy, breaking a portion of the retaining wall just after the entombment (which resisted the power) and allowing further water runoff for the town. In the same catchment area, it is possible to observe an active landslide and its discharge of sediments into the floodplain of the Tenetra creek (Fig. 14 - 2). In this river, whose discharge is not specified but could be estimated to be less than 1 m^3/s, a large deposit of highly heterogeneous debris has accumulated in the central part. Measured sizes ranging from 1.5/2 m in diameter to 0.01 m (Fig. 14 - 1). In some cases, as mentioned above, the sediments are sandier, allowing them to be transported further downstream. This is the case in the upper part of the Burano basin (Fig. 14 - 7-8) and a small part of its tributary, the Bevano. In the Bevano River, it has been observed that the increase in sediments in the riverbed mainly began following a major landslide on the right bank (Fig. 14 - 5). Severe and large mass movements were observed over the entire basin for validation. However, smaller events were also considered (Fig. 14 - 3). In the affected sites for which the surveys had suffered uncertainty in recognition, especially for the smallest landslides, due to the vegetation cover and the steep slopes, the output maps helped to identify their location and their areal distribution and then confirm the robustness of the method’s results.

2.7 Discussion

Recent literature provides a wide range of tools to investigate sediment connectivity, from empirical or index-based approaches (Borselli et al., 2008; Cavalli et al., 2013; Heckmann et al., 2018) to physically based or cellular automata models (Baartman et al., 2020). While these models can reproduce sediment fluxes with high accuracy, they often rely on complex parametrization and heterogeneous datasets, including rainfall erosivity, soil erodibility, and land-use factors (Staffilani et al., 2019). Such requirements restrict their application in mountainous basins where monitoring networks are sparse and rapid evaluations are essential, particularly after major flood or landslide events. The present work addresses this limitation by adopting a simplified but integrated geomorphometric framework, which reduces input data and computational time without compromising interpretative quality. Compared the work with the integrated HOTSED model of La Licata et al. (2025), which also focuses on identifying sediment sources at the catchment scale, the approach presented here differs in both structure and objectives. In contrast, our method is entirely morphometric and quantitative, avoiding subjectivity in parameter assignment and minimising data demand. The workflow can be executed

within a short computational time using only a digital terrain model, basic geological layers, and pre- and post-event landslide inventories. Furthermore, while HOTSED primarily evaluates the spatial distribution of sediment sources, our framework explicitly incorporates the linear hydraulic dimension through the Stream Length-Gradient Index, capturing in-channel energy variations and sediment routing that are not directly represented in HOTSED.

Similar studies have been conducted in a mountainous basin in the paper by Zingaro et al., 2019, where, as previously reported in the literature (Borselli et al., 2008; Zhao et al., 2020; Michalek et al., 2020; Guo et al., 2023; Abebe et al., 2023), the main factor taken into consideration is land use. This proves to be limiting when dealing with environments with complex morphologies. Instead, by using a parameter more suited to steep slopes and lithological variations, such as roughness, it is possible to obtain a good estimate in terms of connectivity. IC alone shows limited predictive capability for functional connectivity, especially under dynamic post-disturbance conditions—since many structurally connected areas did not actually deliver sediment during storm events (Martini et al., 2022). Our method addresses these limitations by integrating multiple indices and morphological criteria, validated through field surveys and remote sensing after the specific 2022 event.

By combining geomorphometric parameters and a geomorphological interpretation within a fully GIS-based environment, the method enables rapid identification of sediment source areas and their degree of coupling with the drainage network. The integration of the SPI, IC, and SL allows the assessment of both the potential energy for sediment mobilisation and the structural pathways controlling transfer processes. This combination bridges traditional morphometric analysis with a process-oriented understanding of sediment delivery, offering a flexible tool. Analyses for sediment availability to morphogenetic processes are important as they try to identify specific areas that can represent the source of material that could be mobilised. From this perspective, the geomorphological map obtained (Fig. 7) enabled the identification of slope and fluvial margin deposits, facilitating the first assessment of sediment availability within the study area. In trying to isolate the areas most prone to sediment production, landslides retrieved from the national database exhibiting signs of evolution, thus mostly recent, were mainly considered. It was observed that depending on the basin areas of the three considered watercourses, 5.3% of the Burano area is affected by landslides, while in its tributary's basins, it is about 4.4% for the Bevano Creek and 4.5% for the Tenetra Creek. Considering the extent of each, it can be identified that the Bevano and Tenetra basins are the most receptive regarding sediment availability. In Bevano Creek, areas of material deposition have been identified both at the foot of Catria Mount near the village of Chiaserna (about 4 km upstream of Cantiano) and along the valley floor road that connects this locality to Cantiano through the activation of run-off deposits from the slope (Fig. 12). On the contrary, the upper part of the Bevano has not undergone important changes, being present a very extensive landslide area that has not shown signs of large evolution for at least 20 years according to available information. In Tenetra Creek, the situation is still different due to its high slopes in the upstream part and material availability. The sediment transfer is more significant and concentrated along the main network; it shows less on the slopes, except for the main channel set on Fucoid Marl formation with high erodibility.

Using the stream power index map (Fig. 8), it was possible to delineate the slopes along which the flow may gain energy, thereby increasing the likelihood of material entrainment from both slope deposits and channel sediments. The upper Burano contains 4.3% of the pixels, the Bevano contains 17%, and the Tenetra contains 22.5%. Both the area's overall slope and the lithology, a topic covered in detail in the preceding paragraphs, help to explain this aspect. It is observed that when considering the involved areas, the zones that accelerate the water represent 4.1 km² in Tenetra, 14.8 km² in Bevano, and 59.8 km² in Burano.

The connectivity index map (Fig. 9) provided an expedient means of assessing sediment dynamics at the basin scale. The resulting depiction graphically illustrates the probability of material entering the river system and indirectly indicates the locations of the source areas. In the Burano basin, these source areas are responsible for mobilising material, which sometimes reaches roads and settlements and can be traced back to active superficial landslides, as mentioned above. The availability of sediment is an essential factor in being able to define which areas are more productive and which are less so. Through a pixel-based statistical analysis, the proportion of positive values for each basin was determined relative to its total pixel count. Specifically, 2.5% of the pixels in Burano, 2% in Bevano, and 2.7% in Tenetra exhibited high sediment connectivity. In terms of spatial extent, 0.12 km² in Tenetra, 0.3 km² in Bevano, and 1.67 km² in Burano were affected.

The Stream length gradient index (Fig. 10) identified the knickpoints on the stream profiles, measuring the clustering of values with the sharpest changes in hydraulic gradient. The percentages of anomalies along the network were assessed thanks to the statistics applied to the SL; this analysis was done on the V class of the isolated quantile mode symbology. According to this, Burano accounts for 56.5% of the anomalies, Bevano for 33.4%, and Tenetra for 10%. Observing anomalies with values greater than 400, the highest percentage was identified in Bevano (17.8%) while Burano and Tenetra were characterised by 10% and 7.5%, respectively.

The analysis of the longitudinal profiles (Fig. 11) supported the interpretation of the previous index, better characterising the geometric nature of the morphological leap and differentiating the profile anomalies between those of an anthropic nature and natural ones. Natural factors were almost attributable to lithological variations, thus due to differential erosion of the substrate. This allowed attention to focus on knickpoints that could show an interaction between slope and fluvial processes.

An expertise-based interpretation of the sediment production map (Fig. 12) makes it possible to reveal the most critical areas and to isolate sectors with greater sediment production where it is important to provide more attention, especially in the hydrogeological occurrence of high-magnitude. The upper part of the Tenetra basin had a strong mobilisation due to the availability of sediment; on the contrary, in the upper Bevano basin, the non-availability caused less connectivity of material, which, however, led the flows to accelerate at the foot of the slope, creating a strong erosion zone on the main channel with a bridge collapse. The areas with the highest productivity and likelihood of flowing into the river network are mainly represented by secondary tributaries and small, steep ditches. Three large areas can be highlighted: i) the Tenetra basin where a land change of 2.9% of its total area was seen; ii) the transition between the Tenetra and Bevano basins where several landslides of debris flow have been mapped; iii) the highest orders tributaries of upper Burano basin that led fine material along the river network (mud that reached the town of Cantiano). According to the considerations made above,

the area with the highest propensity for sediment discharge according to the results map under discussion is the Tenetra area, approximately 1 km from the confluence with the Burano. Due to its reduced width, high slope and flow accumulation values, and low stream frequency values, the basin exhibits more sediment production and a stronger connectivity between slopes and the river water system. The strong spatial correspondence observed between high-index areas and the post-event landslide inventory validates the method's capacity to delineate active sediment source zones and preferential transport channels.

It should be considered that for the current research, the DTM used in the processing was neither high-resolution nor up to date, making the methodology highly implementable. Moreover the landslides inventory is an important factor for the availability map and if constantly updated, make the procedure extremely solid. Nevertheless, with this type of basic data, we can obtain a good level of information to use practically. Our approach introduces notable methodological refinements by combining multiple indicators - such as the SPI, the IC, and the SL - within an integrated and scalable framework. This combination allows for a more detailed distinction between areas of potential sediment supply and those likely to be activated under extreme rainfall conditions. Results suggest that, especially under short-duration, high-intensity rainfall events like the one recorded in the Burano basin in September 2022 (419 mm in 12 hours), terrain-based connectivity indices such as the IC (Cavalli et al., 2013) and geomorphic energy proxies like SPI and SL become more predictive when interpreted in combination with topographic discontinuities (e.g., slope breaks, knickzones, and convexities). These features, which often act as sediment traps or thresholds, help explain the selective functional activation of source areas under extreme conditions and are not always explicitly represented in traditional terrain-based models when used in isolation (Crema and Cavalli, 2018; Wainwright et al., 2011). This study contributes to current research in two main respects. Firstly, it presents a procedure featuring a replicable methodology applicable to similar mountainous environments for broader-scale screening, which is both rapid and straightforward and does not necessitate high-performance computing resources. Secondly, the approach is widely expandable so that it may support land management practices, particularly in the context of post-extreme event risk mitigation, by identifying the most vulnerable areas and informing the development of targeted protection strategies.

2.8 Conclusion

Sediment production is a sensitive issue in fluvial geomorphology and investigating hillslope-channel coupling in a system that facilitates sediment transfer across a mountainous river basin is a significant challenge faced in this research. The study area is located in the Northern Apennines, and in particular in a mountainous sub-basin which includes three neighbouring and different hydrographic basins. These areas were affected by an extreme pluviometric event in September 2022. The proposed approach provides an innovative and operationally efficient framework for analysing sediment dynamics in mountainous catchments. A progressive process of seven working steps from the hydro-geomorphological characterisation through four key GIS analysis methods is proposed to identify the potential material sources and availability, the channel flow power, the basin sediment connectivity, and the river network oddity regions in each basin. The suggested method was designed and tested

by using geospatial data available previous to the 2022 event, validating the model results by observing the geomorphological changes induced by the extreme event. The working process calculates a series of maps with morphometric indices applied to the territory and creates a model that provides information on the sediment mobilisation during pluviometric events, assessing the cascade of processes triggered by intense precipitations. The research has demonstrated that the three river basins have high sediment productivity, which is also consistent with the post-event field observations. The Bevano and the Tenetra basins are more prone to sediment production than the Burano. Both rivers represent the greatest threat to the valleys converging on the urbanised areas due to the areal extent of the mass movements and their lithological composition. The observed morphological changes and the NDVI variations validate this statement.

The geomorphometric parameters in Tables 3 and 4 confirm these data, which show important consistency. In particular, the parameters (Nu), (Lu) and (Fs) denote that the hydrographic network is much more articulated in the Burano basin, allowing it to be more effective in the water distribution during extreme events than in the other two basins. The considerable increase in runoff in the Tenetra and Bevano creeks, as well as high values of relief ratio and gradient ratio, indicate a higher propensity to runoff, erosion, and sediment transport. Sediment accumulations conducted by the flow in the city of Cantiano can be partly attributed to coarse and very poorly sorted carbonate material transported by Tenetra and Bevano creeks. The fine sediment portion comes from eluvial-colluvial deposits along the highest-order branches of the Burano River, which are supplied by the more erodible siliciclastic Miocene formations. In the latter, even the less steep channels are highly productive during ordinary and exceptional rainfall events, such as the 2022 one.

This study contributes to the growing effort to develop connectivity-based approaches that are both scientifically robust and operationally practical. By coupling morphometric indices with a geomorphological interpretation, the proposed framework complements existing models (e.g., Borselli et al., 2008; Cavalli et al., 2013; La Licata et al., 2025) and provides a scalable methodology for investigating sediment transfer processes in mountainous landscapes. Furthermore, the procedure, build upon established approaches in the recent literature and here tested, could be applied to forecast the territory evolution in ordinary and extreme morphogenetic conditions in similar geo-environmental contexts. Despite its proven effectiveness, potential improvements can be glimpsed based on the input data. The more up to date the DEM, land use, geology, and landslide data are, the more efficient the methodological procedure becomes. This can increase the result accuracy and improves the preventive mitigation and management measures. The proposed workflow can be an important, smooth and easy-to-apply support to public administrations. The chain of processes can be wrapped into a single automated model, which also includes functional connectivity, working as part of a monitoring system. Overall, the method proved to be a suitable support tool for both sediments supply mapping and post-event planning, especially in poorly instrumented catchments. While this approach does not replace detailed process-based sediment transport models, it offers a reliable and scalable solution for first-order sediment assessment and planning interventions under climate-driven flood risk scenarios.

CHAPTER III

Modelling river geomorphic responses to abrupt sediment inputs and grain size variability during floods: insights from Burano River (Italy)

In the submission phase

Guidi E. [a], Ruiz-Villanueva V. [b-c], Bladè Castellet E. [d], Borga M. [e], Dallan E. [e], Pappafico G.F. [a], Ottaviani F. [a], Morelli S. [a].

a Department of Pure and Applied Sciences, University of Urbino Carlo Bo, Urbino 61029, Italy

b Geomorphology, Natural Hazards and Risks Research Unit, Institute of Geography, University of Bern, 3012 Bern, Switzerland

c Oeschger Centre for Climate Change Research, University of Bern, Switzerland

d FLUMEN - Institute of River Dynamics and Hydrological Engineering, Polytechnic University of Catalonia, Barcelona, 08034, Spain

e Department of Land, Environment, Agriculture and Forestry, University of Padua, Padua 35122, Italy

ABSTRACT

Predicting geomorphic changes in rivers after floods remains a significant scientific challenge due to the complex interplay among hydrodynamic forces, sediment supply, and sediment availability. These factors play a crucial role in determining how rivers respond to extreme events, including channel morphology, sediment transport, and deposition patterns. Exploring these aspects is the primary objective of this article. Effective sediment control and management are increasingly recognized as critical to promoting the sustainable use of natural resources and mitigating environmental impacts. On 15-16 September 2022, the Marche region experienced an exceptional meteorological event, with localized rainfall reaching 419 mm in twelve hours—a record intensity over the past decades. This huge amount of rain water was derived by a self-regenerating storm system and led to the overflow of watercourses and widespread flooding, with peak rainfall intensities of up to 90 mm/h. In the municipal territory of Cantiano, one of the most severely affected areas, intense soil erosion led to the mobilization of substantial amounts of mud and debris, exacerbating damage to built-up areas. The research focuses on a sub-basin of the Burano River, which experienced profound morphological changes due to the mobilization of coarse sediments during the event. This study seeks to advance understanding of these processes to improve predictive models and inform sustainable river management practices. The Iber model, a two-dimensional numerical tool designed for simulating free surface flow in rivers, is employed to investigate erosion and deposition processes in Tenetra stream. The objectives of this research are to explore the impact of sediment grain size variation on morphology and bed-load capacity and to assess the effect of sediment input and the efficiency of structures under 2022 flood conditions. The modelling incorporated various (D_{50}) values to explore the dynamics governing the coarse sediments transport and better understand the underlying mechanisms driving these changes. An assessment of the efficiency of hydraulic works in relation to grain size

variations has been set up, and the sediment supply from a high-productivity secondary channel is also being explored. The results of the above-mentioned applied methods are expected to provide critical insights into the role of sediment availability and its influence on morphological changes during flood events, not only in the studied river but also in analogous fluvial systems. This enhanced understanding will contribute to developing more effective flood management and river restoration strategies, aiding in designing of sustainable measures to mitigate flood impacts and improving sediment management practices across similar geomorphic contexts.

3.1 Introduction

Floods play an essential role in the geomorphic and ecological functioning of rivers; however, they also pose significant risks to infrastructure and human populations. Floods were the most costly natural disaster worldwide in terms of the total number of people affected between 2000 and 2019 (Vázquez-Tarrío et al., 2024). River flooding occurs when the channel's capacity to convey flow is exceeded, causing water levels to rise above the banks and inundate the floodplain and nearby areas (Benito & Vázquez-Tarrío, 2022). The geomorphologic and stratigraphic signatures of floods provide the basis for understanding the linkages between climate change, environmental variability, flood hydrology, and the geomorphic evolution of fluvial landscapes (Benito & Vázquez-Tarrío, 2022). Moreover, rapid channel adjustments during high-magnitude flood events are often associated with intense sediment mobilisation and transport, which can cause severe damage to riverine infrastructure and surrounding settlements (Vázquez-Tarrío et al., 2024).

Sediment mobilisation and transport, whether naturally occurring or human-induced, poses significant global challenges, including soil resource depletion, waterway siltation, infrastructure damage, reduced hydropower efficiency, and difficulties in flood control (Liu et al., 2018). Although human activities such as land-use change and sediment trapping behind dams have intensified erosion and disrupted land–ocean sediment fluxes, fluvial processes continue to play a fundamental role in shaping the Earth's surface through erosion, deposition and denudation (Walling et al., 2006). To address these challenges, UNESCO's International Hydrological Programme launched the International Sediment Initiative (ISI) in 2002 with the objective of promoting sustainable sediment management on a global scale. The ISI provides a decision-support framework for developing institutional and legislative solutions that consider both physiographic and socioeconomic contexts within the broader framework of global environmental change. It also compiles case studies to assist policymakers in the effective management of river basins and water resources.

Predicting the geomorphic response of river channels to flooding remains a formidable challenge, given the complex interplay of hydraulics, sediment transport and channel form, and field studies continue to reveal highly variable morphological outcomes even under broadly similar flood conditions (Ziliani et al., 2020; Kashyap et al., 2025). The handling of abrupt or pulsed sediment supplies — for example via mass movements or cliff-fall events — further complicates morphodynamic prediction, as such inputs can overwhelm transport capacity and fundamentally alter river response trajectories (Müller & Hassan, 2018; Barbosa et al., 2024). Moreover, variability in bed-sediment grain-size distributions exerts a critical control on transport thresholds, sediment

mobility and morphological change, yet many models simplify this to a single representative size, limiting their predictive power (Guerit et al., 2018).

Modelling these types of phenomena, especially under unusual conditions, is complicated and requires a specific approach based on effective strategies that enable land conservation. The sediments that characterise a mountain environment are heterogeneous in several respects and depend on several factors such as the slope of the channel, the inflow of sediments, and the size of the channel (Mir & Patel, 2024). A numerical approach based on St. Venant's equations and the conservation of mass of the mobile bed and sediment transport was used. The results obtained for hypothetical scenarios are consistent with field observations. The model underwent calibration and validation processes using different sets of experimental data acquired over time. This approach aims to predict geomorphic changes in rivers during floods by examining the interplay of hydrodynamic forces, sediment supply, and availability. It emphasizes the importance of effective sediment control and management for sustainable resource use and environmental mitigation. The study involves a hydro-geodynamic simulation using IBER model to understand the effect of variability grain size on river morphology during flood conditions. The open-source, non-commercial IBER software is particularly well suited for working in river environments with open channel flow, flood modelling in extreme conditions, with manageable computational time and the possibility of entering local parameters that can be adapted to a site-specific conditions. It uses advanced numerical schemes that are particularly stable and robust in any situation but especially suitable for discontinuous flows and, specifically, for torrential channels and irregular regimes (Bladè et al., 2014).
The main purposes of this research are: i) set up and calibrate a numerical model to simulate river morpho-dynamics, including a sensitivity analysis of the main input parameters; ii) assess the effects of an abrupt sediment supply from one tributary; iii) explore the effect of sediment grain size by designing several scenarios; iv) evaluate the efficiency of existing retention structures in the channel. In this paper, several scenarios of sediments transfer that are characterised by a significant variation in D_{50} will be examined for the simulation of particle movement. The models are based on meteorological data collected by the civil protection agency during the flood event. The study was applied to a small stream, free from anthropogenic influence, which was affected by the 2022 flood in the Marche region and underwent profound morphological changes. This sub-basin of the Burano River situated in Marche region (Italy) was chosen for its small size and the number of factors that came into play in hydraulic modelling.
The study's results will offer crucial insights into the impact of sediment availability on morphological changes during flood events, not only in the studied river but also in similar fluvial systems, aiding in the development of effective flood management strategies and sustainable flood mitigation measures.

3.2 Case study

3.2.1 Geomorphological and geological settings

The area chosen for the simulation is in the northern Apennines of Umbria and Marche (central Italy, Figure **1**), near the border between the regions of Umbria and Marche, about 50 km from the Adriatic coast. It is a predominantly mountainous area whose slopes descend eastwards towards the Adriatic coast, transforming into

hills that gently slope down towards the coastal area. The most imposing peak is Mount Catria (1701 m a.s.l.), part of a complex structure of almost parallel orographic features, trending in a N/NW-S/SE direction. The Umbrian-Marche ridge area is characterized by the large Mount Nerone - Mount Tenetra anticlinal structure, which is divided into smaller lateral structures. The presence of anticlines with Mesozoic formations creates longitudinal valleys along narrow synclines. Watercourses in this area are often carved into the substrate, creating steep valleys and gorges.

Figure 1 Tenetra river basin on the left: the highest point of the basin is Mount Tenetra, while the town of Cantiano is located at the bottom of the image. On the right, the segment analysed shows the geometry designed in QGIS, used for the construction of the mesh in the numerical model.

The river basin investigated is called the Tenetra basin and is a sub-basin of the main watercourse, the Burano River. It is located at the foot of the main anticline (Mt. Catria), which is composed of Jurassic-Paleogene carbonate-marl lithostratigraphic units (mainly Scaglia *Rossa, Scaglia Bianca, Maiolica, and Corniola formation*). The Tenetra catchment has the distinctive feature of being a morphological amphitheatre with an unmistakable circular shape linked to its structural layout and the erosive action of water. It is possible that the area was involved in the past in glacial processes (Savelli et al., 1995; Nesci 2005; Bendia et al., 2025), later resumed and amplified by karstification and other erosional phenomena. It is a straight course with N/NE-S/SW direction that suggests tectonic control. Downstream, near the locality of Tenetra, the valley suddenly narrows due to the closure of the sides by two flatirons (Bendia et al., 2025). The lithological characteristics have allowed the development of a steep valley that quickly connects to the valley floor. The upper part is marked by dense forests and almost vertical limestone walls. At the foot of the steep wall that rises rapidly to the summit, called Mt. Acuto, there are Quaternary deposits attributable to slope deposits and active and historical landslides. Land cover consists of a mosaic of woodland and pasture, with limited agricultural areas in the lower sectors, the river basin shows almost no anthropogenic influence, except for a small part in the valley area where it connects with the main watercourse. The average slope and width of this stretch are 24% and 1.7 km, respectively. Observing the morphometric characteristics of the basin, the Tenetra is a small watercourse with a total stream number (Nu) of 220 and a total stream length (Lu) of 30.75 km with a stream frequency (Fs) of 36.67 (for more information, see CHAPTER 2 – geomorphological results). The drainage density (Dd) of 5.12 and its lower

bifurcation rate are related to the complex morphology with also has high relief rate (Rh=0.27). High values of lower circularity (Rc) and elongation (Re), 0.90 and 0.80 respectively, indicate a greater propensity for runoff and sediment transport within the basin with much more intense energy involved. Morphometric values (area, slope, length, etc.) were derived from GIS and DEM analysis (TINITALY- Tarquini et al., 2007).

3.2.2 Hydrology and climate

The hydrographic networks of this region largely follow main structural features, being strongly controlled by tectonics and localised erosion. The river under investigation, the Burano River, originates near Monte Cerrone (Umbria) at an altitude of approximately 870 metres above sea level. It collects water from two minor tributaries, the Bevano and the Tenetra, and flows through the town of Cantiano, running very close to residential areas. It was decided to focus on a 1.5 km stretch of the Tenetra stream, a right tributary of the Burano. The Tenetra stream drains a small mountainous catchment in the northern Apennines, with a drainage area of about 6.25 km^2. The basin is characterised by steep slopes and a short main channel, typical of flash-flood prone Apennine torrents. The maximum height of the Tenetra catchment area is 1319 m a.s.l., and the minimum height is 360 m a.s.l. There is a difference in height of 959 metres spread over a river length of 2.8 km. Along the watercourse there are three hydraulic structures that can be classified as weirs. The flow rate is often strongly influenced by seasonal rainfall patterns, a clear sign of rapid underground circulation (PTA- Regione Marche). These morpho-hydrological characteristics, together with limited storage capacity and thin soils, result in a very short concentration time and a high susceptibility to flash flood events.

The climate has Mediterranean characteristics and becomes progressively continental towards the Apennine areas, with a decrease in marine influence as one moves away from the Adriatic Sea (Soldini & Darvini, 2025). The typical continental climate is found in inland regions, with hot summers that frequently reach temperatures above 30°C and cold winters that frequently fall below freezing (Soldini & Darvini, 2025). The mean annual precipitation calculated from the Cantiano gauge is 1279,0 mm (PTA- Regione Marche) with a difference between summer and winter of approximately 100 mm. The mean annual temperature recorded in the Apennines ranges from 10.0 to 14.4 °C, with a mean temperature of the coldest month from 4.0 to 5.9 °C and three months with a mean temperature above 20.0 °C (Donnini et al., 2023). According to Köppen's climate classification system (Köppen, 1936), the territory is classified as having a moderate climate (class C). In particular, the climate can be identified with the sub-category Cfb (Latini, 2018), which is characterised by average annual temperatures ranging between 13° and 10°C, a temperature range that reaches 14°-15°C and annual rainfall that oscillates between 1000 and 1500 mm.

3.2.3 Extreme rainfall event

Lack of observational data with a spatial and temporal resolution appropriate to the complex topography and the significant challenge of accurately capturing these complex geologies make it difficult to gain a thorough grasp of the climatic features of mountain regions. Mountains are important factors in the disruption of large-scale atmospheric flows; they also influence cloud formation and precipitation in their vicinity, which in turn are indirect mechanisms for the vertical transfer of heat and moisture (Beniston, et al., 1997). The

geomorphology of the Marche region includes many rivers with torrential characteristics that flow from west to east, making them particularly sensitive to rainfall intensity (Tartaglione, 2025).

Between 15 and 16 September 2022, following a sudden and intense rainfall event, a self-regenerating, stationary V-shaped storm cell originating from the Tyrrhenian Sea mainly affected the northern part of the Marche region. The event affected inland areas, which were the first to be hit, and subsequently the hilly and coastal areas, covering a total of approximately 5000 km² (Santangelo et al., 2023). High amounts of rainfall were recorded in a very short time, causing widespread critical issues in the basins of the Candigliano River (particularly in the Burano River sub-basin), the Cesano River, the Misa River and the Sentino River (Morelli et al., 2023). Rain gauges in Frontone, Arcevia, and Sassoferrato recorded totals nearing 200 mm, while gauges within the Misa and Esino Valleys registered rainfall above 100 mm (Tartaglione, 2025; Corti et al., 2024). The rain gauge station in Cantiano (Mt. Catria/Acuto) measured the highest value of 419 mm of rainfall in 12 hours (Morelli et al., 2023). An intensity with peaks of approximately 90 km/h was calculated, and it is estimated that 30% of the annual average rainfall fell (Morelli et al., 2023). The Donnini's 2023 paper estimated a more precise duration of the event, namely 8 hours and 15 minutes, with a significant peak of 39.0 mm in 15 minutes. The Marche region had already experienced other heavy rainfall and flooding before 15 September 2022, like the Misa flood of 2014, which affected Senigallia or another in 2011 (Tartaglione, 2025) .

3.2.4 Floods and consequences

This alignment of thunderstorms facilitated intense and continuous rainfall over the same areas, amplifying the severity of the flooding as each successive cell contributed to the accumulation of precipitation. The heavy rainfall caused a rapid rise in water levels in the basins of the central mountain range of the Marche region, leading to widespread flooding. The flood caused extensive damage and loss of life.

The event triggered intense mobilisation of material on the slopes. A total of 1243 landslides (Donnini et al., 2023) larger than 225 m^2 were recorded (as polygon) and classified according to the type of material and movement. In terms of material and therefore origin, 60% involved earth, 39% debris and only 1% rock. In terms of movement, most landslides involved earth (49%), followed by debris flows (17%) (Donnini et al., 2023). Considering the spatial distribution of the landslides triggered during the event, it was observed that a significant percentage occurred near roads, homes and commercial activities. In fact, 50% of the total area of the landslides occurred within 50 m of a road embankment. The Tenetra basin has been affected by significant sediment movement. Specifically, we are referring to debris flows that have mobilised sediments attributable to different lithological formations and, consequently, of different sizes (Figure **2**). The geomorphological impact on the river course has been significant, to the extent that it has altered its bed along its entire course up to the town of Cantiano. The existing morphologies, due to tectonics and lithological changes imposed on them, are activated during periods of heavy rainfall, triggering the activation of certain deposits. There are accumulations resulting from debris flows transported to the riverbed along an erosive channel marked in regional databases as an active landslide (Figure **2**, C). The hydraulic weirs were filled with sediments that arrived both from the main valley, with the movement of large blocks, and from the introduction of lateral material, as well as from

erosion of the riverbed. The Tenetra watercourse continues underground beneath the city, and during the event, the underpass was blocked by a 70%. No damage was reported in the city from the Tenetra stream.

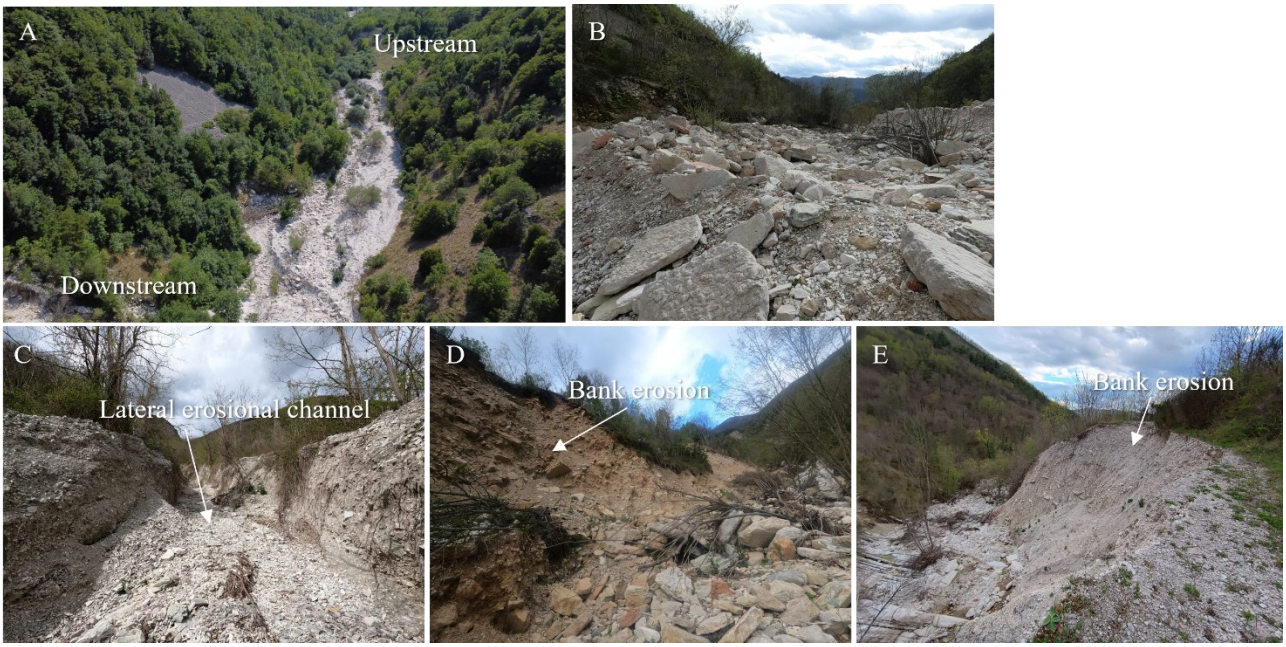

Figure 2 Damage caused by the flood event of September 2022. A) Drone photo of the central area of the Tenetra; B) heterogeneous sediments deposited at the end of the flood event; C) tributary of the Tenetra river, high mobilisation of material entering the main system. High density debris flow; D and E) intense erosion of river banks.

3.3 Materials and methods

3.3.1 Hydrological analysis

Precipitation analysis was based on data from a network of 31 rain gauges in the study area and rainfall estimates from the C-band weather radar covering the region and provided the input to the hydrological model (Amponsah et al., in preparation).

Flood peak discharges for the study basin were reconstructed through post-flood surveys by using methods reported by Borga, 2019 and Amponsah, 2018. More specifically, peak discharge was reconstructed by surveying channel cross-sections and the energy slope of a straight channel reach, as well as by applying the Manning–Strickler equation. The uncertainties associated with these estimates were evaluated by taking into account the uncertainties affecting the retrieval of maximum flow depth for the weir equations and by using the method described by Amponsah, 2016 for the application of the Manning–Strickler equation and are reported in Zaramella, 2020 and Zaramella, 2023. Following Amponsah, 2022, uncertainty parameters of 37.1%, which corresponds to major geomorphic effects as in the case of Tenetra, were used to estimate the likely lower and upper bounds of the peak discharge estimates, accounting for several factors that may have affected the accurate estimation of peak discharges in complex terrains.

Flood hydrographs were obtained by applying the KLEM model (Zaramella et al., 2020). KLEM based on the availability of raster information of the landscape topography and of the soil, geology and vegetation properties. In the model, the SCS-CN approach is applied on a grid-by-grid way for the spatially distributed representation

of runoff generating processes, while a simple description of the drainage system response (Da Ros and Borga, 1997) is used to represent runoff propagation by means of a kinematic model. The distributed runoff propagation procedure is based on the identification of drainage paths and requires the characterization of hillslope paths and channelled paths as well as the specification of two invariant hillslope and channel velocities, respectively. The hillslope and channelled flow paths are determined by a using drainage threshold area parameter.

3.3.2 Iber software

IBER is a free and open source numerical model, allowing modifications and implementations of existing equations. Equipped with a powerful and friendly interface, it facilitates understanding and use. This software calculates the water depth and the two horizontal components of the depth-averaged velocity by solving the 2D depth-averaged surface water equations. The Iber hydrodynamic module solves two-dimensional St. Venant equations in order to compute flow velocity, water depth, bed shear stress and critical diameter (Bladè et al., 2014). An unstructured finite volume solver that is explicit in time is used to solve these equations. It is able to model subcritical and supercritical flows. It uses boundary conditions that are applied to the geometry defining the model of the area.

3.3.3 Hydro-morphodynamic module

The sediment transport module solves the 2D Exner equation to calculate the evolution of bed elevation due to sedimentation and erosion processes, considering both bed-load and suspended load (Bladè et al., 2014, Cea and Bladé, 2015). Iber works with homogeneous or quasi-homogeneous sediment grain sizes, where grain size is characterized by the median diameter D_{50}. The bed-load solid flow is calculated from empirical formulations based on bed tension. The 2-D Exner equation allows to adjust the riverbed elevation according to erosion or deposition due to bedload. The Shields threshold, or critical Shields stress, is considered for initiating the sediment motion (Bladè et al., 2014). Iber use a rock layer position for non-erodible condition, this is particularly important for flood simulations, where neglecting bedrock can compromise predictions of channel morphology and sediment fluxes.

3.3.4 Reference scenario and sensitivity of morphodynamic response

Calibration of the model was performed by comparison with a reference scenario, represented by the extreme rainfall event that occurred in the Marche region in September 2022. In order to explore the importance, and select the set of parameters that result in a more reliable results a sensitivity analysis was performed (Figure **3**). This approach aims to identify which model components most strongly control bed-level variations and sediment fluxes, and to evaluate the model's robustness under different parameter configurations.

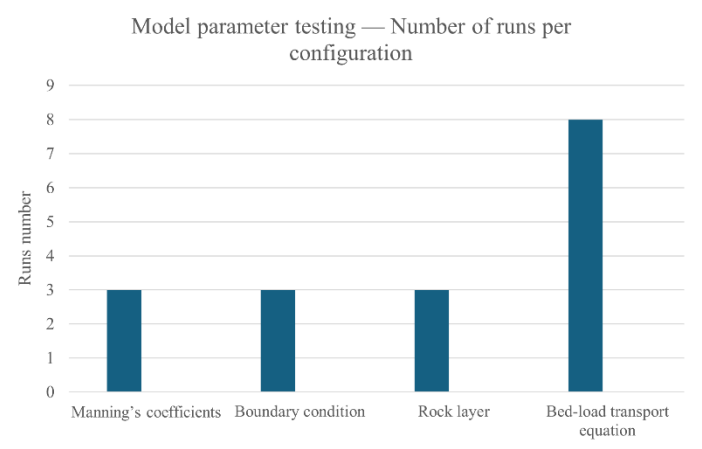

Figure 3 tacked bar chart showing the number of simulation runs performed to test each model parameter. Each segment represents a different aspect of the model setup. Bed-load transport equations required the highest number of simulations, followed by mesh configuration and rock layer definition.

The parameters selected for the sensitivity test are: i) spatial distribution of Manning's roughness coefficients; ii) boundary conditions at the inlet and outlet; iii) definition of the underlying rock layer; iv) choice of the bedload transport equation. These characteristics directly influence the model's ability to represent flow resistance, shear stress distribution and the onset of sediment movement. A total of 17 model runs (Figure **3**) were performed, varying one parameter and keeping the others constant. Three runs were conducted to test the influence of Manning coefficients assigned to geomorphologically homogeneous areas, in particular for the bedrock and the upstream part of the channel. Three runs were conducted to define the influence of boundary conditions: in output, tested subcritical and supercritical flow, and in input tested the influence of the influx of a secondary lateral channel. Three runs were conducted to define the rock layer by varying the thickness of erodible materials. Finally, eight runs were conducted to define the influence of the bed-load equation. Initially, the Meyer-Peter and Muller equation was tested, followed by the Recking equation, and finally adjusted with the AdHoc equation. The latter equation was tested on different grain size scenarios to evaluate the response. Model sensitivity was quantified by analysing changes morphodynamic indicators like maximum bed elevation change (Δz_max), spatially averaged erosion and deposition areas and channel width variations. The results were compared to the field observations. Aerial photographs, Google Street View and private testimonies were used to support the data collected in the field to compare the results of the analysis in areas that are difficult to access or that have undergone post-event changes.

3.3.5 Hydrodynamic Model Setup

3.3.5.1 Input data

A 1 m precision DTM was used, derived from LiDAR scanning on an aerial platform acquired by the Ministry of the Environment and Protection of Land and Sea as part of the Extraordinary Environmental Remote Sensing Plan. The geometry of the floodplain and the channel was defined using LiDAR and interpretation based on field experience. The geometry underwent changes following the introduction of the secondary lateral canal, extending over an area of 50 m. The software uses a friction value based on the roughness of the terrain, which

was not extracted from the DTM but evaluated according to land use. The floodplain was divided into geomorphologically homogeneous areas defined by a unique roughness value. The Manning coefficients were defined according to the bibliography (Table 2) and are based on the roughness created by each surface. The most accurate values chosen were those of the river channel, which was divided into two units, one downstream representing the most stable part (0.3), and one upstream which, due to the presence of calcareous lithologies, is coarser (0.4). The bedrock value was adjusted from 0.020 to 0.025 as it had a high influence on the flow velocity.

Table. 2 Manning's values based on Chow, 1959 classification and adjusted for the local case study

Homogeneous geomorphic unit	**Manning's value**
Forest	0.12
Sparse vegetation (field)	0.028
Upstream channel	0.04
Downstream channel	0.03
Bedrock	0.025
Road	0.02
City	0.02

It was possible to define the rock layer using data provided by the region on geology, creating geological sections and attempting to define the thicknesses of the older and more recent deposits. These values were then adjusted based on sensitivity analysis, defining ranges of erodible soil not exceeding 3 m.

3.3.5.2 Boundary and initial conditions

The inflow condition is represented by the hydrograph under flood conditions (Figure **4**, a); another inflow has been defined in the secondary side channel. The maximum flow rate modelled within this catchment area derives mainly from the main channel and, to a lesser extent, from a tributary channel. The peak flood flow reconstructed on the basis of measured rainfall data is defined within a range of estimated values, between a lower uncertain bound of 40,88 m^3/s and an upper uncertain bound of 89,11 m^3/s. The estimated discharge value used in the simulation is 61.97 m^3/s. A value defined based on the morphological characteristics of the small tributary was used as a second input. Since no input sedimentograms were available, the minimum flow rate value leads to a possible transport based on bed-load capacity (sediment boundary conditions). A uncertain flow peak of 10 m^3/s was set for the tributary. Outlet boundary conditions is a free surface with a defined supercritical flow. In order to define a model that is as close as possible to the real case, the most upstream hydraulic structure was added

to the DTM by imposing internal conditions. Specifically, two structures were used in combination, gates and weirs, in the aim of reconstructing the weir shown in the Figure **4**, b. The sediment boundary condition is a fundamental piece of data, as the sediment load is defined by the programme based on the water flow passing through the starting section 'bed-load capacity'. Using a combination of theoretical models and empirical formulae, the transport capacity was calculated using hydraulic factors like as velocity, shear stress, and sediment grain size.

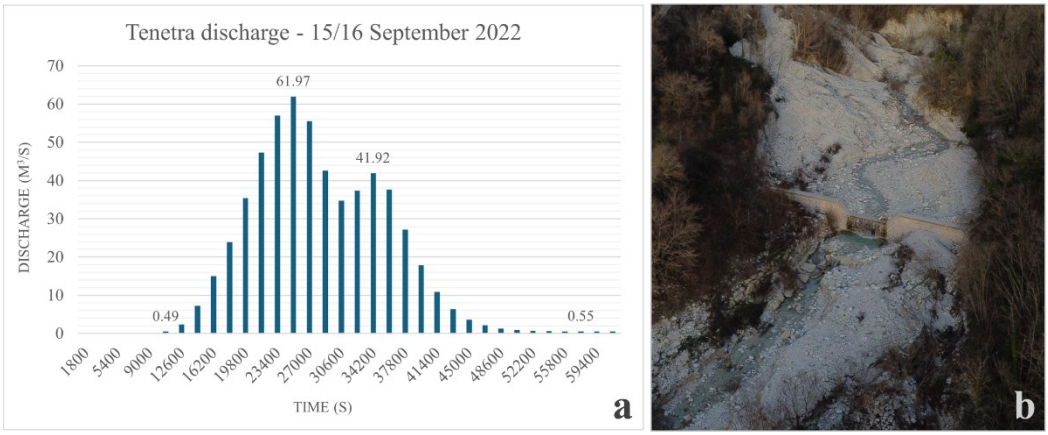

Figure 4 a) boundary conditions, input flow. b) hydraulic structures post event - designed in the model with internal conditions.

3.3.5.3 Mesh setting

The modelled reach extends approximately 1.2 km and includes both the main channel and adjacent floodplain zones. Digital elevation data were derived from pre-event LIDAR DTM from 'Geoportale nazionale - Regione Marche' with accuracy of 1x1m. The domain was discretized using an unstructured triangular mesh with variable resolution: 2 m elements within the active channel to capture local hydraulics and bed evolution, and 5 m elements in the remaining areas to optimize computational efficiency. The quality of the mesh was evaluated within the software, attempting to reduce elements that were too small and caused the numerical calculation to slow down. The computational mesh consists in a grid with 30427 triangular elements with a maximum element edge of 12.6 and a minimum element edge of 0.97.

3.3.5.4 Bed-load transport equation

The AdHoc equation was used, introducing some morphological factors into the alpha coefficient that had been considered in Recking's automatic assessment, in which, however, the D_{50} value had been lowered to 0.1. The alpha coefficient of 0.505 and the beta coefficient of 1.5 were maintained according to the standards defined in the bibliography (Recking, 2013).

The bed-load equation that best describes the processes, in this case is the AdHoc equation.

$$q_{sb} = \alpha (\tau_{bs} - \tau_c)^{\beta}$$

The equation describes the unit bedload transport rate (q_{sb}) considering the shear stress at the bed, the effective shear stress (τ_{bs}) and the critical shear stress for triggering movement (τ_c). An empirical scalar coefficient (α) is applied, which is adjusted according to grain size, slope, roughness and local conditions, and a dimensionless

empirical exponent that describes how transport increases as shear stress rises above the threshold (β). The values α and β can be set manually within the ad hoc (user-defined) equation. Within the equation selection window, it is also used the stabilisation of bottom slopes in case studies with steep slopes and erosion (Avalanche Model BT).

3.3.5.5. Scenarios

Four scenarios were defined to study the impacts that grain size variation in bedload transport causes in a river system under extreme conditions. Highly heterogeneous grain sizes are typical of flood events followed by a gradual sediment discharge curve. Through two grain size analyses (Wolman, 1957 - Pebble Count Methods), upstream depositional areas were investigated to define the range of diameters involved in exceptional transport during the event. Diameters ranging from 0.003 m to 1.5 m were measured. An important hydrodynamic result factor for defining the different study scenarios is the critical diameter. This represents the maximum diameter that the specific flow described is potentially capable of mobilising, and therefore depends exclusively on the hydraulic parameters and model.

Based on these concepts, four modelling scenarios were developed, differing in D_{50} size.

i) D_{50} = 0.01 m
ii) D_{50} = 0.1 m;
iii) D_{50} = 0.75 m;
iv) D_{50} = 1 m.

The four scenarios, modelled using the same set-ups defined above, varying in D_{50} factors, setting up a simulation with homogeneous grain size. The results were analysed by evaluating the different morphological changes and the different bed-load capacity resulting from the predictive scenarios. A maximum simulation time of 60'000 seconds was set in order to simulate 16 h of the extraordinary event departing and returning to the base river flow level.

3.4 Results

3.4.1 Hydraulic results

Hydraulic modelling also allows to obtain an interesting parameter called critical diameters. The result, which is returned in ASCII format, was displayed in GIS as a raster. It represents the potential grain size diameter that a given flow, depending on the morphological characteristics of the riverbed, is capable of mobilising. This does not imply that these particles will be transported, nor can we know the distance reached by the hypothetical particle. It can be observed that the coarser grain sizes are activated as the river flow rates increase. The value returned by the model is determined by the velocity and bed shear stress parameters, both of which are calculated during hydraulic modelling. Four moments were analysed, which correspond to different flow rates in the hydrograph. In order, these are 5400 seconds (15 m³/s); 10800 seconds (45 m³/s); 14400 seconds (60 m³/s); and 26200 seconds (30 m³/s). For each of them, a pixel count was performed based on the seven size classes defined

in Figure **5**. The bars indicate the diameter (in metres) that could potentially be mobilised by the flow rate (m^3/s) defined in the considered second.

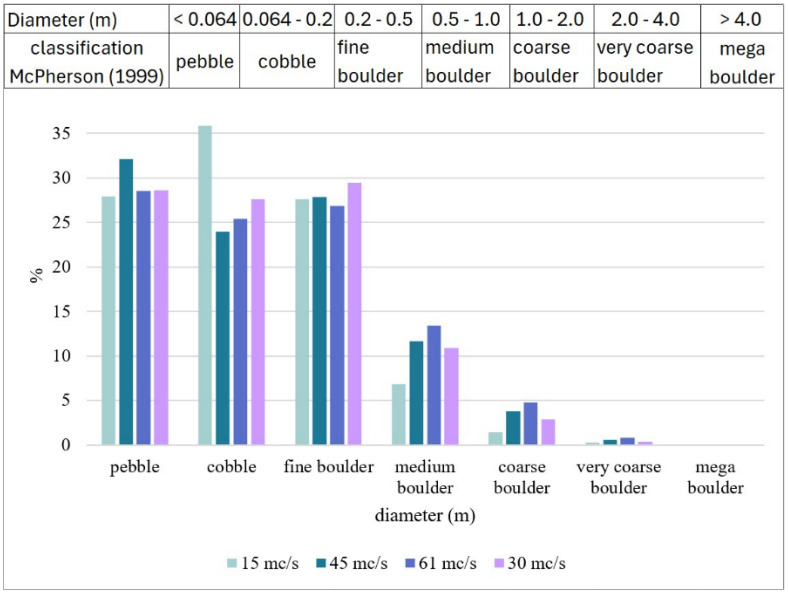

Figure 5 Pixel analysis of critical diameter on QGIS classifying the sediments diameter in 7 classes (MCPherson, 1999). Colours indicating the discharge involved in the model in the seconds previously explained.

3.4.2 Bed-load transport

The results are displayed in Iber's post-processing, from which you can download '.asc' files and process it in GIS environment. The accuracy of the resulting raster is defined according to the accuracy of the input data and the mesh size. Working with a 2 m mesh and a 1 m of DTM, the results were downloaded with a cell size of 1 m. The figure shows the bed-load transport obtained from Iber in m^2/s. The maximum values were standardised in order to obtain a clear comparison of the four scenarios previously designated. On the right is an enlargement of the upstream area where the most critical values are found. The four scenarios show different mobilisation patterns (Figure **6**). The first two show a high concentration in the upper part and especially in the secondary side channel, although they also show significant sediment transport in the parts of the channel where the velocity increases. The last two scenarios with coarse grain sizes have high values defined in some peaks of the mesh triangles, so transport is not continuous but indicates sediment mobilisation over very short distances. A significant amount of sediment is mobilised by the lateral erosion channel on the right bank. Maximum values higher of 0.0042 m^2/s were registered in the SC2 – D 0.1.

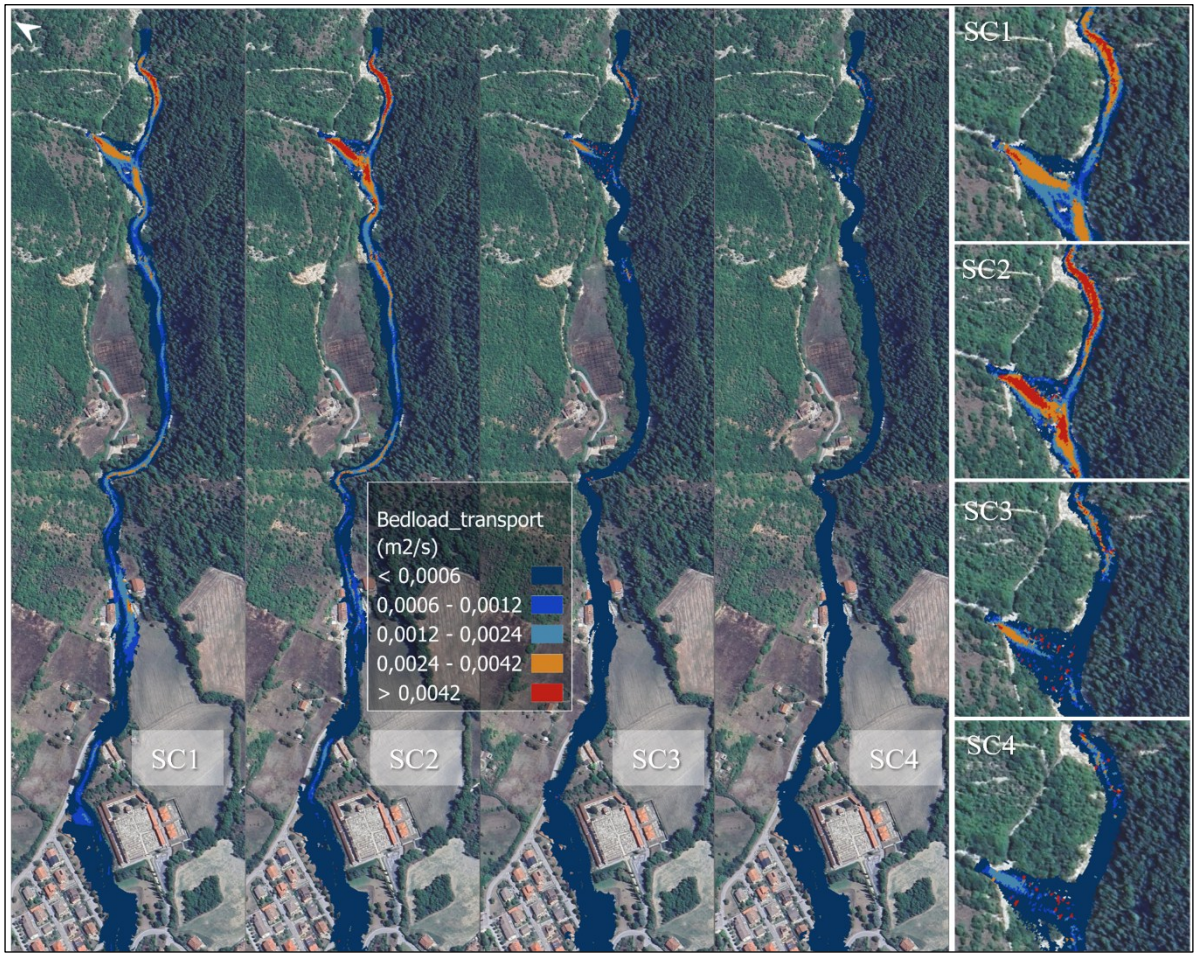

Figure 6 Bed-load transport (m^2/s) defined for each grain size scenarios. SC1 (D_{50}0.01m); SC2 (D_{50}0.1m); SC3 (D_{50}0.75m); SC4 (D_{50}1m). Red colour high transport, blue colour low transport, in the right the zoom of the upstream area.

The bed-load results are displayed in the software post-processing in m^2/s and were analysed integrating along the cross-sections, which transform the results in m^3/s. The image highlights the sections chosen for analysis, six cross-sections called CS or CUT were defined in Iber's post-processing (Figure **7**).

Figure 7 Cross-sections defined to analyse the bed-load capacity over the event times.

The bar chart (Figure **8**) defines the material passing through each section. Cross-section number two, 'CUT2', represents the incoming material transported by the secondary erosion channel that enters immediately before the uppermost hydraulic structure , which is why it has not been included in this chart. It is possible to observe the input material in the main channel and the quantity transported along the main hydraulic network, with particular attention paid to the retained material.

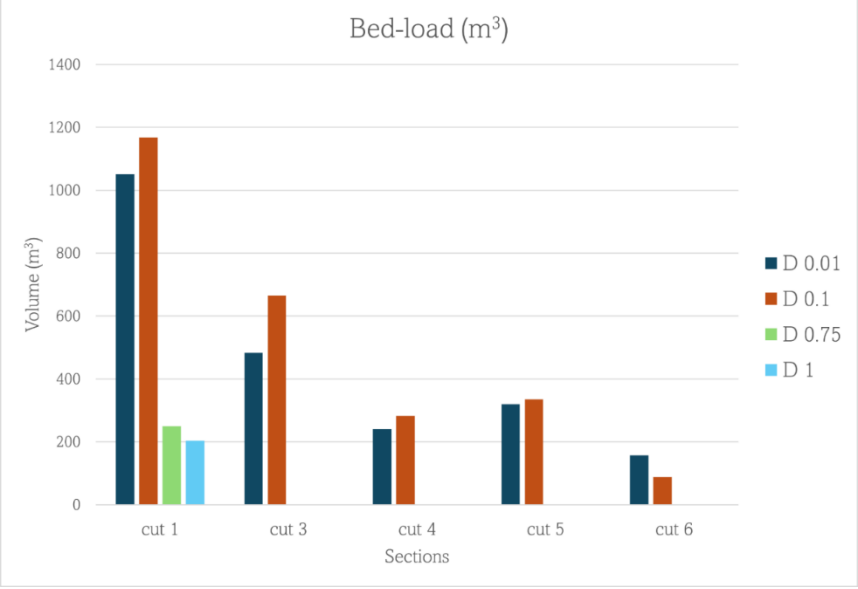

Figure 8 Bars graph showing the volume of material passing through the sections described along the Tenetra Stream.

The graph in Figure **9** represents the integration along the cross-section, thus describing the curve in terms of volumes defined in m^3/s. The x-axis shows the seconds of the simulation, while the y-axis shows the volumes in m^3. There are six sections in total, one at the input and one at the output (Fig. CUT 1 and CUT 6) to assess what enters and what leaves the system. By comparing these two curves, it is possible to define the quantity of

material deposited within the system. Two peaks values are shown in CS-CUT-1 for each scenario, respectively: 0.052 m^3 around 11'200 s and 0.051 m^3 at 14'400; 0.068 m^3 at 9'600 s and 0.065 m^3 at 12'400; 0.031 m^3 at 10'000 s and 0.030 m^3 at 11'000; 0.019 m^3 at 10'000 s and 0.023 m^3 at 12'800 s. The peak values defined by the output curves, cs-cut6, are respectively: 0.0062 m^3 at 5'800 and 0.0077 m^3 at 14'600 s; 0.0050 m^3 at 5'400 s and 0.0048 m^3 around 15'600 s.

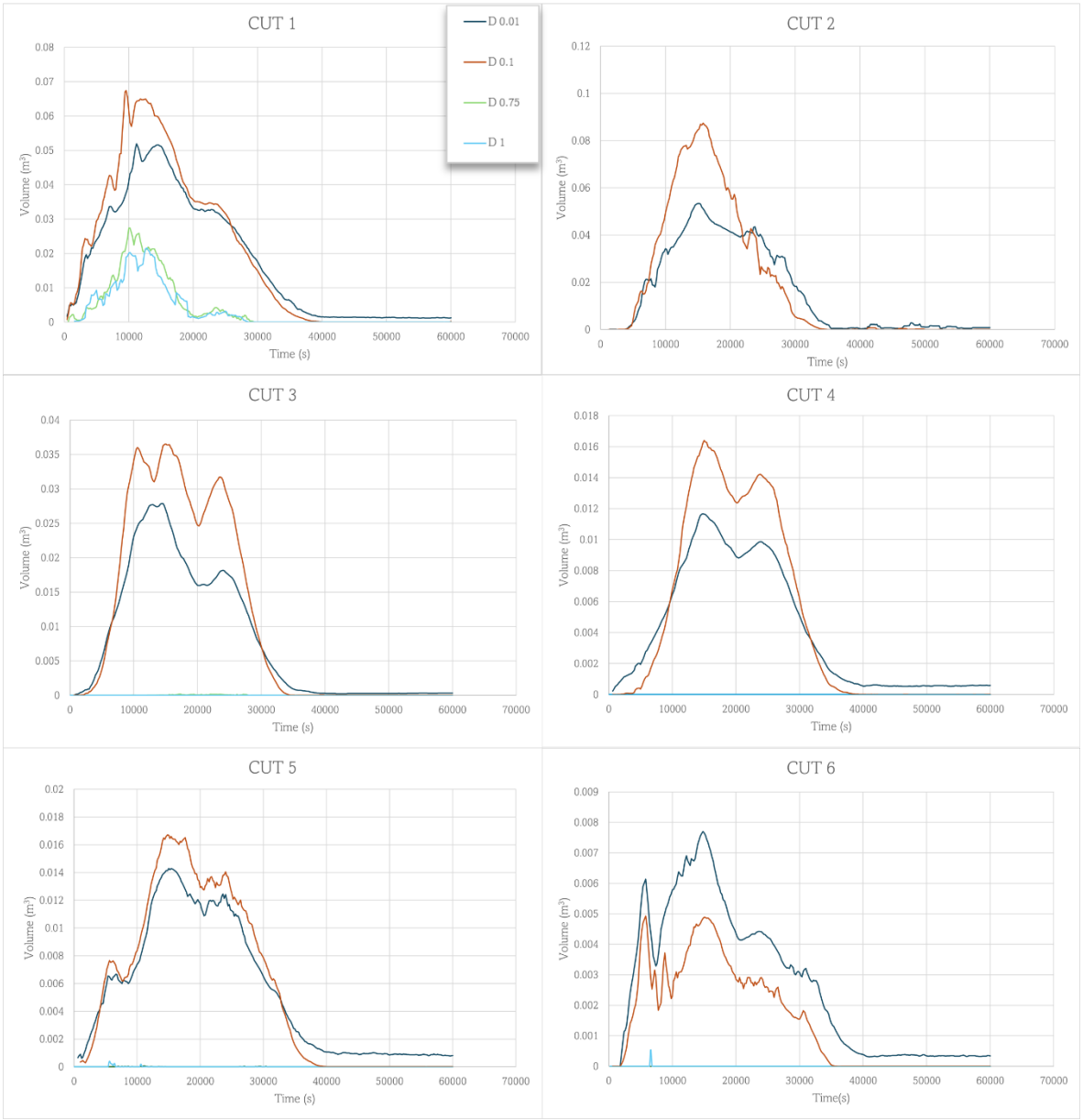

Figure 9 Integration along cross-section of the bed-load transport m^3/s. The max simulation was set to 60'000 seconds in order to simulate 16 hours of flooding with a maximum peak recorded at around 14'000 seconds. Recording intervals of 200 s.

The inflow bed-load quantity according to the defined equation and based on the event discharge is: 1051.8 m^3 for SC1, 1167.9 m^3 for SC2 (Figure **10**), 250 m^3 for SC3 and 204.2 m^3 for the last, SC4 with larger grain size. Section number 2 (CUT-2) represents the input fed into the system by the lateral tributary channel. Only two curves are shown, as it was not possible to include grain sizes with a diameter greater than 0.1 m due to the high level of noise, which created very high peaks, making it impossible to identify the real quantity. Based on these

reconstructed scenarios, the efficiency of the hydraulic structures along the riverbed was assessed. These consist of three work, two are located further downstream and are older, while one is located upstream where the channel's slope decreases. The bedload graphs (Figure **9** CUT-3, CUT-4, and CUT-5) describing the sediment flow curve before and after each hydraulic structures during the event were examined.

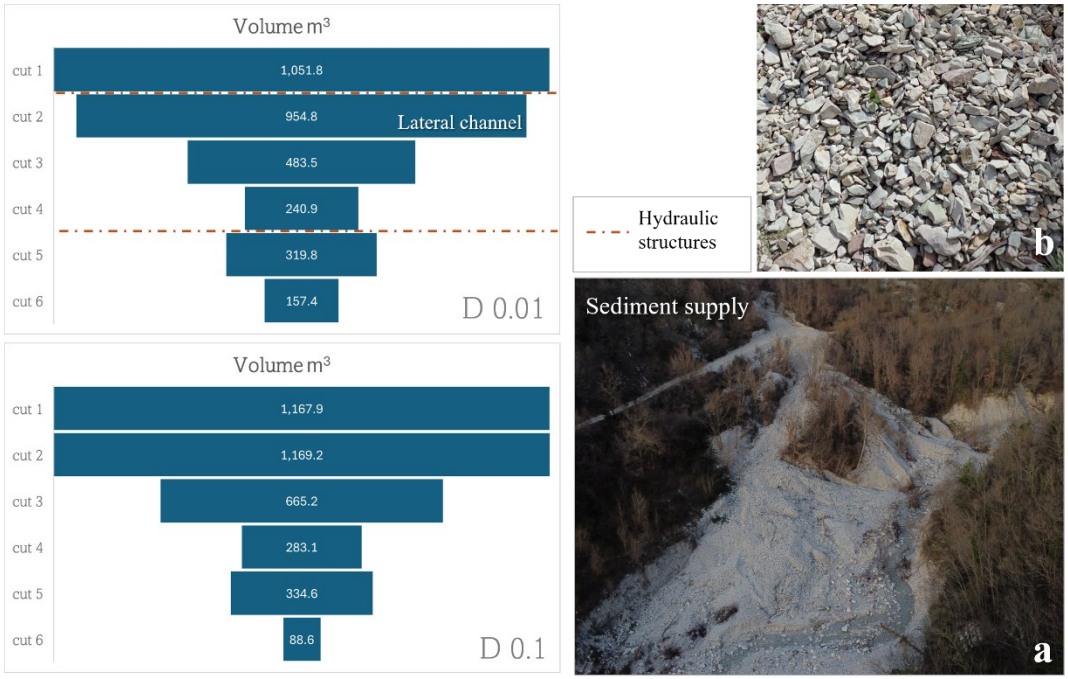

Figure 10 Assessment of the sediment volume (m^3) per cross-section analysed. SC1 – D 0.01 m; SC2 – D 0.1 m.

The sediment contribution from the secondary side channel was assessed using cross-section number 2 (CS - CUT 2). The quantity defined by the bed-load transport curves defines a total value in m^3 that is equal to 954.8 m^3 for SC1 and 1169.2 m^3 for SC2. As previously mentioned, the results of sediment input in the last scenarios were not considered as the values were not representative. A quick comparison shows that the quantity of material carried into the main channel by the tributary is similar to the quantity mobilised in the main river itself.

3.4.3 Morphological impact analysis

Using the results returned by the model under the name 'Erosion' the river morphological impacts were analysed. For statistical data analysis, erosion raster were extracted from post-processing in Iber at the final time of 60'000 s with an accuracy of 0.2 m and processed in a GIS environment. They describe the altimetric variation caused by the transport of sediments during the flood. The range of values goes from an average of -4, which in this case represents aggradation, to +2.5, erosion. Each scenario analysed has different values, especially in terms of areas. The erosion values were extracted with a specific threshold of 0.1 for positive values and -0.1 for negative values. Through statistical analysis of the data, it is possible to see in Figure **11** how the morphological processes differed. On the x-axis, the areas undergoing erosion are divided from those undergoing aggradation, while on the y-axis there is the area expressed in m^2. The morphological impact is significantly higher in the first scenarios, those with a lower D_{50}. Furthermore, erosion processes occupy a larger area overall, clearly predominating over deposition processes.

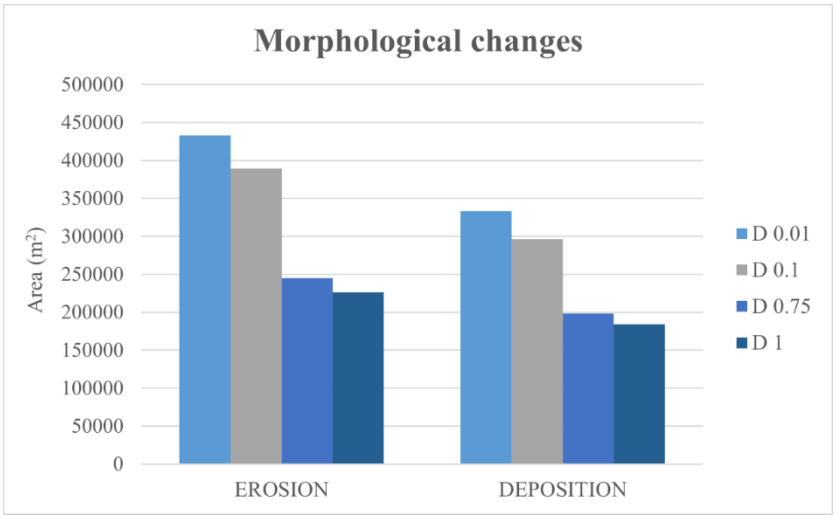

Figure 11 Morphological changes - area affected from erosion or deposition. Calculated in QGIS with pixel statistic analysis.

The total morphological impact is the total morphological changes that occurred during a given event, representing the sum of the morphological processes involved (Figure **12**). An algebraic sum of the areas undergoing erosion and the areas undergoing deposition to assess the result of the granulometric change. The graph in the Figure 11 shows how the first scenarios have significantly higher values in terms of affected area. SC1 - D 0.01m produced a change of 0.76 km^2; SC2 - D 0.1m produced a change equal to 0.68 km^2; SC3 - D 0.75m produced a change of 0.44 km^2; compared to 0.41 km^2 in the last scenario, SC4 - D 1m.

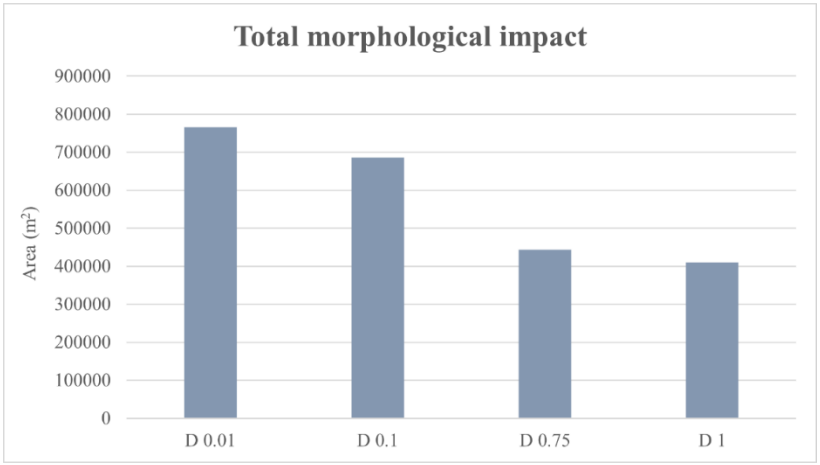

Figure 12 Total morphological impact – Sum of erosion and deposition processes for all scenarios studied.

By extracting the erosion values and categorising them into three ranges defined on the basis of erosion depth, we obtain the graph shown in Figure **13**. The defined ranges are:

- ✓ less than 1 metre, not including 1 metre;
- ✓ between 1 and 2 metres, not including 2 metres;
- ✓ greater than 2 metres.

The colours defining (Figure 12) the different scenarios modelled; each value relates to the total area of erosion.

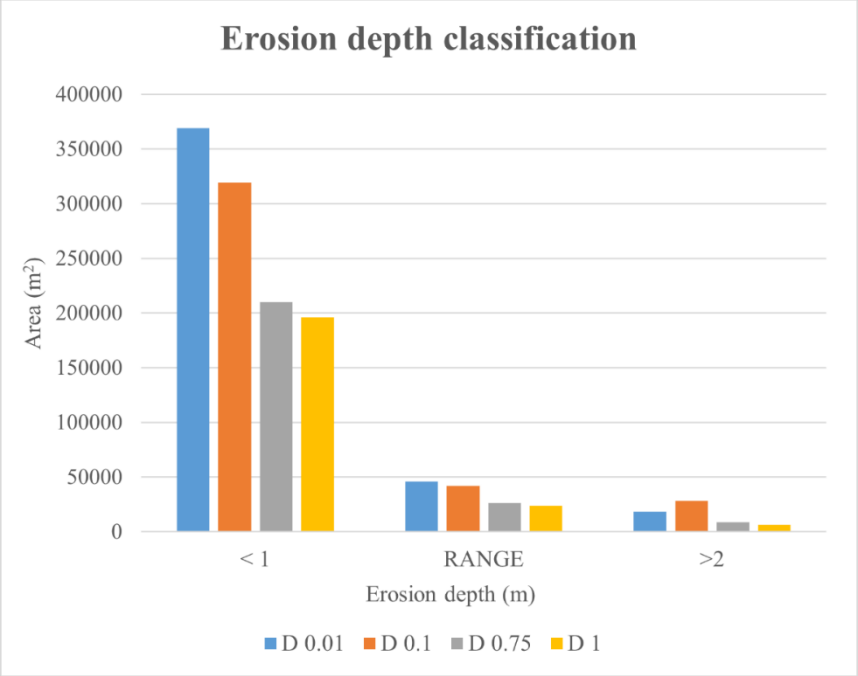

Figure 13 Graph showing the erosive aggressiveness of the four designated scenarios. The x-axis shows the three ranges describing the depth of erosion, while the y-axis shows the area in square metres.

The area that has been eroded by less than 1 metre represents the majority of the total area and is respectively, for the different scenarios: 0.37 km^2, 0.32 km^2, 0.24 km^2, 0.23 km^2. The area affected by erosion between 1 and 2 metres is respectively: 0.046 km^2, 0.042 km^2, 0.026 km^2, 0.024 km^2. Finally, the area that has undergone the most drastic changes in terms of erosion, i.e. changes greater than 2 metres, defined for each scenario is: 0.018 km^2, 0.028 km^2, 0.008 km^2 and 0.006 km^2.

3.4.4 Model validation

The model was validated by comparing the results with field observations. As there were no sensors available to measure the amount of sediment that had been mobilised, qualitative methods were used. Qualitatively, some areas were compared with the post-event scenario, in particular eroded banks, flooded areas, material thicknesses and drone observations (Figure **14**). The fieldwork included a series of general inspections carried out after the event in September 2022. A lot of targeted examinations in the Tenetra drainage areas in November 2023 and in April 2024.

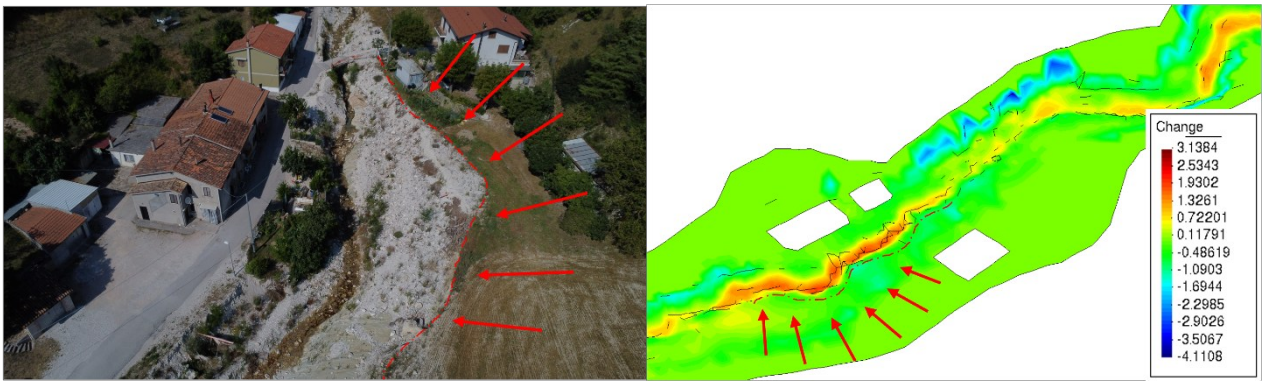

Figure 14 comparation and validation of the model, lateral erosion and morphological changes calculated versus observed.

The simulated erosion maps were visually compared to the difference of DEM (DoD) in order to assess the model's qualitative performance. The oldest DTM, 2008, with 1 meter ground resolution was derived from LiDAR scanning on an aerial platform acquired by the Ministry of the Environment and Protection of Land and Sea as part of the Extraordinary Environmental Remote Sensing Plan. The survey involved the 1st and 2nd order river rods. The Difference of DEM was made possible by a second survey carried out by the University of Urbino in February 2025 with Dj Matrice 350 rtk equipped with a LIDAR sensor. Considering that there is a 17-year gap between the two surveys, not all the changes can be attributed to the 2022 flood, even though its magnitude was such that it caused extreme radical changes. For this reason, DoD was used for a qualitative comparison. The results of comparing (Figure **15**) the erosion model with the DoD show consistency in the most affected areas by the 2022 event.

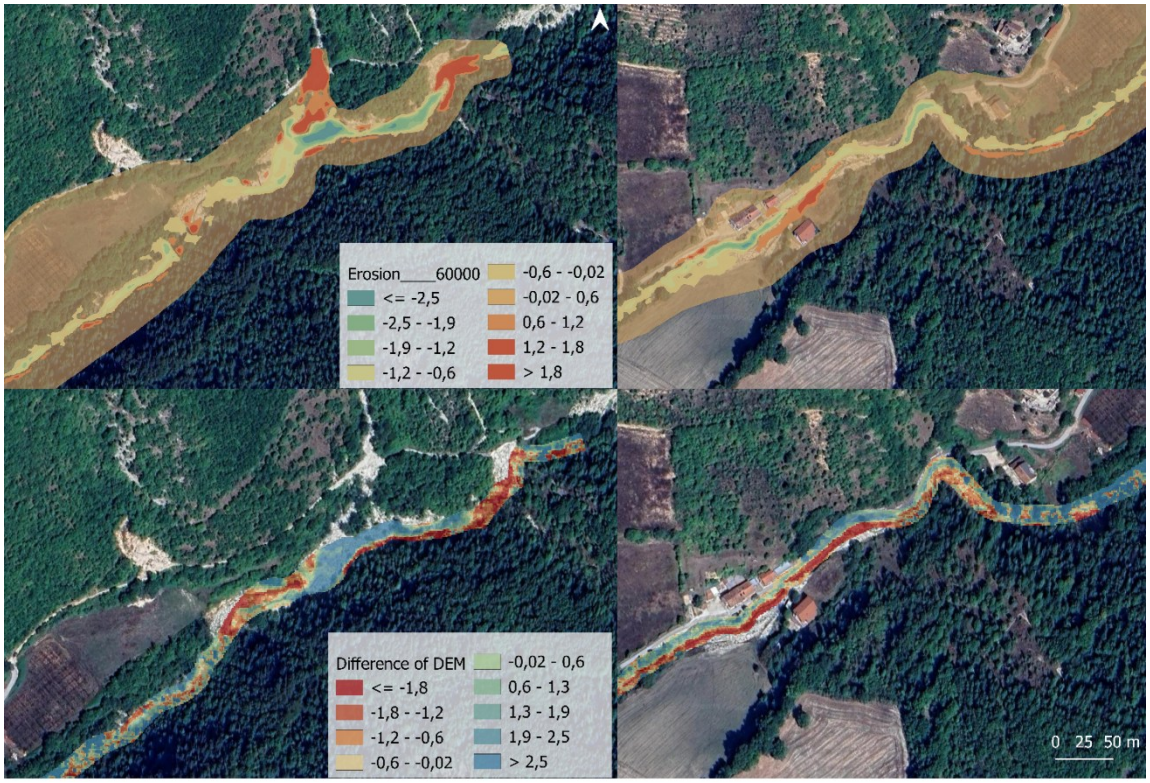

Figure 15 Above: erosion map categorised in 9 classes defining morphological processes. Erosion value in red, positive value (Iber output); aggradation value in blue. Below: DoD – difference of DEM categorised in 9 classes with erosion in red and deposition in blue. Visual comparison for the qualitative validation of the model.

Furthermore, the measurement campaign undertaken in the summer of 2024 made it possible to characterise the sediment in terms of grain size. A pebble count (Wolman, 1954) was performed with a random sampling coarse riverbed material, ZIG – ZAG method. Two main sampling points were defined from downstream to upstream along zigzag trajectories, for a total of 100 randomly measured samples. The value of axis B was taken with a caliber. The results of the campaign were represented by a linear graph in which the values in centimeters (cm) sampled for both sections are defined (Figure **16**). The ordinate shows the diameter expressed in centimetres and the colours represent the grain size as defined in the characterisation by Brunte & Abt, 2001. The blue line represents the upstream grain size taken before the first hydraulic structure (Figure 16, a); the red line represents the downstream grain size, taken just before the closure section (Figure 16, b). The results show that in the upper part of the Tenetra, extremely heterogeneous particles ranging from a minimum of 2 mm to a maximum of 1.10 m are found, with a higher concentration between 0.064 m and 0.256 m. In contrast, the results of the downstream analysis show that only measurements below 0.126 m were found, with a higher concentration between 0.016 m and 0.09 m.

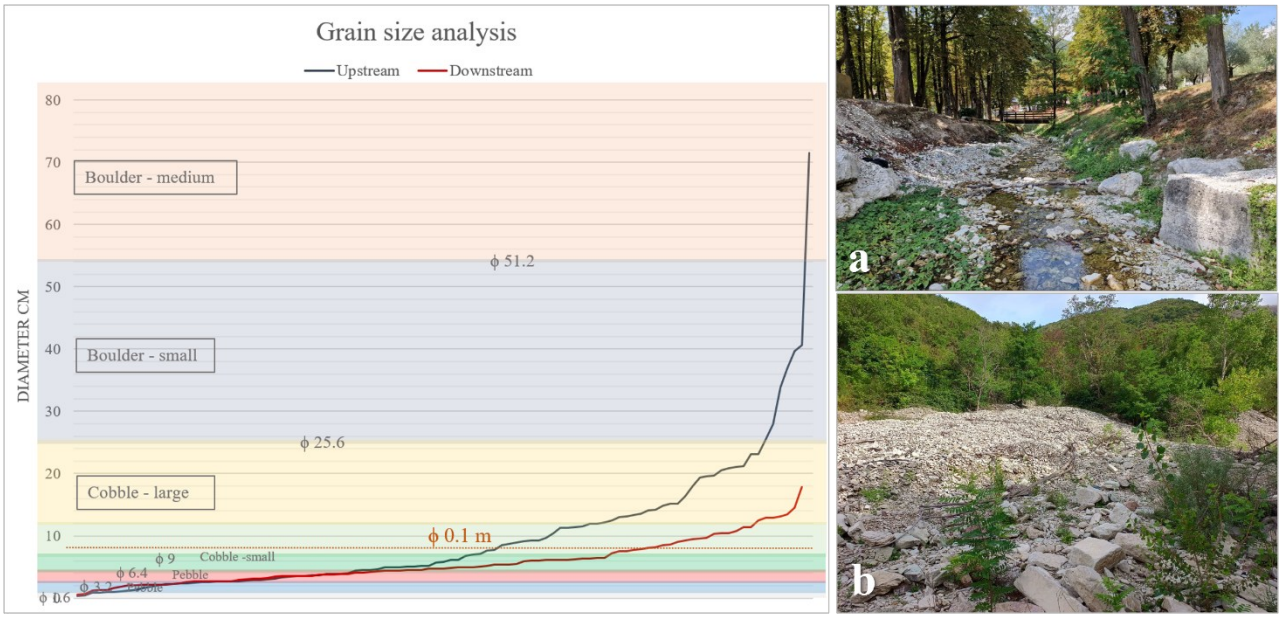

Figure 16 Grain size distribution (Bunte & Abt, 2001) – red line describing an analysis performed downstream close to the end section; blue line describing the result of the pebble count method applied in the upstream part of the river, before the first hydraulic structure. The colours indicate the diameter sizes according to the classification of Bunte & Abt, 2001. a) downstream area sampled, b) upstream area sampled.

3.5 Discussions

Understanding and predicting the geomorphological response of river channels to extreme flood events remains a complex topic, especially considering the interaction between hydrodynamic forces, sediment transport, and morphological feedback (Ziliani et al., 2020; Kashyap et al., 2025). Highly non-linear behaviours are difficult to reproduce in numerical models. Field observations of recent catastrophic floods have shown that, even under comparable hydrological conditions, channel responses can vary from localised incision to extensive sediment accumulation, depending on pre-event morphology and sediment availability (Kashyap et al., 2025). When sediment supply increases suddenly, for example due to slope failures or debris inputs, channels can react in unexpected ways (Müller & Hassan, 2018; Barbosa et al., 2024), moreover variations in grain size strongly affect sediment mobility and bed stability (Guerit et al., 2018). These factors explain why reproducing geomorphological changes during extreme events is challenging and highlight the need for modelling approaches that consider sediment heterogeneity and supply dynamics.

This work shows similarities with the study by Wang et al. (2019), which used flume experiments and morphodynamic modelling to investigate the influence of hydrograph magnitude on sediment transport, focusing on different grain-size classes and their lag effects. The concepts of hysteresis and time-lag identified by Wang et al. (2019) are consistent with the results obtained in this study; however, their analysis was not tested using real flood events as boundary conditions. Moreover, the effect of D_{50} was isolated under controlled laboratory conditions, and the assumption of zero upstream sediment supply represents a simplification of natural torrential systems. In contrast, the Iber model allows sediment input to be defined as a function of discharge, enabling the representation of sediment supply dynamics associated with extreme rainfall events. A comparable modelling-based investigation was conducted by **Yassine et al. (2022)** using the TELEMAC–

SISYPHE framework. While TELEMAC offers a highly flexible numerical environment and advanced options for sediment transport and morphodynamic coupling, their study was limited by the assumption of homogeneous sediment particles. A similar simplification is adopted in the present work; however, this limitation is addressed through the implementation of multiple grain-size scenarios, allowing the influence of sediment calibre on morphological impact and bedload dynamics to be systematically assessed.

The work focuses on simulating riverbed changes during an extreme flood through a calibrated 2D model, with the goal of understanding how parameter variability, sediment supply, and grain size influence morphodynamics, and how effective the current control structures are in limiting sediment transfer. Through sensitivity analysis, it was discovered that bed-load transport is most affected by the bed material characteristics (rock layer), by the transport equation and, obviously, the flow discharge.

3.5.1 Influence of grain size variation on bed-load capacity

By means of hydraulic results and, in particular, critical diameters, it was possible to observe the likelihood of occurrence in relation to different discharges. Analysing the Tenetra section, it can be seen that the potential for movement of particles smaller than 'fine boulders' is high and independent of the flow rate. This leads us to believe that morphological control for grain sizes smaller than 'fine boulders' is mainly topographical. Above values of 0.5 m, the movement of coarse debris depends heavily on the hydraulic flow rate involved. In fact, it can be seen that the three bars mirror the hydrograph curve, showing sediment activation in relation to river flow. The hydro-morphodynamic modelling of the Tenetra channel defined under extreme conditions with a discharge reaching a peak of 61 m^3/s, allows us to develop the following discussions. With the aim of exploring the bed-load mobilised in different granulometric scenarios, the raster resulting from numerical modelling were analysed. The quantity of sediments transported are significantly dependent on granulometric sizes, as well as, of course, on velocity, bed shear stress and water flow rates. Considering extreme conditions such as those experienced during the 2022 flood event and bearing in mind that in such a steep system characterised by calcareous lithologies, the values of the factors described above are high. The results shown are four different possible situations with increasing homogeneous grain sizes. The quantity transported in m^2/s is high in the first two scenarios (SC1 and SC2) and is particularly concentrated in the upstream part, on the main channel and at the confluence with the tributary. Following the hydraulic works, there is a decrease in energy and therefore in transport, which returns to higher values following the channelling of the river along a rocky gorge (where the bedrock is exposed in the river bed), causing sharp increases in speed and enhancing the transport of material downstream. The energy decreases shortly afterwards at the junction with the city, due to tectonic control that causes the valley to open up into a semi-confined river section downstream. A higher value of transported sediments is recorded for scenario SC2, which leads to maximum damage especially in the upstream part. On the contrary, it can be observed that SC1, unlike the second scenario, carries sediments over a greater distance. In fact, this difference can be seen in the downstream part, near to where the first inhabited houses are located. The trend changes and the maximum values from here to the end are given by SC1. For scenarios SC3 and SC4, the movements are more precise and only in rare cases is there a movement of a few metres in the same direction.

Multiple sediments of this size have been found upstream, most of them collapsed from the banks due to lateral erosion or created by the disintegration of coarser material in the riverbed. These debris are carried by the waters that had the energy to transport them only during the peak discharge, failing to maintain continuous transport.

The amount of sediment input, given the water flow and slope, is considerable, but it is evident that it is not at all comparable to the output. Furthermore, observing the curves in Figure **9** (CUT 1, CUT 6), we note that the peak of sediment input coincides with the peak flow entering the system, while the output curve is shifted, defining an arrival delay. Analysing the individual scenarios, it is possible to see that in SC1 - (D 0.01), 15% of the incoming sediments leave the system, while in SC - 2 only 7.6% leave, and finally 0% in SC - 3 and 4.

A validation step that allowed to evaluate these results is the granulometric characterisation carried out in the field in the summer of 2024 (Figure **16**). Sediments with diameters greater than ϕ 0.1 m were found in 10% of the downstream section, probably due to lateral erosion of the banks slightly upstream. This, coupled with the field observations, confirms that the model produced valid results in terms of solid transport.

3.5.2 Sediment retention efficiency

The bottom material transported during the event is retained within the basin. To understand where it is located, several sections were examined. SC3 and SC4 (D 0.75 and D 1) are completely blocked before section number 3, which is located immediately after the hydraulic structure, indicating that 99% of sediments with diameters greater than 0.75 m are retained by the hydraulic structure. A volume of sediment equal to 954.8 m^3 is added from the side channel for SC1; 1169.2 m^3 for SC2. This represents the external sediment input entering the system, which has led to the accumulation of material with metric heights. Consequently, this was added to the channel value to assess the percentage of material retained for the first two scenarios. 75% of sediments with a diameter of 0.01 m are retained by the first hydraulic structure, while 71% of sediments with diameters of 0.1 m are retained. The structure examined proves to be efficient in retaining sediments with diameters greater than 0.75 m, even in extreme flood conditions. By analysing the other hydraulic structures, we can estimate that, in relation to the passing material, 50% is retained in the second structure in SC1, while 57% is retained in SC2. The last structure is old and consists of a wall that essentially creates a significant hydraulic jump, resulting in a considerable increase in speed, that allows the flow to transport more sediment without blocking its path.

3.5.3 Sediment supply influence

In order to characterise the sediment supply of the Tenetra River, the inputs of material entering the river system were analysed. The main source of bed load is the main course, where intense mobilisation was observed, especially in the upstream part of the model. However, the contribution from the side channel was also significant, producing deposits several metres thick due to the presence of a weir that blocked most of the material coming from upstream. The erosive tributary channel was already deeply incised over the years but proved to still have a recharge that allows it to discharge sediments in extreme conditions. In particular, the transported sediments have a rather homogeneous grain size due to the lower consistency of the original lithological formation. It should also be noted that the value of the sedimentary contribution from the landslide,

defined for the first two scenarios with grain sizes consistent with field assessments, represents quantities comparable to the input into the main system (Figure **10** – CUT 2). This allows us to conclude that the influence on morphological change and sediment load is high and that not considering this additional material would have greatly altered the results. The importance of considering the connectivity channels that introduce material into natural mountain river systems is extremely high and useful in terms of prevention and management of emergency systems.

As there are no data relating to the measurement of solid bed-load transport, nor any monitoring stations, the data presented in these last two paragraphs have been qualitatively validated. Field observations show that the contribution of the secondary channel has completely changed the response of the system. The material released by the tributary, coupled with that mobilised upstream, quickly filled the hydraulic structure, creating the highest values in terms of sedimentation. The DoD confirms values of around 4 metres of aggradation, while models show sedimentation processes with values ranging between 2 and 4 metres.

3.5.4 Influence of grain size variation on morphological changes

The geomorphological impact, assessed through statistical analysis of raster, shows that an increase in grain size corresponds to a decrease in response (Figure **11**). This is explained by the energy required to mobilise particles with different grain sizes. The lower mobility of particles with $\phi > 0.75$ m and their greater retention by hydraulic structures reduce the morphological impact in the downstream part of the analysis basin in terms of erosion and deposition. In terms of area, SC1 and SC2 have an erosive impact of 13% and 12% respectively. Scenarios SC3 and SC4 have an impact of 7% and 6.5% respectively. Erosion is similar in the upper part of the basin, especially in the secondary channel, as the geometry was significantly altered during the extreme event. The downstream area, on the other hand, has values reaching a maximum of 1.5 m of erosion, concentrated on the banks of the channel, which have been significantly altered. The aggradation resulting from the presence of the structure and the severe erosion in the upper part of the channel has high values reaching almost 4 metres in the area upstream of the first structure. This phenomenon is also due to the fact that the slope in this area decreases, allowing the velocity to decrease and sedimentation to occur. Percentages of 9.6% and 8.6% represent the area occupied by deposition phenomena for the first two scenarios. Since the last two scenarios are similar and deposit more in the same upstream area, they represent 5.8% and 5.3% respectively. The total geomorphological impact or total morphological change described in Figure **12** allows us to conclude that sediments with $\phi > 0.75$ m have a lesser impact on the analysed area and require exceptional flood flows to be mobilised, and that even if the peak value managed to activate them, they are not transported over long distances in terms of time. Coarse sediments are removed and deposited in a very short time without travelling long distances. On the contrary, sediments with $\phi < 0.1$ m represent a potential factor of greater danger because they have a greater transport capacity that is only partially retained by the structures. The transport of these materials allows them to reach velocities enough to produce significant erosive effect, in terms of both area and volume. Looking at the graph in Figure **13** we can see that intense erosion, with depths > 2 m, is mainly caused by sediments with diameters of 0.1 m, representing the most impactful scenario in terms of area.

The results of comparing the erosion model with the DoD show consistency in the main areas most affected. In particular, the deposition area upstream has values of approximately +4 metres, which, although differing in range between the model and the DoD, represents a critical area in both, with maximum values due to the addition of material from the side channel. In addition to the areas undergoing aggradation upstream, correspondences were noted between some eroding banks and flooded areas with the flood simulated by the model. Comparisons in this regard were made through interpretative assessments in the field, validating the data qualitatively. Extensive erosion is evident at the first group of houses in the area. In fact, although this area has not been aggressively damaged, the river course has suffered a water overflow, causing intense erosion of both the road and the agricultural field, which represent its banks at this point.

It is possible to conclude that the scenarios that manage to sustain a continuous transport rate and that could create risk scenarios, due to their lower retention, even in high-energy systems, are grain sizes characterised by $\phi < 0.1$ m. These sediments can in turn be divided according to the energy of the system. In high-energy environments, it is important to focus on sediments with diameters of 0.1 m, while in valley areas, the greatest transport comes from diameters of 0.01 m. Overall, the study demonstrates that combining high-resolution numerical modelling with field observations provides valuable insights into sediment behaviour during extreme events. Furthermore, the model was implemented with a minimum input value and has amply demonstrated that with an increase in calibration and validation data, more accurate simulations could be obtained and emergency scenarios predicted, which are increasingly relevant in many countries.

3.6 Conclusions

This study investigated the geomorphological response of the Tenetra stream during the September 2022 extreme flood through a two-dimensional morphodynamic model. The modelling approach allowed to test how sediment grain size, supply conditions, and hydraulic works influence bed-load transport and morphological evolution. This river basin has a strong topographical control due to its chemical-physical characteristics, which make it more prone to sediment mobilisation. It can be observed that grain sizes larger than ‘fine boulders’ indicate a direct relationship of likelihood as a function of the flow involved. To examine how the river would react to the sedimentation and erosion processes that cause the morphological changes in the riverbed, many scenarios of grain size variation were created: D_{50} 0.01 m; D_{50} 0.1 m; D_{50} 0.75 m; D_{50} 1 m. Results indicate that grain size strongly controls sediment mobility: finer sediments ($\phi < 0.1$ m) are easily mobilised and travel over longer distances, generating the most significant erosion and deposition patterns. Coarser materials ($\phi > 0.75$ m), on the other hand, are largely retained upstream of hydraulic structures and require exceptional discharges to be set in motion. They require high energy to be removed, and it has been observed that they are quickly deposited along a short path. Although ϕ 0.01 is responsible for erosion downstream of the analysed section, a value of ϕ 0.1 represents the most impactful scenario, the least restrained and the most dangerous. The retention structures were generally efficient, especially for large particles, but finer fractions can still pass through and pose downstream risks. It is interesting to note, however, that works of the right size and positioned in series

are able to retain sediments with $\phi > 0.75$, and attention can be focused on defence systems for sediments with $\phi < 0.1$. The model also highlighted that sediment contributions from lateral channels and slope-derived debris significantly increase morphological impact. This confirms the importance of including sediment connectivity and tributary inputs in flood-related morphodynamic simulations. The proposed methodology can support the design of sediment management strategies and improve the assessment of flood-related geomorphic hazards in similar mountainous basins. Considering the transport of coarse sediments in extreme events is essential, as is predicting the geomorphological impact and monitoring over time. When large quantities of coarse material are mobilised, they can modify the channel geometry, altering cross-sectional profiles, slope, and local roughness conditions. These changes directly influence hydraulic behaviour in subsequent floods, potentially increasing water levels, modifying conveyance capacity, and redirecting flow paths. Morphodynamic feedbacks demonstrate that flood hazard is not a static condition but a dynamic continuous process which must be understood for effective management and planning in emergency conditions. In emergency contexts, this information can guide rapid interventions such as sediment clearance, temporary retention barriers, or river training works to stabilise critical reaches before the next high-flow event (Rickenmann et al., 2016).

CHAPTER IV
Discussion and conclusion

Climate change in mountainous regions introduces significant uncertainty due to complex orography, sparse observations, and the difficulty of accurately representing high-elevation processes in numerical models (Beniston et al., 1997). In these environments, river channel morphodynamics exert a central influence on hydraulic and hydrogeological risk management. Bank protection structures and sediment retention works can trigger complex feedbacks between flow, sediment, and morphology, highlighting the need to integrate geomorphic sensitivity into flood risk mapping and planning (Dingle et al 2019; Nones et al., 2023). Considering the current increase in the intensity of rainfall events, it is necessary to have rapid and practical responses, aligning with the objectives of global shared agendas. The impacts of changes on extreme precipitation and flood frequency should be quantified for design guidelines. The impacts of changes on extreme precipitation and flood frequency should be quantified in order to define design guidelines. Understanding future risk profiles and finding flexible, process-oriented modelling tools to anticipate system responses are increasingly necessary (Madsen et al., 2014). In a non-stationary context, where hydrological regimes, sediment budgets, and climatic forcing are shifting, the traditional assumption of stationarity is no longer valid. Quantifying the impacts of non-stationarity on precipitation extremes and flood frequency is essential for developing adaptive design standards and improving the understanding of future risk profiles (Madsen et al., 2014; Blöschl et al., 2019). The impact of bed shape and sediment transport on flood risk, inundation levels and extent require more attention than in the past (Sinnakaudan et al., 2003; Liu et al., 2022; Nones et al., 2023; Hamidifar et al., 2024). One of the new approaches developed is the flash flood risk assessment, which includes the influence of sediment by estimating potential sediment risk is described in Liu et al., 2022.

The approach developed in this thesis shares conceptual similarities with network-scale sediment connectivity models, such as the D-CASCADE framework proposed by Tangi et al. (2022). This framework quantifies sediment budgets and explores reservoir sediment management strategies at a basin scale. While these models offer valuable insights into long-term sediment transfer and storage patterns, they do not explicitly resolve event-scale hydraulics or morphodynamic processes. In contrast, the present study focuses on extreme flood conditions, combining catchment-scale identification of sediment source areas with two-dimensional (2D) morphodynamic modelling to explicitly simulate bed-load transport, grain-size effects and channel adjustments during a real flood event. Therefore, the two approaches are complementary, addressing sediment connectivity from long-term planning and short-term hazard perspectives, respectively. Other similarities have been highlighted in Pinel's (2016) study, which adopts a two-dimensional framework to explicitly simulate the interaction between hydraulics and sediment transport during extreme events. However, while Pinel's work and several comparable studies commonly rely on advanced modelling platforms such as TELEMAC-SISYPHE, which are characterised by high numerical flexibility, the use of IBER in this research reflects a deliberate trade-off between physical detail and operational applicability. While TELEMAC offers a comprehensive treatment

of sedimentary processes, it requires greater computational effort, longer configuration times, and specialist expertise, which may limit its use in contexts requiring a rapid response or where data are scarce. In contrast, IBER provides a robust, computationally efficient 2D solution that is particularly suited to steep, torrential channels and unstable flows. It allows for systematic sensitivity analyses of grain size and sediment input under real flood conditions.

The study concern the purpose of impact reduction of extreme events on mountainous catchments. This research proposes an integrated methodology that links the identification of sediment source areas at the basin scale with detailed morphodynamic simulations at the reach scale. The approach combines individual event-based analyses into a comprehensive framework that reproduces system behaviour under extreme rainfall. This integration of approaches at different scales allows for the assessment of cascade effects, in which a main event triggered a series of processes involving the mobilisation of material and the consequent influence of solid transport and its interactions with other factors. Quantifying sediment transport rates, especially under high-flow conditions, is fundamental to understanding channel evolution and flood hazard. However, direct measurements during major floods remain logistically difficult and often uncertain (Khosravi et al., 2020). The modelling framework developed here therefore offers a rapid and operationally replicable approach, particularly useful in data-scarce mountainous basins. Adopting a cascading disaster perspective allows for a proactive understanding of system dynamics and promotes anticipatory risk reduction strategies (Huggins et al., 2021). An important aspect of the thesis is the use of open-source software (Iber, QGIS, and SedIN) and reproducible indices (Connectivity Index, Stream Power Index, and Stream Length-Gradient Index), which make the procedure reliably replicable on similar case studies.

The study area, representative of torrential rivers in the northern Apennines, was selected to analyse sediment source activation, grain-size variability, and morphodynamic response during the extreme event of September 2022. The results integrate two complementary scales of investigation. At the catchment scale, a GIS-based approach enabled rapid detection of sediment source zones and their connectivity to the drainage network through morphometric indices such as the Stream Power Index (SPI), the Index of Connectivity (IC), and the Stream Length-Gradient (SL). This method proved efficient even in data-limited mountainous environments, providing valuable information for emergency response and post-event assessment (Borselli et al., 2008; Cavalli et al., 2013). Identifying highly connected sediment pathways supports the prioritisation of areas prone to mobilisation during intense rainfall, offering a fundamental input for both modelling and risk mitigation planning. At the reach scale, a two-dimensional numerical model (Iber) was used to simulate the morphodynamic evolution of the Tenetra stream, a tributary of the Burano River, during the 2022 flood. The model explored the sensitivity of sediment transport and channel response to variations in sediment grain size, sediment supply, and structural interventions. The results demonstrated that coarse sediment supply and bed composition strongly control erosion–deposition patterns, influencing channel geometry and the effectiveness of retention structures. Parameters such as transport equations, grain-size distribution, and discharge regime were found to exert major influence on model outcomes, underscoring the need for calibrated and context-

specific parameterisation in morphodynamic simulations. Together, these two research components illustrate the importance of a multi-scale and integrated approach to sediment management in mountain basins. The first component captures the spatial organisation and geomorphic predisposition of the catchment, while the second quantifies the dynamic behaviour of sediment transport during extreme floods. The combination of geomorphometric mapping and process-based modelling provides a holistic understanding of how sediment availability and system connectivity drive morphological change. From a broader management perspective, the proposed framework contributes to more effective hydraulic and hydrogeological risk management. Predicting geomorphic responses under future extreme conditions remains a challenge due to the non-linear feedbacks between flow, sediment, and morphology. However, the results demonstrate that coupling topographic indicators with physically based models yields reliable, scalable, and operationally relevant outcomes. Bed-load transport processes must be explicitly considered in flood management, as they reshape cross-sections, alter roughness, and change the hydraulic conveyance capacity of river systems. Neglecting these processes can lead to underestimation of flood risk and to maladaptive interventions. Integrating geomorphic feedbacks into hazard mapping and infrastructure design enhances the capacity to anticipate system responses and supports long-term resilience planning (Rinaldi et al., 2020; Wohl et al., 2019). Ultimately, this thesis bridges geomorphological interpretation and numerical simulation, offering both diagnostic and predictive tools. By linking sediment source detection with downstream morphodynamic modelling, it delivers a transferable framework for mountain basins prone to flash floods and sediment hazards. The integration of geomorphometric, hydraulic, and sediment transport perspectives represents a step toward more comprehensive and process-based strategies for landscape resilience and emergency preparedness.

4.1 Future perspective

Extreme climatic events are increasingly recognised as the outcome of multiple interacting drivers rather than isolated phenomena (Seneviratne et al., 2012). Recent research demonstrates that compound and cascading hazards, where several processes occur simultaneously or sequentially, are becoming more frequent and are responsible for many of the most severe climate-related disasters (Zscheischler et al., 2020; Lee et al., 2024). Mountain regions, with their steep terrain and geomorphic sensitivity, are particularly prone to such interactions, where hydrological, geomorphological, and cryospheric processes combine to amplify risks (Alcántara-Ayala, 2025). Future researches should therefore adopt a cascading-hazard perspective, recognising that river catchments operate as interconnected systems where multiple processes co-evolve and influence one another. Developing numerical models capable of simulating coupled processes within a unified framework remains a key research frontier. Integrating this systemic understanding into hydraulic and hydrogeological risk management will enable the anticipation of multi-process responses and support the design of adaptive, robust, and sustainable mitigation strategies.

Acknowledgements

This work is a PNRR project made possible thanks to the supervision of Professor Morelli Stefano, who guided me on this path of academic growth, and Professor Alberto Renzulli, who has never missed one of my milestones, the co-supervisor of the thesis.

I would like also to extend my thanks to:

The scientific support provided by Institute of Geography in Bern – Natural Hazard section. Virginia Villanueva, who taught me with great passion, organisation and empathy. Maha and Mauro, two very special people.

The Flumen Intitute, in particular Ernest Castellet Bladé who welcomed me during my period abroad and trained me with his smart and inspiring critical thinking. And to all the PhD students and workers who welcomed me in Barcelona.

Thanks to all my colleagues who have supported and helped me, especially to Mahnoor, who has been a companion to my soul for all these three years, becoming part of me. Thank you to Fedi, Franci, Carla, Nico, Giulio, and Alberto because I feel at home with all of you.

I am grateful for people that life has decided to bring into… and for these years full of adventures and tears and laughter and waiting for refunds and sleepless nights waiting for you, ah no, waiting for the article to be accepted.

Thanks to my dog, who follows me everywhere and is the geologists' mascot. Finally, I'd like to say thank you to my family, who have supported me at every moment of my life, giving me the opportunity to grow with my strong ideas and a big heart to experience all emotions that makes this world amazing.

Reference

Abebe, N., Eekhout, J., Vermeulen, B., Boix-Fayos, C.,Vente, J., Grum, B., Hoitink, T., Baartman, J., 2023. The potential and challenges of the 'RUSLE-IC-SDR' approach to identify sediment dynamics in a Mediterranean catchment. CATENA, Volume 233, 107480, ISSN 0341-8162, https://doi.org/10.1016/j.catena.2023.107480

Abu El-Magd, S.O., Orabi, H.O., Ali, S.A., Parvin, F., Pham, Q.B., 2021. An integrated approach for evaluating the flash flood risk and potential erosion using the hydrologic indices and morpho-tectonic parameters. Environ. Earth Sci. 80, 694. https://doi.org/10.1007/s12665-021-10013-0.

Alcántara-Ayala, I., 2025.Cascading hazards and compound disasters. npj Nat. Hazards 2, 54. https://doi.org/10.1038/s44304-025-00111-5

Alfieri, L., Bisselink, B., Dottori, F., Naumann, G., de Roo, A., Salamon, P., Wyser, K., & Feyen, L., 2017. Global projections of river flood risk in a warmer world. Earth's Future, 5(2), 171–182. https://doi.org/10.1002/2016EF000485.

Amici, M., Spina, R., 2002. Campo medio della precipitazione annuale e stagionale sulle Marche per il periodo 1950-2000. Protezione Civile Regione Marche, Centro di Ecologia e Climatologia. Osservatorio Geofisico Sperimentale Macerata.Barchi, M.R., Alvarez, W., Shimabukuro, D.H, 2012. The Umbria-Marche Apennines as a double orogen: Observations and hypotheses. Ital. J. Geosci. 131, 258–27. https://doi.org/10.3301/IJG.2012.17.

Amponsah, W., Ayral, P.-A., Boudevillain, B., Bouvier, C., Braud, I., Brunet, P., Delrieu, G., Didon-Lescot, J.-F., Gaume, E., Lebouc, L., Marchi, L., Marra, F., Morin, E., Nord, G., Payrastre, O., Zoccatelli, D., Borga, M., 2018. Integrated high-resolution dataset of high-intensity European and Mediterranean flash floods. Earth System Science Data. 10. 1783-1794. 10.5194/essd-10-1783-2018.

Amponsah, W., Marchi, L., Zoccatelli, D., Boni, G., Cavalli, M., Comiti, F., Crema, S., Lucía, A., Marra, F., Borga, M., 2016. Hydrometeorological Characterization of a Flash Flood Associated with Major Geomorphic Effects: Assessment of Peak Discharge Uncertainties and Analysis of the Runoff Response. Journal of Hydrometeorology. 17. 3063-3077. 10.1175/JHM-D-16-0081.1.

Amponsah, W., Marra, F., Zoccatelli, D., Marchi, L., Crema, S., Pirastru, M., Borga, M., 2022. Scale-dependence of observational and modelling uncertainties in forensic flash flood analysis. Journal of Hydrology. 607. 127502. 10.1016/j.jhydrol.2022.127502.

Baartman, E.M. J., Nunes, P. J., Masselink, R., Darboux, F., Bielders, C., Degré, A., Cantreul, V., Cerdan, O., Grangeon, T., Fiener, P., Wilken, F., Schindewolf, M., Wainwright, J., 2020. What do models tell us about water and sediment connectivity? Geomorphology, Volume 367, 107300, ISSN 0169-555X, https://doi.org/10.1016/j.geomorph.2020.107300.

Barbosa, N., Leinauer, J., Jubanski, J., Dietze, M., Münzer, U., Siegert, F., Krautblatter, M., 2024. Massive sediment pulses triggered by a multi-stage 130 000 m³ alpine cliff fall (Hochvogel, DE-AT). Earth Surf. Dynam., 12, 249–269. https://doi.org/10.5194/esurf-12-249-2024.

Barchi, M.R.; Alvarez, W.; Shimabukuro, D.H. The Umbria-Marche Apennines as a double orogen: Observations and hypotheses. Ital. J. Geosci. 2012, 131, 258–27. https://doi.org/10.3301/IJG.2012.17.

Bendia, F., Bufalini, M., Farabollini, P., and Materazzi, M.: The 15 September 2022 floods in northern Marche (Central Italy): disaster analysis, case studies and mitigation strategies for geomorphological- hydraulic risk, EGUsphere [preprint], https://doi.org/10.5194/egusphere-2025-4405, 2025.

Beniston, M., Diaz, H., Bradley, R., 1997. Climatic Change at High Elevation Sites: An Overview. Climatic Change. 36. 233-251. 10.1023/A:1005380714349.

Beniston, M., Diaz, H., Bradley, R., 1997. Climatic Change at High Elevation Sites: An Overview. Climatic Change. 36. 233-251. 10.1023/A:1005380714349.

Benito, G., & Vázquez-Tarrío, D., 2022. Hazardous Processes: Flooding. Treatise on Geomorphology. Elsevier. http://doi.org/10.1016/b978-0-12-818234-5.00081-x.

Bladé Castellet, E., Cea, L., & Corestein, G., 2014. Numerical modelling of river inundations. Ingeniería del agua, 18(1), 71-82. https://doi.org/10.4995/IA.2014.3144.

Bladé, E., Cea, L., Corestein, G., Escolano, E., Puertas, J., Vázquez-Cendón, E., Dolz, J., Coll, A., 2014. Iber: herramienta de simulación numérica del flujo en ríos, Rev. int. métodos numér. cálc. diseño ing., 30(1), p 1-10. URL https://www.scipedia.com/public/Blade_et_al_2012a.

Bladé, E., Gómez-Valentín, M., Dolz, J., Aragón-Hernández, J. L., Corestein, G., and Sánchez-Juny, M., 2012. "Integration of 1D and 2D Finite Volume Schemes for Computations of Water Flow in Natural Channels." Advances in Water Resources, 42, 17–29. https://doi.org/10.1016/j.advwatres.2012.03.021.

Borga, M., Comiti, F., Ruin, I., Marra, F., 2019. Forensic analysis of flash flood response. WIREs Water. 6:e1338. https://doi.org/10.1002/wat2.1338.

Borga, M., Stoffel, M., Marchi, L., Marra, F., Jakob, M., 2014. Hydrogeomorphic response to extreme rainfall in headwater systems: Flash floods and debris flows, Journal of Hydrology, Volume 518, Part B, Pages 194-205, ISSN 0022-1694, https://doi.org/10.1016/j.jhydrol.2014.05.022.

Borrelli, P., Robinson, D. A., Panagos, P., Lugato, E., Yang, J. E., Alewell, C., Wuepper, D., Montanarella, L., & Ballabio, C., 2020. Land use and climate change impacts on global soil erosion by water (2015–2070). Proceedings of the National Academy of Sciences of the United States of America, 117(36), 21 994–22 001. https://doi.org/10.1073/pnas.2001403117.

Borselli, L., Cassi, P., Torri, D., 2008. Prolegomena to sediment and flow connectivity in the landscape: A GIS and field numerical assessment. CATENA. 75. 268-277. https://doi.org/10.1016/j.catena.2008.07.006.

Borselli, L., Cassi, P., Torri, D., 2008. Prolegomena to sediment and flow connectivity in the landscape: A GIS and field numerical assessment. CATENA. 75. 268-277. https://doi.org/10.1016/j.catena.2008.07.006.

Bracken, L.J., Turnbull, L., Wainwright, J., Bogaart, P., 2015. Sediment connectivity: a framework for understanding sediment transfer at multiple scales. Earth Surface Processes and Landforms. 40(2), 177-188. https://doi.org/10.1002/esp.3635.

Bracken, L.J., Turnbull, L., Wainwright, J., Bogaart, P., 2015. Sediment connectivity: a framework for understanding sediment transfer at multiple scales. Earth Surface Processes and Landforms. 40(2), 177-188. https://doi.org/10.1002/esp.3635.

Brenna, A., Scorpio, V., Finotello, A., Zarabara, F., Surian, N., (2025). Suspended transport of gravel in rivers: Empirical evidence from the 2022 flood in the Misa River (Eastern Apennines, Italy). Earth Surface Processes and Landforms. 50. 10.1002/esp.70081.

Brierley, G., Fryirs, K. and Jain, V. (2006), Landscape connectivity: the geographic basis of geomorphic applications. Area, 38: 165-174. https://doi.org/10.1111/j.1475-4762.2006.00671.x

Bunte, K. & Abt, S., 2001. Sampling Surface and Subsurface Particle-Size Distributions in Wadable Gravel- and Cobble-bed Streams for Analyses in Sediment Transport, Hydraulics, and Streambed Monitoring. USD A-Rocky Mountain Research Station, General Technical Report RMRS-GTR-74. 74.

CARG Project—Geologic and geothematic cartography. (1988). Geologic and Geothematic Cartography. https://www.isprambiente.gov.it/en/projects/soil-and-territory/carg-project-geologic-and-geothematic-cartography-1(accessed 14 October 2025).

Cavalli, M., Trevisani, S., Comiti, F., Marchi, L., 2013. Geomorphometric assessment of spatial sediment connectivity in small Alpine catchments. Geomorphology. 188, 31-41. https://doi.org/10.1016/j.geomorph.2012.05.007.

Cavalli, M., Trevisani, S., Comiti, F., Marchi, L., 2013. Geomorphometric assessment of spatial sediment connectivity in small Alpine catchments. Geomorphology. 188, 31-41. https://doi.org/10.1016/j.geomorph.2012.05.007.

Cea, L., Bermudez, M., Puertas, J., Blade, E., Corestein, G., Escolano, E., Conde, A., Bockelmann-Evans, B., and Ahmadian, R., 2016. IberWQ: new simulation tool for 2D water quality modelling in rivers and shallow estuaries. Journal of Hydroinformatics 18, 816–830. DOI: 10.2166/hydro.2016.235.

Cea, L., and E. Bladé, 2015. A simple and efficient unstructured finite volume scheme for solving the shallow water equations in overland flow applications, Water Resour. Res., 51, 5464–5486, doi:10.1002/2014WR016547.

Chow, V.T. 1959. Open-channel Hydraulics. MacGraw-Hill Book Co., NY.

Chowdhury, Md.S., 2023. Modelling hydrological factors from DEM using GIS. MethodsX. 10, 102062. https://doi.org/10.1016/j.mex.2023.102062.

Church, M. & Hassan, M. A., 1992. Size and distance of travel of unconstrained clasts on a streambed, Water Resour. Res., 28(1), 299–303, doi:10.1029/91WR02523.

Coe, J. & Godt, J., 2012. Review of approaches for assessing the impact of climate change on landslide hazards. Landslides and Engineered Slopes, Protecting Society Through Improved Understanding. 1. 371-377.

Comendador, G. J., 2021. Sediment fingerprinting and hydro-sedimentary monitoring as tools for catchment management in Mediterranean environments. PhD thesis Universitat de les Illes Balears. Doctorat en Història, Història de l'Art i Geografia.

Confuorto, P., Franceschini, R., Scarpitta, L., Casagli, N., Morelli, S., Raspini, F., Tofani, V., Moretti, S., (2025). Event-based landslide inventory through very high-resolution optical images and field surveys. Geoenvironmental Disasters. 12. 10.1186/s40677-025-00328-6.

Corti, M., Francioni, M., Abbate, A., Papini, M., & Longoni, L. (2024). Analysis and modelling of the September 2022 flooding event in the Misa Basin. Italian Journal of Engineering Geology and Environment, 69–76. https://doi.org/10.4408/IJEGE.2024-01.S-08.

Corti, M., Francioni, M., Abbate, A., Papini, M., Longoni, L., (2024). ANALYSIS AND MODELLING OF THE SEPTEMBER 2022 FLOODING EVENT IN THE MISA BASIN. Italian Journal of Engineering Geology and Environment. 1. 69-76. 10.4408/IJEGE.2024-01.S-08.

Cossart, É., Fressard, M., 2017. Assessment of structural sediment connectivity within catchments: insights from graph theory. Earth Surf. Dynam., 5, 253–268. https://doi.org/10.5194/esurf-5-253-2017.

Crema, S., Cavalli, M., 2018. SedInConnect: a stand-alone, free and open source tool for the assessment of sediment connectivity. Computers & Geosciences. 111. 39-45. https://doi.org/10.1016/j.cageo.2017.10.009.

Da Ros, D., & Borga, M., 1997. Use of digital elevation model data for the derivation of the geomorphological instantaneous unit hydrograph. Hydrological processes, 11(1), 13-33.

Dijkstra, T.A. & Dixon, N., 2010. Climate change and slope stability: Challenges and approaches. Quarterly Journal of Engineering Geology and Hydrogeology, 43, 4, 371-385.

Dingle, E. H., Paringit, E. C., Tolentino, P. L. M., Williams, R. D., Hoey, T. B., Barrett, B., Long, H., Smiley, C., Stott, E., 2019. Decadal-scale morphological adjustment of a lowland tropical river, Geomorphology, Volume 333, Pages 30-42, ISSN 0169-555X, https://doi.org/10.1016/j.geomorph.2019.01.022.

Donnini, M., Santangelo, M., Gariano, S.L. et al. Landslides triggered by an extraordinary rainfall event in Central Italy on September 15, 2022. Landslides 20, 2199–2211 (2023). https://doi.org/10.1007/s10346-023-02109-4.

Donnini, M., Santangelo, M., Gariano, S.L., Bucci, F., Peruccacci, S., Alvioli, M., Althuwaynee, O., Ardizzone, F., Bianchi, C., Bornaetxea, T., Brunetti, M.T., Cardinali, M., Esposito, G., Grita, S., Marchesini, I., Melillo, M., Salvati, P., Yazdani, M., Fiorucci, F., 2023. Landslides triggered by an extraordinary rainfall event in Central Italy on September 15, 2022. Landslides. 20(10), 2199-2211. https://doi.org/10.1007/s10346-023-02109-4.Gennari, E., Biagiotti, F., Mengarelli, D., Striglio, G., Cristallo, C., 2023. La gestione dell'emergenza nell'ultimo miglio: il caso dell'alluvione nelle Marche del 15 settembre 2022. SIGEA Società Italiana di Geologia Ambientale – APS. ISSN 1591-5352.

European Commission – Joint Research Centre, 2020. Land use and climate change impacts on global soil erosion by water (2015–2070). Global Soil Erosion – Future projections. https://esdac.jrc.ec.europa.eu/themes/global-soil-erosion-future-projections

Fryirs KA, Brierley GJ, Hancock F, et al. Tracking geomorphic recovery in process-based river management. Land Degrad Dev. 2018;1-24. https://doi.org/ 10.1002/ldr.2984.

Fryirs, K., 2013, (Dis)Connectivity in catchment sediment cascades: a fresh look at the sediment delivery problem. Earth Surf. Process. Landforms, 38: 30-46. https://doi.org/10.1002/esp.3242.

Gariano, S. L. & Guzzetti, F., 2016. Landslides in a changing climate, Earth-Science Reviews, Volume 162, Pages 227-252, ISSN 0012-8252, https://doi.org/10.1016/j.earscirev.2016.08.011.

Gariano, S. L. & Rianna, G., 2025. How will the projected climate change influence rainfall-induced landslides in Europe? A review of modelling approaches. Landslides. 10.1007/s10346-025-02550-7.

Gentilucci, M., Materazzi, M., Pambianchi, G., Burt, P., Guerriero, G., 2020. Temperature variations in Central Italy (Marche region) and effects on wine grape production. Theoretical and Applied Climatology.140. 10.1007/s00704-020-03089-4.

Guerit, L., Barrier, L., Liu, Y., Narteau, C., Lajeunesse, E., Gayer, E., Métivier, F., 2018. Uniform grain-size distribution in the active layer of a shallow, gravel-bedded, braided river (the Urumqi River, China) and implications for paleo-hydrology. Earth Surf. Dynam., 6, 1011–1021. https://doi.org/10.5194/esurf-6-1011-2018.

Guo, Z., Wu, L., Liu, S., Zhang, H., Du, B., Ruan, B., 2023. An integrated watershed modelling framework to explore the covariation between sediment connectivity and soil erosion. European Journal of Soil Science. Volume 74. https://doi.org/10.1111/ejss.13412

Hack, J.T., 1973. Stream-profile analysis and stream-gradient index. Journal of Research of the U.S. Geological Survey, 1(4), 421-429. https://pubs.usgs.gov/publication/70161653 (accessed 30 July 2024).

Hamidifar, H., Keshavarzi, A., & Rowiński, P. M. 2020. Influence of Rigid Emerged Vegetation in a Channel Bend on Bed Topography and Flow Velocity Field: Laboratory Experiments. Water, 12(1), 118. https://doi.org/10.3390/w12010118.

Hamidifar, H., Nones, M., Rowiński, P., 2024. Flood modeling and fluvial dynamics: A scoping review on the role of sediment transport. Earth-Science Reviews. 253. 104775. 10.1016/j.earscirev.2024.104775.

Haque, U., da Silva F. P., Devoli, G., Pilz, J., Zhao, B., Khaloua, A., Wilopo, W., Andersen, P., Lu, P., Lee, J., Yamamoto, T., Keellings, D., Wu, J-H., Glass, E. G., 2019. The human cost of global warming: Deadly landslides and their triggers (1995–2014), Science of The Total Environment, Volume 682, Pages 673-684, ISSN 0048-9697, https://doi.org/10.1016/j.scitotenv.2019.03.415.

Harvey, A. M. 2001. Coupling between hillslopes and channels in upland fluvial systems: implications for landscape sensitivity, illustrated from the Howgill Fells, northwest England *CATENA*, Landscape sensitivity: principles and applications in Northern, 42 (2): 225–50. https://doi.org/10.1016/S0341-8162(00)00139-9

Heckmann, T., Cavalli, M., Cerdan, O., Foerster, S., Javaux, M., Lode, E., Smetanová, A., Vericat, D., Brardinoni, F., 2018. Indices of sediment connectivity: opportunities, challenges and limitations. Earth Sci. Rev. 187, 77–108. https://doi.org/10.1016/j.earscirev.2018.08.004.

Heckmann, T., Cavalli, M., Cerdan, O., Foerster, S., Javaux, M., Lode, E., Smetanová, A., Vericat, D., Brardinoni, F., 2018. Indices of sediment connectivity: opportunities, challenges and limitations. Earth Sci. Rev. 187, 77–108. https://doi.org/10.1016/j.earscirev.2018.08.004.

Hjulström, F. (1935). Studies of the morphological activity of rivers as illustrated by the River Fyris. Bulletin of the Geological Institute, University of Uppsala, 25, 221–527.

Hooke, J., 2003. Coarse sediment connectivity in river channel systems: a conceptual framework and methodology, Geomorphology, Volume 56, Issues 1–2, Pages 79-94, ISSN 0169-555X, https://doi.org/10.1016/S0169-555X(03)00047-3.

Huggins, T.J., Yang, L., Sornette, D., 2021. Introduction to the Special Issue on Cascading Disaster Modelling and Prevention. Int J Environ Res Public Health. Apr 30;18(9):4813. doi: 10.3390/ijerph18094813. PMID: 33946425; PMCID: PMC8124500.

IPCC Special Report on the Ocean and Cryosphere in a Changing Climate, 2023. [H.-O. Pörtner, D.C. Roberts, V. Masson-Delmotte, P. Zhai, M. Tignor, E. Poloczanska, K. Mintenbeck, A. Alegría, M. Nicolai, A. Okem, J. Petzold, B. Rama, N.M. Weyer (eds.)]. by DRI Lexicon Project Expert Panel.

IPCC Special Report on the Ocean and Cryosphere in a Changing Climate, 2023. [H.-O. Pörtner, D.C. Roberts, V. Masson-Delmotte, P. Zhai, M. Tignor, E. Poloczanska, K. Mintenbeck, A. Alegría, M. Nicolai, A. Okem, J. Petzold, B. Rama, N.M. Weyer (eds.)]. by DRI Lexicon Project Expert Panel.

IPCC, 2021: Climate Change 2021: The Physical Science Basis. Contribution of Working Group I to the Sixth Assessment Report of the Intergovernmental Panel on Climate Change[Masson-Delmotte, V., P. Zhai, A. Pirani, S.L. Connors, C. Péan, S. Berger, N. Caud, Y. Chen, L. Goldfarb, M.I. Gomis, M. Huang, K. Leitzell, E. Lonnoy, J.B.R. Matthews, T.K. Maycock, T. Waterfield, O. Yelekçi, R. Yu, and B. Zhou (eds.)]. Cambridge University Press, Cambridge, United Kingdom and New York, NY, USA, In press, doi:10.1017/9781009157896.

IPCC, 2021: Climate Change 2021: The Physical Science Basis. Contribution of Working Group I to the Sixth Assessment Report of the Intergovernmental Panel on Climate Change[Masson-Delmotte, V., P. Zhai, A. Pirani, S.L. Connors, C. Péan, S. Berger, N. Caud, Y. Chen, L. Goldfarb, M.I. Gomis, M. Huang, K. Leitzell, E. Lonnoy, J.B.R. Matthews, T.K. Maycock, T. Waterfield, O. Yelekçi, R. Yu, and B. Zhou (eds.)]. Cambridge University Press, Cambridge, United Kingdom and New York, NY, USA, In press, doi:10.1017/9781009157896.

Jiang, S., Tarasova, L., Yu, G., & Zscheischler, J. (2024). Compounding effects in flood drivers challenge estimates of extreme river floods. Science Advances. DOI: 10.1126/sciadv.adl4005.

Kashyap, A., Cook, K. L. & Behera, M. D. (2025) Geomorphic imprint of high-mountain floods: insights from the 2022 hydrological extreme across the upper Indus River catchment in the northwestern Himalayas. Earth Surf. Dynam., 13, 147. https://doi.org/10.5194/esurf-13-147-2025.

Kemp, D. B., Sadler, P. M., & Vanacker, V., 2020. The human impact on North American erosion, sediment transfer, and storage in a geologic context. Nature Communications, 11, 6012. https://doi.org/10.1038/s41467-020-19744-3 .

Kharin, V., Flato, G., Zhang, X., Gillett, N., Zwiers, F., Anderson, K.,2018. Risks from Climate Extremes Change Differently from 1.5°C to 2.0°C Depending on Rarity. Earth's Future. 6. 10.1002/2018EF000813.

Kharin, V.V., Zwiers, F.W., Zhang, X. et al., 2013. Changes in temperature and precipitation extremes in the CMIP5 ensemble. Climatic Change 119, 345–357. https://doi.org/10.1007/s10584-013-0705-8.

Khosravi, K., Cooper, J. R., Daggupati, P., Thai Pham, B., Tien Bui, D., 2020. Bedload transport rate prediction: Application of novel hybrid data mining techniques, Journal of Hydrology, Volume 585, 124774, ISSN 0022-1694, https://doi.org/10.1016/j.jhydrol.2020.124774 .

Köppen, W., 1936. Das geographische System der Klimate. In: Köppen, W., Geiger, R. (eds). Handbuch der Klimatologie. Gebrüder Borntraeger, Berlin, p 1−44.

Koreňová, S., Michalková, M. Š., Máčka, Z., Pöppl, R., & Donoval, J. (2024). Linking sediment connectivity with sediment transport risk assessment in small forested catchments in the Czech Republic. River Research and Applications, 40(7), 1343-1362.

La Licata, M., Bosino, A., Sadeghi, S. H., De Amicis, M., Mandarino, A., Terret, A., Maerker, M., 2025. HOTSED: A new integrated model for assessing potential hotspots of sediment sources and related sediment dynamics at watershed scale, International Soil and Water Conservation Research, Volume 13, Issue 1, Pages 80-101, ISSN 2095-6339, https://doi.org/10.1016/j.iswcr.2024.06.002.

Latini, I., 2018. Floristic-vegetational analysis and the changes of biodiversity in the moist environments of Metauro river's final stretch. Unpublished thesis. Università Politecnica delle Marche.

Latini, I., 2018. Floristic-vegetational analysis and the changes of biodiversity in the moist environments of Metauro river's final stretch. Unpublished thesis. Università Politecnica delle Marche.

Lee, R., White, C.J., Sarfaraz Gani Adnan M., Douglas, J., Mahecha, M.D., O'Loughlin, F.E., Patelli, E., Ramos, A.M., Roberts, M.J., Martius, O., Tubaldi, E., van den Hurk, B., Ward, P.J., Zscheischler, J., 2024. Reclassifying historical disasters: From single to multi-hazards, Science of The Total Environment, Volume 912, 169120, ISSN 0048-9697, https://doi.org/10.1016/j.scitotenv.2023.169120.

Liu, C., Walling, D.E., He, Y., 2018. The International Sediment Initiative case studies of sediment problems in river basins and their management. Int. J. Sediment Res.33(2), 216-219. https://doi.org/10.1016/j.ijsrc.2017.05.005.

Liu, C., Walling, D.E., He, Y., 2018. The International Sediment Initiative case studies of sediment problems in river basins and their management. Int. J. Sediment Res.33(2), 216-219. https://doi.org/10.1016/j.ijsrc.2017.05.005.

Liu, H., Du, J., Yi, Y., 2022. Reconceptualising flood risk assessment by incorporating sediment supply, CATENA, Volume 217, 2022, 106503, ISSN 0341-8162, https://doi.org/10.1016/j.catena.2022.106503.

Marche Regione, 2022. SIRMIP - Sistema Informativo Regionale Meteo-Idro-Pluviometrico (Weather-Hydro-Pluviometric Regional Information System). http://app.protezionecivile.marche.it/sol/indexjs.sol?lang=it (accessed 12 July 2024).

Martini, L., Cavalli, M., Picco, L., 2022. Predicting sediment connectivity in a mountain basin: a quantitative analysis of the Index of Connectivity. Earth Surf. Process. Landforms, 47, https://doi.org/10.1002/esp.5331

Messenzehl, K., Hoffmann, T., Dikau, R., 2014. Sediment connectivity in the high-alpine valley of Val Müschauns, Swiss National Park—linking geomorphic field mapping with geomorphometric modelling. Geomorphology. 221, 215-229. https://doi.org/10.1016/j.geomorph.2014.05.033.

Michalek, A., Zarnaghsh, A., Husic, A., 2021. Modeling linkages between erosion and connectivity in an urbanizing landscape, Science of The Total Environment, Volume 764, 144255, ISSN 0048-9697, https://doi.org/10.1016/j.scitotenv.2020.144255.

Mir, A. A. & Patel, M., 2024. "A Comprehensive Review on Sediment Transport, Flow Dynamics, and Hazards in Steep Channels." Journal of Water Management Modeling 32: C517. https://doi.org/10.14796/JWMM.C517 www.chijournal.org ISSN: 2292-6062 © Mir and Patel 2024.

Moore, I.D., Grayson, R.B., Ladson, A.R., 1991. Digital terrain modelling: A review of hydrological, geomorphological, and biological applications. Hydrol. Process., 5: 3-30. https://doi.org/10.1002/hyp.3360050103.

Moosdorf, N., Cohen, S., Hagke, C., 2018. A global erodibility index to represent sediment production potential of different rock types, Applied Geography, Volume 101, Pages 36-44, ISSN 0143-6228, https://doi.org/10.1016/j.apgeog.2018.10.010.

Morelli, S., Bonì, R., Guidi, E., De Donatis, M., Pappafico, G., Francioni, M., 2023. L'alluvione delle Marche del 15 settembre 2022, cause e conseguenze, in: "La Dinamica fluviale. La conoscenza del Fiume per la pianificazione e la salvaguardia del territorio". Cencetti, C., Di Matteo, L. (Eds.), Cult. Territ. Linguaggi. 24, 136-147. ISBN 9788894469783.Najafi, S., Dragovich, D., Heckmann, T., Hamidreza S. S., 2021. Sediment connectivity concepts and approaches. CATENA, Volume 196, 104880, ISSN 0341-8162. https://doi.org/10.1016/j.catena.2020.104880.

Morelli, S., Bonì, R., Guidi, E., De Donatis, M., Pappafico, G., Francioni, M., 2023. L'alluvione delle Marche del 15 settembre 2022, cause e conseguenze, in: "La Dinamica fluviale. La conoscenza del Fiume per la pianificazione e la salvaguardia del territorio". Cencetti, C., Di Matteo, L. (Eds.), Cult. Territ. Linguaggi. 24, 136-147. ISBN 9788894469783.Najafi, S., Dragovich, D., Heckmann, T., Hamidreza S. S., 2021. Sediment connectivity concepts and approaches. CATENA, Volume 196, 104880, ISSN 0341-8162. https://doi.org/10.1016/j.catena.2020.104880.

Müller, T. & Hassan, M. A., 2018. Fluvial response to changes in the magnitude and frequency of sediment supply in a 1-D model. Earth Surf. Dynam., 6, 1041–1057. https://doi.org/10.5194/esurf-6-1041-2018.

Najafi, S., Dragovich, D., Heckmann, T., Hamidreza S. S., 2021. Sediment connectivity concepts and approaches. CATENA, Volume 196, 104880, ISSN 0341-8162. https://doi.org/10.1016/j.catena.2020.104880.

Najafi, S., Dragovich, D., Heckmann, T., Hamidreza S. S., 2021. Sediment connectivity concepts and approaches. CATENA, Volume 196, 104880, ISSN 0341-8162. https://doi.org/10.1016/j.catena.2020.104880.

Nanni, T., & Vivalda, P. M. (2009). Idrogeologia degli acquiferi carbonatici, terrigeni ed alluvionali tra i fiumi Cesano e Potenza (Marche centrali). GNDCI–CNR, Unità Operativa 10. ISBN 9788890455414. DOI: 10.13140/2.1.3450.6883

Nanni, T., Vivalda, P., Clemente, F., Caprari M., Siciliani M. (2018). Carta idrogeologica dell'area compresa tra i fiumi Cesano e Potenza (Marche centrali). Scala 1:100.000. CNR- GNDCI, Unità operativa 10 (Responsabile Scientifico Torquato Nanni). La nuova Lito . Firenze.

Nesci, O., Savelli, D., Diligenti, A., Mariangeli, D., 2005. Geomorphological sites in the northern Marche (Italy). Examples from autochthon anticline ridges and from Val Marecchia allochthon. Il Quaternario Italian Journal of Quaternary Sciences. 18. 79-91.

Nones, M., Guo, Y., 2023. Can sediments play a role in river flood risk mapping? Learning from selected European examples. Geoenviron Disasters 10, 20. https://doi.org/10.1186/s40677-023-00250-9

Nordio, G., Koyanagi, K., Comiti F., Andreoli, A., 2024. Change in Hydrological and Erosion Dynamics in an Alpine River Basin Affected by Forest Cover Change: Field Data Collection and Modeling, the Case of Vaia Windstorm, 2024 IEEE International Workshop on Metrology for Agriculture and Forestry (MetroAgriFor), Padua, Italy, pp. 376-381, doi: 10.1109/MetroAgriFor63043.2024.10948850.

Papalexiou, S. M., & Montanari, A., 2019. Global and regional increase of precipitation extremes under global warming. Water Resources Research, 55, 4901–4914. https://doi.org/10.1029/2018WR024067.

Parsons, A.J., Bracken, L., Poeppl, R.E., Wainwright, J., Keesstra, S.D., 2015. Introduction to special issue on connectivity in water and sediment dynamics. Earth Surface Processes and Landforms, 40(9), 1275-1277. https://doi.org/10.1002/esp.3714.

Piacentini, D., Troiani, F., Marini, M., Menichetti, M., Nesci, O., 2020. GIS-based geomorphometric analysis of stream networks in mountainous catchments. Implications for slope stability, in: Alvioli, M., Marchesini, I., Melelli, L., Guth, P. (Eds.). Proceedings of the Geomorphometry 2020 Conference. Perugia, Italy, CNR Edizioni, 270 p, 254-257. https://doi.org/10.30437/GEOMORPHOMETRY2020_68.

Pinel, S., Cherif, F., Meslard, F., Labrousse, C., Bourrin, F., 2020. Development of a hydro-morphodynamic model for simulation of bed load and morphological changes of flash-floods (Têt River, France). In: Breugem, W. Alexander; Frederickx, Lesley; Koutrouveli, Theofano; Chu, Kai; Kulkarni, Rohit; Decrop, Boudewijn (Hg.): Online proceedings of the papers submitted to the 2020 TELEMAC-MASCARET User Conference October 2020. Antwerp: International Marine & Dredging Consultants (IMDC). S. 46-52.

Poeppl, R. E., Polvi, L. E., Turnbull, L. (2023). (Dis)connectivity in hydro-geomorphic systems – emerging concepts and their applications. Vol. 48. Earth Surface Processes and Landforms 1089 – 1094. https://doi.org/10.1002/esp.5574.

Poesen, J.,2018. Soil erosion in the Anthropocene: Research needs. Earth Surf. Process. Landforms, 43: 64–84. doi: 10.1002/esp.4250.

PTA – Regione Marche. L'Assemblea legislativa regionale delle Marche ha approvato il Piano di Tutela delle Acque (PTA) con delibera DACR n.145 del 26/01/2010. La pubblicazione è avvenuta con il supplemento n. 1 al B.U.R. n. 20 del 26/02/2010 (parte 1 - parte 2).

Raphael, A., Ngaga, Y., Lalika, M., 2023. Watershed degradation and water provision in Morogoro Municipality, Tanzania. Ecohydrology & Hydrobiology, 23(2), 272-279. https://doi.org/10.1016/j.ecohyd.2022.12.004.

Recking, A., 2010. A comparison between flume and field bed load transport data and consequences for surface-based bed load transport prediction, Water Resour. Res., 46, W03518, doi:10.1029/2009WR008007.

Recking, A., 2013. An analysis of nonlinearity effects on bed load transport prediction, J. Geophys. Res. Earth Surf., 118, 1264–1281, doi:10.1002/jgrf.20090.

Remondo, J., Forte, L. M., Cendrero, A., Cienciala, P., Beylich, A. A., 2024. Human-driven global geomorphic change, Geomorphology, Volume 457,109233, ISSN 0169-555X, https://doi.org/10.1016/j.geomorph.2024.109233.

Rickenmann, D.. 2016. Debris-Flow Hazard Assessment and Methods Applied in Engineering Practice. International Journal of Erosion Control Engineering. 9. 80-90. 10.13101/ijece.9.80.

Rinaldi, M., Surian, N., Comiti, F., Bussettini, M., 2020. The role of sediment processes in river management: A review. *Earth-Science Reviews, 210*, 103334. https://doi.org/10.1016/j.earscirev.2020.103334.

Ruiz-Villanueva, V., and G. Consoli. 2025. Instream Large Wood Enhances the Benefits of e-Floods in Regulated Mountain Rivers. River Research and Applications 1–15. https://doi.org/10.1002/rra.70009.

Santangelo, M., Althuwaynee, O., Alvioli, M., Ardizzone, F., Bianchi, C., Bornaetxea, T., Brunetti, M.T., Bucci, F., Cardinali, M., Donnini, M., Esposito, G., Gariano, S.L., Grita, S., Marchesini, I., Melillo, M., Peruccacci, S., Salvati, P., Yazdani, M., Fiorucci, F., 2023. Inventory of landslides triggered by an extreme rainfall event in Marche-Umbria, Italy, on 15 September 2022. Scientific data. 10(1), 427. https://doi.org/10.1038/s41597-023-02336-3.

Santangelo, M., Althuwaynee, O., Alvioli, M., Ardizzone, F., Bianchi, C., Bornaetxea, T., Brunetti, M.T., Bucci, F., Cardinali, M., Donnini, M., Esposito, G., Gariano, S.L., Grita, S., Marchesini, I., Melillo, M., Peruccacci, S., Salvati, P., Yazdani, M., Fiorucci, F., 2023. Inventory of landslides triggered by an extreme rainfall event in Marche-Umbria, Italy, on 15 September 2022. Scientific data. 10(1), 427. https://doi.org/10.1038/s41597-023-02336-3.

Savelli D., Nesci O., B. Asili M., 1995. Evidenze di un apparato glaciale pleistocenico sul massiccio del Catria (Appennino Marchigiano) - Geogr. Fis.Dinam. Quat., 18, pp. 331-335.

Scisciani, V. Styles of positive inversion tectonics in the Central Apennines and in the Adriatic foreland: Implications for the evolution of the Apennine chain (Italy). J. Struct. Geol. 2009, 31, 1276–1294. https://doi.org/10.1016/j.jsg.2009.02.004.

Semnani, S., Han, Y., Bonfils, C., White, J., 2025. Assessing the impact of climate change on rainfall-triggered landslides: a case study in California. Landslides. 22. 1-18. 10.1007/s10346-024-02428-0.

Seneviratne Sonia I., Wartenburger Richard, Guillod Benoit P., Hirsch Annette L., Vogel Martha M., Brovkin Victor, van Vuuren Detlef P., Schaller Nathalie, Boysen Lena, Calvin Katherine V., Doelman Jonathan, Greve Peter, Havlik Petr, Humpenöder Florian, Krisztin Tamas, Mitchell Daniel, Popp Alexander, Riahi Keywan, Rogelj Joeri, Schleussner Carl-Friedrich, Sillmann Jana and Stehfest Elke 2018Climate extremes,

land–climate feedbacks and land-use forcing at 1.5°CPhil. Trans. R. Soc. A.37620160450 http://doi.org/10.1098/rsta.2016.0450.

Seneviratne, S.I., N. Nicholls, D. Easterling, C.M. Goodess, S. Kanae, J. Kossin, Y. Luo, J. Marengo, K. McInnes, M. Rahimi, M. Reichstein, A. Sorteberg, C. Vera, and X. Zhang, 2012: Changes in climate extremes and their impacts on the natural physical environment. In: Managing the Risks of Extreme Events and Disasters to Advance Climate Change Adaptation [Field, C.B., V. Barros, T.F. Stocker, D. Qin, D.J. Dokken, K.L. Ebi, M.D. Mastrandrea, K.J. Mach, G.-K. Plattner, S.K. Allen, M. Tignor, and P.M. Midgley (eds.)]. A Special Report of Working Groups I and II of the Intergovernmental Panel on Climate Change (IPCC). Cambridge University Press, Cambridge, UK, and New York, NY, USA, pp. 109-230.

Seneviratne, S.I., X. Zhang, M. Adnan, W. Badi, C. Dereczynski, A. Di Luca, S. Ghosh, I. Iskandar, J. Kossin, S. Lewis, F. Otto, I. Pinto, M. Satoh, S.M. Vicente-Serrano, M. Wehner, and B. Zhou, 2021: Weather and Climate Extreme Events in a Changing Climate. In Climate Change 2021: The Physical Science Basis. Contribution of Working Group I to the Sixth Assessment Report of the Intergovernmental Panel on Climate Change [Masson-Delmotte, V., P. Zhai, A. Pirani, S.L. Connors, C. Péan, S. Berger, N. Caud, Y. Chen, L. Goldfarb, M.I. Gomis, M. Huang, K. Leitzell, E. Lonnoy, J.B.R. Matthews, T.K. Maycock, T. Waterfield, O. Yelekçi, R. Yu, and B. Zhou (eds.)]. Cambridge University Press, Cambridge, United Kingdom and New York, NY, USA, pp. 1513–1766, doi:10.1017/9781009157896.013.

Shekar, P.R., Mathew, A., 2022. Morphometric analysis for prioritizing sub-watersheds of Murredu River basin, Telangana State, India, using a geographical information system. J. Eng. Appl. Sci. 69, 44. https://doi.org/10.1186/s44147-022-00094-4.

Shekar, P.R., Mathew, A., 2024. Morphometric analysis of watersheds: A comprehensive review of data sources, quality, and geospatial techniques. Watershed Ecology and the Environment. 6. 13-25. https://doi.org/10.1016/j.wsee.2023.12.001.

Shi, C., Liang, Y., Qin, W., Ding, L., Cao, W., Zhang, M., & Zhang, Q. (2025). Review of sediment connectivity: Conceptual connotations, characterization indicators, and their relationships with soil erosion and sediment yield. Earth-Science Reviews, 105091.

Sinnakaudan, S., K., Ghani, A. A., Sanusi S. M. A., Zakaria, N. A., 2003. Flood risk mapping for Pari River incorporating sediment transport, Environmental Modelling & Software, Volume 18, Issue 2, Pages 119-130, ISSN 1364-8152, https://doi.org/10.1016/S1364-8152(02)00068-3.

Soldini, L., & Darvini, G., 2025. Variation in the Extreme Temperatures and Related Climate Indices for the Marche Region, Italy. Climate, 13(3), 58. https://doi.org/10.3390/cli13030058.

Soldini, L., Darvini, G., 2025. Variation in the Extreme Temperatures and Related Climate Indices for the Marche Region, Italy. Climate, 13(3), 58. https://doi.org/10.3390/cli13030058.

Staffilani, F., Bonaposta, D., & Marucci, F. E. (2019). Carta dell'Erosione idrica attuale della Regione emilia-romagna. Servizio Geologico, Sismico e Suoli. Regione Emilia-Romagna.

Stryker, J., Wemple, B., Bomblies, A., 2018. Modeling the impacts of changing climatic extremes on streamflow and sediment yield in a northeastern US watershed, Journal of Hydrology: Regional Studies, Volume 17, Pages 83-94, ISSN 2214-5818, https://doi.org/10.1016/j.ejrh.2018.04.003.

Syvitski, J. P. M., Vörösmarty, C. J., Kettner, A. J., Green, P., 2005. Impact of humans on the flux of terrestrial sediment to the global coastal ocean. Science, 308(5720), 376–380. https://doi.org/10.1126/science.1109454.

Tal, M. & Paola, C., 2007. Dynamic single-thread channels maintained by the interaction of flow and vegetation. Geology; 35 (4): 347–350. doi: https://doi.org/10.1130/G23260A.1

Tangi, M., Bizzi, S., Fryirs, K., & Castelletti, A. (2022). A dynamic, network scale sediment (dis) connectivity model to reconstruct historical sediment transfer and river reach sediment budgets. Water Resources Research, 58(2), e2021WR030784.

Tangi, M., Bizzi, S., Schmitt, R., & Castelletti, A. (2022). D-CASCADE: a basin-scale sediment (dis) connectivity model to quantify sediment budgets and explore reservoir sediment management strategies.

Tarquini S., I. Isola, M. Favalli, A. Battistini, G. Dotta, 2023. TINITALY, a digital elevation model of Italy with a 10 meters cell size (Version 1.1). Istituto Nazionale di Geofisica e Vulcanologia (INGV). https://doi.org/10.13127/tinitaly/1.1.

Tarquini S., Isola I., Favalli M., Battistini A., 2007. TINITALY, a digital elevation model of Italy with a 10 m-cell size (Version 1.0) [Data set]. Istituto Nazionale di Geofisica e Vulcanologia (INGV). https://doi.org/10.13127/TINITALY/1.0.

Tarquini, S., Isola, I., Favalli, M., Mazzarini, F., Bisson, M., Pareschi, M.T., Boschi, E., 2007. TINITALY/01: a new Triangular Irregular Network of Italy. Annals of Geophysics. 50(3), 407-425. https://doi.org/10.4401/ag-4424.

Tarquini, S., Nannipieri, L., 2017. The 10 m-resolution TINITALY DEM as a trans-disciplinary basis for the analysis of the Italian territory: Current trends and new perspectives. Geomorphology, 281, 108-115. https://doi.org/10.1016/j.geomorph.2016.12.022.

Tartaglione, N. (2025). Unprecedented Flooding in the Marche Region (Italy): Analyzing the 15 September 2022 Event and Its Unique Meteorological Conditions. Meteorology, 4(1), 3. https://doi.org/10.3390/meteorology4010003.

Trigila, A., Iadanza, C., 2008. Landslides in Italy, Special Report. Italian National Institute for Environmental Protection and Re-774 search-Geological Survey of Italy/Land Protection and Georesources Department, Rome, Italy.

Trigila, A., Iadanza, C., Guerrieri, L., 2007. The IFFI Project (Italian Landslide Inventory): Methodology and Results, in: Proceedings 772 of the Guidelines for Mapping Areas at Risk of Landslides in Europe; Javier Hervás: Ispra, Italy, October 23, 2007; p. 60. 773.

Trigila, A., Iadanza, C., Spizzichino, D., 2010. Quality Assessment of the Italian Landslide Inventory Using GIS Processing. Landslides. 7, 455–470. https://doi.org/10.1007/s10346-010-0213-0.

Troiani, F., Galve, J.P., Piacentini, D., Della Seta, M., Guerrero, J., 2014. Spatial analysis of stream length-gradient (*SL*) index for detecting hillslope processes: A case of the Gállego River headwaters (Central Pyrenees, Spain). Geomorphology. 214, 183-197. https://doi.org/10.1016/j.geomorph.2014.02.004.

Tunas, I. G., Azikin, H., Oka, G., 2021. Impact of Extreme Rainfall on Flood Hydrographs. IOP Conference Series: Earth and Environmental Science. 884. 012018. 10.1088/1755-1315/884/1/012018.

Turnbull, L., Hütt, M.T., Ioannides, A.A., Kininmonth, S., Poeppl, R., Tockner, K., Bracken, L.J., Keesstra, S., Liu, L., Masselink, R., Parsons, A.J., 2018. Connectivity and complex systems: learning from a multi-disciplinary perspective. Appl Netw Sci. 3, 1-49. https://doi.org/10.1007/s41109-018-0067-2.

UNESCO, 2022. IHP-IX: strategic plan of the intergovernmental hydrological programme: science for a water secure world in a changing environment, ninth phase 2022–2029. UNESCO, Paris, 51 pp. https://unesdoc.unesco.org/ark:/48223/pf0000381318 (accessed 30 July 2024).

UNISDR, 2015. Sendai Framework for Disaster Risk Reduction 2015–2030. United Nations Office for Disaster Risk Reduction, Geneva, Switzerland. Vandekerkhove, E., Bertrand, S., Mauquoy, D., et al., 2020. Neoglacial increase in high-magnitude glacial lake outburst flood frequency, upper Baker River, Chilean Patagonia (47S). Quaternary Science Reviews 248, 106572.

Vázquez-Tarrío, B.T.D., Batalla, R.J., Piégay, H., 2024. A multi-site and hypothesis-driven approach to identify controls on the bedload transport regime of an anthropised gravel-bed river. Earth Surface Processes and Landforms, 49(12), 3913–3933. Available from: https://doi.org/10.1002/esp.5945.

Vázquez-Tarrío, D., Peeters, A., Cassel, M., Piégay, H., 2023. Modelling coarse-sediment propagation following gravel augmentation: The case of the Rhône River at Péage-de-Roussillon (France), Geomorphology, Volume 428, 108639, ISSN 0169-555X, https://doi.org/10.1016/j.geomorph.2023.108639.

Villaret, C., Hervouet, J. M., Kopmann, R., Merkel, U., Davies, A. G., 2013. Morphodynamic modeling using the Telemac finite-element system, Computers & Geosciences, Volume 53, Pages 105-113, ISSN 0098-3004, https://doi.org/10.1016/j.cageo.2011.10.004.

Wainwright, J., Turnbull, L., Ibrahim, T.G., Lexartza-Artza, I., Thornton, S.F., Brazier, R.E., 2011. Linking environmental régimes, space and time: Interpretations of structural and functional connectivity. Geomorphology. 126 (3–4), 387–404. https://doi.org/10.1016/j.geomorph.2010.07.027.

Wainwright, J., Turnbull, L., Ibrahim, T.G., Lexartza-Artza, I., Thornton, S.F., Brazier, R.E., 2011. Linking environmental régimes, space and time: Interpretations of structural and functional connectivity. Geomorphology. 126 (3–4), 387–404. https://doi.org/10.1016/j.geomorph.2010.07.027.

Walling, Des., 2006. Human Impact on Land–Ocean Sediment Transfer by the World's Rivers. Geomorphology. 79. 192-216. 10.1016/j.geomorph.2006.06.019.

Walling, Des., 2008. Studying The Impact Of Global Change On Erosion And Sediment Dynamics: Current Progress And Future Challenges.

Wang, L, Cuthbertson, A, Pender, G & Zhong, D 2019, 'Bed Load Sediment Transport and Morphological Evolution in a Degrading Uniform Sediment Channel Under Unsteady Flow Hydrographs', Water Resources Research, vol. 55, no. 7, pp. 5431-5452. https://doi.org/10.1029/2018WR024413.

Wartenburger, R., Hirschi, M., Donat, M., Greve, P., Pitman, A., Seneviratne, S., 2017. Changes in regional climate extremes as a function of global mean temperature: an interactive plotting framework. Geosci. Model Dev. Discuss.. 2017. 1-30. 10.5194/gmd-2017-33.

Westra, S., Alexander, L., Zwiers, F., 2013. Global Increasing Trends in Annual Maximum Daily Precipitation. Journal of Climate. 26. 7834-. 10.1175/JCLI-D-12-00502.1.

Wilcock, R. P., 1998. Two-Fraction Model of Initial Sediment Motion in Gravel-Bed Rivers.Science280,410-412.DOI:10.1126/science.280.5362.410

Wilson, J. P., 2012. Digital Terrain Model. Geomorphology. Volume 137. Issue 1. Pages 107-121. ISSN 0169-555X, https://doi.org/10.1016/j.geomorph.2011.03.012.

Wohl, E., 2017. Connectivity in rivers. Prog. in Physical Geography. 41(3), 345-362. https://doi.org/10.1177/0309133317714972.

Wohl, E., Brierley, G., Cadol, D., Coulthard, T.J., Covino, T., Fryirs, K.A., Grant, G., Hilton, R.G., Lane, S.N., Magilligan F.J., Meitzen, K.M., Passalacqua, P., Poeppl, R.E., Rathburn, S.L., Sklar, L.S., 2019. Connectivity as an emergent property of geomorphic systems. Earth Surface Processes and Landforms. 44, 4–26. https://doi.org/10.1002/esp.4434.

Wolman, M.G. (1954) A Method of Sampling Coarse River-Bed Material. Transactions—American Geophysical Union, 35, 951-956. http://dx.doi.org/10.1029/TR035i006p00951.

Wu, J., Liu, W., Zhang, J., Chen, X., Yu, Z., Luan, J., Tian, Y., Lan, T., Li, X., Wang, G., 2025. Sediment transport rate variability over time: Individual and synergistic effects of precipitation and flow. Journal of Hydrology: Regional Studies, Volume 59, 102410, ISSN 2214-5818, https://doi.org/10.1016/j.ejrh.2025.102410.

Yassine, R., Cassan, L., Roux, H., Frysou, O., and Pérès, F.: Numerical modelling of the evolution of a river reach with a complex morphology to help define future sustainable restoration decisions, Earth Surf. Dynam., 11, 1199–1221, https://doi.org/10.5194/esurf-11-1199-2023, 2023.

Zanandrea, F., Michel, G.P., Kobiyama, M., Censi, G., Abatti, B.H., 2021. Spatial-temporal assessment of water and sediment connectivity through a modified connectivity index in a subtropical mountainous catchment. Catena, 204, 105380. https://doi.org/10.1016/j.catena.2021.105380.

Zaramella, M., Dallan, E., Marchi, L., Marra, F., Cavalli, M., Crema, S., Borga, M., 2002. Characterization of the flood response to the Vaia storm (October 27th-30th, 2018) in a catchment of the Eastern Italian Alps. preparation for Journal of Hydrometeorology. Submitted to J. Hydrometeorol. (2023).

Zaramella, M., Marchi, L., Marra, F., Comiti, F., Crema, S., Marchio, M., and Borga, M.: Role of stationary convective bands and antecedent conditions on the flood response to the Vaia storm (October 27-30, 2018) in the Eastern Italian Alps, EGU General Assembly 2020, Online, 4–8 May 2020, EGU2020-18668, https://doi.org/10.5194/egusphere-egu2020-18668, 2020.

Zhao, G., Gao, P., Tian, P., Sun, W., Hu, J., Mu, X., 2020. Assessing sediment connectivity and soil erosion by water in a representative catchment on the Loess Plateau, China, CATENA, Volume 185, 104284, ISSN 0341-8162, https://doi.org/10.1016/j.catena.2019.104284.

Ziliani, L., Surian, N., Botter, G., Mao, L., 2020. Assessment of the geomorphic effectiveness of controlled floods in a braided river using a reduced-complexity numerical model. Hydrol. Earth Syst. Sci., 24, 3229–3246. https://doi.org/10.5194/hess-24-3229-2020.

Zscheischler, J., Martius, O., Westra, S., Bevacqu,a E., Raymond, C., Horton, M. R., Hurk, B., Kouchak, A., Jézéquel, A., Mahecha, M. D., Maraun, D., Ramos, A. M., Ridder, N.. N., Thiery, W., Vignotto, E., 2020. A typology of compound weather and climate events. Nat Rev Earth Environ 1, 333–347. https://doi.org/10.1038/s43017-020-0060-z.